

Movement-related and disease-dependent interactions between subthalamic nucleus and cortex in Parkinson's disease and obsessive-compulsive disorder

Inaugural-Dissertation

zur Erlangung des Doktorgrades der Mathematisch-Naturwissenschaftlichen Fakultät der Heinrich-Heine-Universität Düsseldorf

vorgelegt von

Lucie Winkler

aus Duisburg

aus dem Institut für Klinische Neurowissenschaften und Medizinische Psychologie der Heinrich-Heine-Universität Düsseldorf			
Gedruckt mit der Genehmigung der Mathematisch-Naturwissenschaftlichen Fakultät der Heinrich-Heine-Universität Düsseldorf			
Berichterstatter:			
1. Prof. Dr. Markus Butz			
2. Prof. Dr. Gerhard Jocham			
Tag der mündlichen Prüfung: 30.10.2025			

Table of contents

Glossary	5		
Summary	6		
Zusammenfassung	8		
1. Introduction	10		
1.1. Methods of measuring neural oscillations	10		
1.1.1. Magnetoencephalography	10		
1.1.2. Local field potentials	11		
1.2. Analysis of neural oscillations	13		
1.2.1. Spectral analysis	13		
1.2.2. Connectivity	14		
1.2.3. Source analysis	14		
1.3. The role of physiological neural oscillations	15		
1.3.1. Beta oscillations and movement	15		
1.3.2. Beta oscillations and cognition	17		
1.3.3. The role of the cortico-basal ganglia-thalamo-cortical loop	18		
1.3.3.1. The direct pathway	18		
1.3.3.2. The indirect pathway	19		
1.3.3.3. The hyperdirect pathway	19		
1.3.4. The role of theta and gamma oscillations	20		
1.4. The role of neural oscillations in disease	21		
1.4.1. The role of neural oscillations in PD	23		
1.4.2. The influence of DBS on neural oscillations in PD	24		
1.4.3. The role of neural oscillations in OCD	26		
1.4.4. The influence of DBS on neural oscillations in OCD	26		
2. Aims	27		
3. Study 1: Context-dependent modulations of subthalamo-cortical synchronization du reversals of movement direction in Parkinson's Disease	•		
3.1. Methods	28		
3.2. Results	29		
3.2.1. Movement-related power dynamics	29		
3.2.2. Movement-related connectivity dynamics	30		
3.2.3. The influence of predictability on power and coherence dynamics	30		
3.3. Discussion	31		
3.4. Conclusion	32		
4. Study 2: Deep brain stimulation-responsive subthalamo-cortical coupling in obsessive-compulsive disorder			
4.1. Methods			

4.2.	Res	esults			
4.	2.1. The influence of DBS on beta power and coherence in OCD				
4.2.2.		Modulations of beta and theta power during a Go/NoGo task	35		
4.3.	Dis	cussion	37		
4.4.	Cor	nclusion	37		
5 .	Gene	ral discussion	38		
5.1.	Mer	its	38		
5.1.1. Beta synchronization during cognitive challenge			39		
5.1.2. Beta rebour		Beta rebound signals sequence completion, not temporary halts	39		
5.	5.1.3. Beta oscillations are modulated by DBS in OCD				
5.	1.4.	Beta and theta oscillations distinguish PD and OCD	41		
5.2.	Lim	itations	42		
5.	2.1.	Generalizability beyond Parkinson's disease	42		
5.	2.2.	Sample size	42		
5.	2.3.	Stun effect	43		
5.	2.4.	Ecological validity	43		
5.2.5. Scope of analysis		Scope of analysis	43		
5.	5.2.6. The role of the STN in changes of movement direction		44		
5.	2.7.	Electrode locations	44		
6.	Outlo	ok	45		
6.1.		ommendation 1: Extend research to disorders other than Parkinson's disease and to lthy participants	45		
6.2.	Rec	commendation 2: Take advantage of sensing-capable deep brain stimulation systems	46		
6.3.	S.3. Recommendation 3: Develop complex motor tasks46				
6.4.		commendation 4: Expand research methods beyond magnetoencephalography and loca			
6.5.	Rec	commendation 5: Expand data analysis beyond oscillatory power and coherence	47		
7.	Concl	usion	48		
8.	Refer	ences	49		
9.	Erklärung		64		
10.	Danksagung		65		
11.	Appe	ndix	66		
		ox 1: Deep brain stimulationox 2: Parkinson's disease			
		ox 3: Obsessive-compulsive disorder			

Glossary

STN	Subthalamic nucleus
PD	Parkinson's disease
DBS	Deep brain stimulation
MEG	Magnetoencephalography
LFPs	Local field potentials
OCD	Obsessive compulsive disorder
EEG	Electroencephalography
SQUIDs	Superconducting Quantum Interference Devices
BG	Basal ganglia
GPi	Internal segment of the globus pallidus
SNr	Substantia nigra pars reticulata
DICS	Dynamical Imaging of Coherent Sources
LCMV	Linearly Constrained Minimum Variance
ERS	Event-related synchronization
ERD	Event-related desynchronization
SNc	Substantia nigra pars compacta
GPe	External segment of the globus pallidus
VTA	Ventral tegmental area
M1	Primary motor cortex
ACC	Anterior cingulate cortex
OFC	Orbitofrontal cortex
SSRIs	Serotonin reuptake inhibitors
NAc	Nucleus accumbens
PFC	Prefrontal cortex
ROI	Region of interest
MSMC	Medial sensorimotor cortex

Summary

Neural beta oscillations in the cortico-basal ganglia-thalamo-cortical loop, and particularly within the subthalamic nucleus (STN), have consistently been associated with motor control. These oscillations have been studied extensively in Parkinson's disease (PD) patients who present with pathologically elevated beta activity linked to motor impairments. Deep brain stimulation (DBS), a common treatment for advanced PD, can reduce pathological beta activity, suggesting a connection between beta oscillations and motor symptoms. Many studies have capitalized on the unique opportunity to measure neural oscillatory activity directly from the STN in these patients and have revealed valuable insights into PD pathophysiology, PD treatment, and the neural control of simple motor programs. However, the broader role of beta oscillations in the control of complex movement under cognitive challenge, as well as in neurological and psychiatric conditions other than PD, is still largely unknown.

The present thesis is intended to extend our knowledge of the oscillatory mechanisms of motor control to complex movement contexts, involving continuous movements under conditions varying in cognitive challenge, as well as to patients who do not suffer from PD or motor impairment. Further, this work aimed at revealing the effect of DBS on beta oscillations in patients with diseases other than PD.

Two studies were conducted, in both of which magnetoencephalography (MEG) and STN local field potentials (LFPs) were measured simultaneously. 20 PD patients performed a visually cued motor task, involving changes in direction of a continuously performed movement and two conditions varying in the extent to which the next movement prompt could be predicted (**Study 1**). Additionally, one patient with obsessive-compulsive disorder (OCD) and one PD patient were recorded performing a visually cued Go/NoGo task (Study 2). The OCD patient was further recorded at rest while DBS was either ON or OFF to test the influence of DBS on neural oscillatory activity in OCD. In both studies, changes in oscillatory power and STN-cortex coherence were considered to assess the effects of the motor tasks and, in the case of the OCD patient, the effect of DBS.

Study 1 investigated the oscillatory mechanisms of stopping an ongoing action in comparison to briefly halting an action in the context of a complex motor paradigm and varying levels of predictability of motor commands. To do so, PD patients were instructed to turn a wheel, change movement direction, which involved a brief halt in motion, and stop. The beginning of a motor sequence was marked by the suppression of cortical and subthalamic beta power and STN-cortex coherence. Fully terminating a motor sequence was associated with a beta rebound in motor cortex, STN and STN-cortex coherence, whereas briefly halting a movement in the context of a reversal of movement direction was not. Instead, during changes of movement direction, motor cortical beta power was primarily suppressed in the ipsilateral hemisphere, as it had already reached its low in the contralateral hemisphere in the course of the movement. In the STN, brief modulations of high beta power were observed which differed from the post-movement beta rebound spectrally and in amplitude. Interestingly, it was revealed that an unpredictable movement

context was associated with enhanced movement-related modulations of beta coherence between motor cortex and the STN.

Study 1 therefore suggests that briefly halting in the course of a continuous movement and stopping a movement completely have distinct oscillatory profiles. Possibly, the beta rebound does not occur during brief pauses, because it would hinder the recontinuation of movement. Lastly, the study provides first evidence that beta oscillations are associated with cognitive processes in the context of complex movement. Heightened coherence likely reflected the recruitment of additional neural resources in an unpredictable movement scenario requiring enhanced levels of caution.

Study 2 aimed at assessing the effect of DBS on neural oscillatory activity in a single case of OCD, a disorder not marked by motor dysfunction, as well as changes in brain activity that occur during a motor task requiring intact behavioral inhibition. The study revealed strong peaks in resting-state beta power in the right STN and in coherence between the right STN and sensorimotor cortex in the OCD patient. These peaks were reduced by means of DBS, tallying with the existing literature on PD. During a visually cued Go/NoGo task, both the OCD patient and a control patient with PD demonstrated changes in the beta band in motor cortex, including beta suppression and rebound in Go-trials. In NoGo trials, which involve the inhibition of a prepotent response, the beta suppression was interrupted by an early rebound. Interestingly, the oscillatory patterns differed between patients in the STN. In the PD patient, STN power dynamics were generally comparable to motor cortex and involved the beta band. In the OCD patient, differences occurred in the theta band instead: NoGo trials revealed higher theta power compared to Go-trials.

Study 2 suggests that DBS-responsive beta oscillations are not limited to PD and motor dysfunction. Task-based oscillations distinguished better between PD and OCD than resting-state neural oscillations, indicating a stronger association with the diseases. The theta and beta bands appeared to be selectively linked with OCD and PD pathologies, respectively.

The studies presented here demonstrate the sensitivity of beta oscillations to motor and cognitive demands, as well as their response to DBS in OCD. Beta oscillations across cortico-basal ganglia loops reveal enhanced activity during cognitive challenge and reflect the beginning and end of motor sequences. Power modulations during brief changes of a motor program differ from those at movement termination in amplitude and frequency. The occurrence of beta oscillations and their responsiveness to DBS is, however, not necessarily limited to PD patients but can be observed in the resting state in OCD, a disorder not characterized by motor impairment. In contrast, taskbased power modulations appear to be better suited to differentiate between PD and OCD. These findings broaden our understanding of the role of neural beta oscillations in cortico-basal ganglia loops during movement and in DBS, as well as in the distinction between different disorders. As such, they might aid the advancement of therapeutic interventions in the future.

Zusammenfassung

Neuronale Beta Oszillationen innerhalb der Kortiko-Basalganglien-Thalamo-kortikalen Schleife. insbesondere im Nucleus subthalamicus (STN), stehen in engem Zusammenhang mit der motorischen Kontrolle. Bei Patienten mit Morbus Parkinson (PD) wurde in diesem Netzwerk eine pathologisch erhöhte Beta-Aktivität beobachtet, die mit motorischen Einschränkungen einhergeht. Die tiefe Hirnstimulation (THS), eine gängige Therapie bei fortgeschrittenem PD, reduziert die pathologische Beta-Aktivität, was einen Zusammenhang zwischen dem Beta-Frequenzband und motorischen Symptomen nahelegt. Durch zahlreiche vorherige Forschungsarbeiten, in denen neuronale Oszillationen im STN von PD-Patienten aufgezeichnet wurden, konnten wertvolle Einblicke in die Pathophysiologie von PD, die Behandlung von PD, sowie die neuronale Steuerung einfacher Bewegungsmuster gewonnen werden. Die umfassendere Rolle von Beta-Oszillationen bei der Kontrolle komplexer Bewegungsabläufe unter kognitiver Beanspruchung, sowie bei anderen neurologischen und psychiatrischen Erkrankungen, ist jedoch weitgehend unbekannt.

Die vorliegende Dissertation erweitert unser Verständnis der oszillatorischen Mechanismen der motorischen Kontrolle auf komplexe Bewegungskontexte, die kontinuierliche Bewegungen mit unterschiedlichen kognitiven Anforderungen umfassen, sowie auf Patienten ohne PD oder motorischer Beeinträchtigung. Ein weiteres Ziel war es, die Wirkung der THS auf die Beta-Aktivität bei anderen Krankheitsbildern als PD zu untersuchen.

In zwei Studien wurden jeweils simultan Magnetenzephalographie (MEG) und lokale Feldpotenzialaufzeichnungen (LFPs) aus dem STN erfasst. 20 PD-Patienten führten eine visuell instruierte Bewegungsaufgabe mit Richtungswechseln innerhalb kontinuierlicher Bewegungen durch (Studie 1). Die Aufgabe wurde in zwei Bedingungen unterteilt, die sich im Grad der Vorhersehbarkeit der als nächstes durchzuführenden Bewegung unterschieden. Zusätzlich führten eine Patientin mit Zwangsstörung (OCD) und eine Patientin mit PD eine visuelle Go/NoGo-Aufgabe durch (Studie 2). Die OCD-Patientin wurde darüber hinaus im Ruhezustand sowohl unter aktiver THS als auch ohne Stimulation untersucht, um den Einfluss der THS auf die neuronale Oszillationsaktivität zu analysieren. In beiden Studien wurden Veränderungen in der oszillatorischen Power und der STN-Kortex-Kohärenz erfasst, um die aufgabenspezifischen Effekte, und - im Fall der OCD-Patientin - die Wirkung der THS, zu bewerten.

Studie 1 untersuchte die oszillatorische Dynamik beim Anhalten einer laufenden Bewegung im Vergleich zu einem kurzen Stopp innerhalb eines komplexen Bewegungsparadigmas, sowie die Unterschiede zwischen verschiedenen Vorhersagbarkeitsebenen von Bewegungsanweisungen. Zu diesem Zweck wurden PD-Patienten angewiesen, ein Rad zu drehen, die Drehrichtung zu ändern, was einen kurzen Stopp der Bewegung erforderte, und anzuhalten. Der Beginn einer Bewegungsseguenz war mit der Unterdrückung kortikaler und subthalamischer Beta-Power und STN-Kortex Beta-Kohärenz verbunden. Das vollständige Anhalten einer Bewegungsseguenz ging mit einem Beta-Rebound im motorischen Kortex, im STN und in der STN-Kortex-Kohärenz einher. Kurze Stopps innerhalb einer Richtungsänderung zeigten hingegen keinen Beta-Rebound. Stattdessen traten kurzzeitige Modulationen der Power im höheren Beta-Bereich im STN auf. Im motorischen Kortex zeigte sich vor allem in der ipsilateralen Hemisphäre eine Beta-Suppression, da in der kontralateralen Hemisphäre bereits ein Bodeneffekt erreicht war.

Auffällig war, dass bei geringer Vorhersagbarkeit die bewegungsabhängige Modulation der Beta-Kohärenz zwischen STN und Kortex zunahm.

Studie 1 legt nahe, dass kurze Unterbrechungen und das Anhalten einer kontinuierlichen Bewegung unterschiedliche oszillatorische Profile aufweisen. Möglicherweise unterbleibt der Beta-Rebound bei kurzen Pausen, da er die Wiederaufnahme der Bewegung verzögern würde. Schließlich liefert die Studie erste Hinweise auf eine Beteiligung von Beta-Oszillationen in kognitiven Prozessen im Kontext komplexer Bewegungen. Die erhöhte STN-Kortex-Kohärenz war möglicherweise Ausdruck einer gesteigerten Rekrutierung neuronaler Ressourcen in einer Situation, die aufgrund von geringer Vorhersehbarkeit ein höheres Maß an Vorsicht erforderte.

Studie 2 verfolgte das Ziel, die Effekte der THS auf neuronale Oszillationen bei OCD – einer nichtmotorischen Erkrankung – zu untersuchen, sowie die Gehirnaktivität während einer motorischen Inhibitionsaufgabe zu analysieren. Im Ruhezustand zeigten sich bei einer OCD-Patientin ausgeprägte Beta-Power im rechten STN und verstärkte Kohärenz zwischen dem rechten STN und dem sensomotorischen Kortex, die durch THS signifikant reduziert wurden, vergleichbar mit bisherigen Befunden bei PD-Patienten. Während einer visuellen Go/NoGo-Aufgabe traten sowohl bei der OCD-Patientin als auch bei einer Kontrollpatientin mit PD im motorischen Kortex typische Veränderungen im Beta-Band auf, einschließlich Beta-Suppression und Beta-Rebound in Go-Durchgängen. In NoGo-Durchgängen, welche die Inhibierung einer geplanten Reaktion erfordern, wurde eine Beta-Suppression mit vorzeitigem Rebound beobachtet. Interessanterweise unterschieden sich die Oszillationsmuster zwischen den Patientinnen auf STN-Ebene. Bei der PD-Patientin dominierten Power-Modulationen im Beta-Band, die weitgehend denen im motorischen Kortex entsprachen. Bei der OCD-Patientin waren die Effekte auf das Theta-Band beschränkt: NoGo-Versuche zeigten eine deutlich höhere Theta-Power als Go-Versuche.

Studie 2 deutet darauf hin, dass durch THS modulierte Beta-Oszillationen nicht zwangsläufig auf PD und motorische Dysfunktionen begrenzt sind. Aufgabenbezogene neuronale Oszillationen unterschieden deutlicher zwischen PD und OCD als solche im Ruhezustand und spiegeln demnach die Krankheiten besser wider. Die Theta- bzw. Beta-Band-Aktivität zeigte eine selektive Assoziation mit den Pathologien von OCD und PD.

Die hier vorgestellten Studien verdeutlichen die Responsivität von Beta-Oszillationen gegenüber motorischen und kognitiven Anforderungen sowie deren Reaktion auf die THS bei OCD. Beta-Aktivität in Kortiko-Basalganglien Netzwerken nimmt unter kognitiver Herausforderung zu und markiert den Beginn und das Ende von Bewegungssequenzen. Temporäre Veränderungen innerhalb einer Bewegungsseguenz unterscheiden sich in Bezug auf Freguenz und Amplitude von der vollständigen Beendigung der Bewegung. Beta-Oszillationen und deren Reaktion auf THS sind jedoch nicht auf PD-Patienten beschränkt, sondern werden auch in OCD, einer Krankheit ohne Bewegungsstörung, im Ruhezustand beobachtet. Die aufgabenspezifischen Modulationen neuronaler Oszillationen scheinen die Unterschiede zwischen PD und OCD hingegen deutlicher zu zeigen. Diese Erkenntnisse tragen zu einem tieferen Verständnis der Rolle von Oszillationen in Kortiko-Basalganglien Netzwerken im Zusammenhang mit Bewegung und der THS sowie bei der Unterscheidung verschiedener Krankheiten bei und könnten daher zukünftig zur Weiterentwicklung therapeutischer Interventionen beitragen.

1. Introduction

Neural oscillations are rhythmic patterns of neural activity in the brain, which result from the synchronized activity of neuronal assemblies, reflecting the fluctuation in their excitability (Cohen, 2014). Neural oscillations were first measured in 1929 by Hans Berger (Berger, 1929) by means of scalp electrodes. Berger discovered, among other things, that neural oscillations are associated with specific mental states, such as sleep and wakefulness. Since then, neural oscillations have gained widespread interest from researchers. Today, we know that neural oscillations carry meaningful information with respect to sleep (Adamantidis et al., 2019), cognitive operations, such as attention, learning and memory (Ward, 2003), and movement (Barone & Rossiter, 2021). Furthermore, neural oscillations are clinically relevant. For instance, they are now used in clinical practice to diagnose epilepsy (Földi et al., 2021) and sleep disorders (Parrino et al., 2004). They can further aid our understanding of certain pathologies, such as Parkinson's disease (PD, see Info box 2), which is associated with altered neural oscillatory activity (Kühn et al., 2009), and even guide treatment development, as in the case of deep brain stimulation (DBS, see Info box 1) (Wilkins et al., 2024). The following introduction will first introduce neural oscillations and describe how they can be measured and analyzed. The main part of the introduction will focus on the role of beta oscillations in the cortico-basal ganglia-thalamo-cortical loop in health, e.g. in motor control, and in disease, using the examples of PD and obsessive-compulsive disorder (OCD). Info boxes will provide concise overviews of both diseases, including their symptoms, pathologies and treatment options. DBS will be introduced as a treatment option for these disorders in a separate info box and its effect on neural oscillations will be discussed. The focus on beta oscillations will be complemented by a brief overview of theta and gamma oscillations and their roles in health and disease.

1.1. Methods of measuring neural oscillations

1.1.1. Magnetoencephalography

Neural oscillations can be measured by means of noninvasive procedures, including electroencephalography (EEG) and magnetoencephalography (MEG), and by invasive procedures, encompassing local field potential recordings (LFPs), electrocorticography and single-unit recordings. MEG (see Figure 1), one of the techniques employed in the present work, measures the brain's naturally occurring magnetic activity generated by the synchronized activity of parallel pyramidal cell populations, primarily reflecting postsynaptic currents. The brain's magnetic fields are small, in the range of 50 to 500 fT, and are therefore merely a fraction of those produced by commonly used electrical devices or magnetic items, and a billion times smaller than the earth's static magnetic field. Hence, the MEG is equipped with Superconducting Quantum Interference Devices (SQUIDs) - sensors that are sensitive enough to capture the magnetic fields produced by the brain. Using liquid helium, SQUIDs are kept at a temperature of 4 K, which maintains their superconducting quality. Another cornerstone of the MEG is active and passive shielding from external interference of magnetic activity, which is accomplished by the magnetically shielded

room, as well as the cancellation of external magnetic fields. The advantage of MEG in comparison to other neuroimaging techniques is its high temporal resolution that allows for the detection of short-lived neural events, for example linked with cognitive and motor processes. Neural activity is typically measured at a sampling rate of 2000 Hz. EEG reaches the same temporal resolution as MEG, but has a lower spatial resolution, as electrical currents are more distorted by bones and tissues than magnetic fields (reviewed by Baillet et al., 2001; reviewed by Hansen et al., 2010).



Figure 1. MEG setup. 306-channel MEG system (MEGIN) in a magnetically shielded room at the University hospital Düsseldorf. MEG sensors are cooled by liquid helium which is stored in the dewar.

1.1.2. Local field potentials

In healthy humans, researchers are typically bound to use noninvasive measurement tools, such as MEG and EEG. This bears the disadvantage of having to restrict one's analyses to the cortical level or accepting spatial inaccuracies when intending to study deeper sources of neural activity. In contrast, invasive procedures, such as LFP recordings, can shed light on oscillatory processes occurring within deeper structures of the brain. Patients undergoing surgery for DBS (see Info box 1) offer the unique opportunity to measure neural signals from deep brain structures within the basal ganglia (BG). To record neural activity from DBS electrodes, surgery is performed in two steps. In a first step, the DBS macroelectrodes are implanted and the leads externalized, such that LFPs can be recorded the following day. One day after the recording, the DBS pulse generator is implanted into a subclavicular pocket or the abdominal region and subcutaneously connected with the DBS leads permanently (Neumann et al., 2022). Though under debate, the LFP signal derived from the DBS electrodes likely reflects the summed post-synaptic activity from groups of neurons (reviewed by Brown & Williams, 2005). LFPs can be recorded simultaneously with MEG or EEG, as was done in the present work. More recently, DBS systems have been advanced such that LFPs can be recorded directly from the implanted leads without the need to externalize them (Hnazaee et al., 2023). While introducing some new difficulties in data processing, this new

technology has various advantages, including the possibility to measure neural activity at any point post-implantation, possibly when patients have recovered from surgery.

Info box 1: Deep brain stimulation

Deep brain stimulation (DBS) was first established in 1987 as a last resort to manage symptoms of advanced PD. The procedure involves the surgical implantation of macroelectrodes (1.3 mm in diameter with 4 to 8 contacts at the top) into one of the nuclei of the BG, in either one or both hemispheres (reviewed by Hariz & Blomstedt, 2022). Prominent DBS targets are the STN, the ventralis intermediate nucleus (VIM) and the globus pallidus internus (GPi) in the case of PD, essential tremor, and dystonia. In psychiatric patients, for example with OCD or Tourette syndrome, targets include the STN, the striatum, and the nucleus accumbens (NAc, reviewed by Raviv et al., 2020). Electrical current is applied at high frequencies, typically at 130 Hz with 60 µs pulse width and an amplitude between 1 and 4 mA via an implanted pulse generator that is connected with the electrodes subcutaneously. Both monopolar and bipolar stimulation protocols are possible: monopolar stimulation creates a broad field by using an active electrode contact and a remote reference, while bipolar stimulation confines current between two electrode contacts to achieve more focused targeting. Modern DBS systems feature directional contacts, enabling even more precise stimulation by directing current towards specific neural pathways (reviewed by Hariz & Blomstedt, 2022).

DBS surgery can be performed while patients are awake to guide correct electrode placement. Alternatively, advanced imaging techniques allow for great precision in electrode placement at improved comfort of the patients while under general anesthesia (reviewed by Hariz & Blomstedt, 2022). Typically, the neurologist determines the optimal stimulation settings. However, recent developments in adaptive closed-loop DBS systems enable real-time sensing of neural signals, allowing stimulation to be guided by electrophysiological biomarkers (reviewed by Parastarfeizabadi & Kouzani, 2017). First evidence has demonstrated successful symptom improvement in PD patients (Piña-Fuentes et al., 2020) with the added potential of an increased battery life for these DBS systems (reviewed by Parastarfeizabadi & Kouzani, 2017).

Today, DBS is a standard procedure for the symptomatic treatment of PD and other movement disorders and is considered to be generally safe, particularly when selecting patients carefully (reviewed by Pouratian et al., 2012). Complications, such as infections, bleeding, and inflammation of the wound are rare and typically easy to manage (Mostofi et al., 2021; Olson et al., 2023; reviewed by Pouratian et al., 2012). The outcome of DBS of the STN is best in PD patients who are cognitively unimpaired, young, respond well to levodopa and do not suffer from psychiatric disorders. Side effects of DBS, including dysarthria and non-motor symptoms, depend on the chosen DBS target and typically result from a slight misplacement of the electrode (reviewed by Hariz & Blomstedt, 2022; reviewed by Pouratian et al., 2012).

The exact mechanisms through which DBS works remain debated to date, and various hypotheses have been proposed, encompassing oscillatory and chemical effects in the micro-to-macro scales of the cortico-BG circuit, as well as plasticity, and even neuroprotection and neurogenesis depending on the disorder and DBS target (Herrington et al., 2016). In the case of PD and DBS of the STN, the effect of DBS appears to arise from network-wide changes, including reduced excitatory activation of the STN by cortex via the hyperdirect pathway, as well as local alterations of activity in the STN or GPi that impact the dynamics of down-stream targets of the circuit (reviewed by Herrington et al., 2016; reviewed by Neumann et al., 2023). DBS likely normalizes the pathologically enhanced inhibition of the thalamus by the STN (reviewed by Hariz & Blomstedt, 2022), avoiding a spread of pathological activity to other

brain areas (reviewed by Turner & Desmurget, 2010).

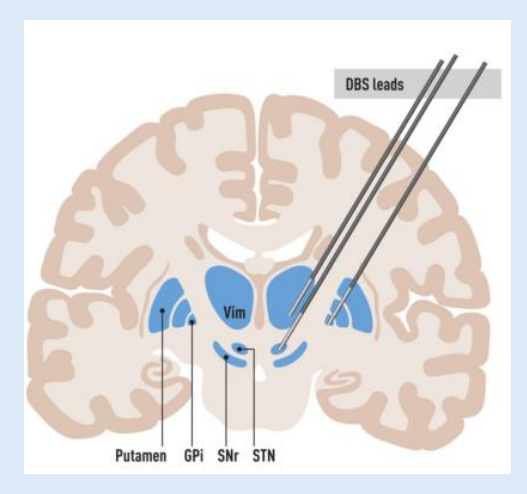


Figure 2. Deep brain stimulation. DBS involves the implantation of electrodes into one of the nuclei of the BG, such as the putamen, GPi, the substantia nigra pars reticulata (SNr) or the STN. The DBS leads are connected subcutaneously to a neurostimulator which applies high frequency stimulation to the DBS target (reproduced from Hariz & Blomstedt, 2022, under the Creative Commons Attribution-NonCommercial-NoDerivatives 4.0 International License (CC BY-NC-ND 4.0)).

1.2. Analysis of neural oscillations

One of the major goals of studying neural oscillations is to understand how they relate to different diseases, symptoms, clinical characteristics (e.g. symptom severity), as well as motor and cognitive processes. They are often studied in the context of neuroscientific experiments to isolate a specific behavior or cognitive process. Performing any of the analyses discussed below requires a thorough cleaning procedure first, ensuring that relevant effects in the data are not masked or altered by the presence of artifacts from sources outside the brain.

1.2.1. Spectral analysis

Most research on neural oscillations is focused on the signal's power in a given frequency band. The power of an oscillation is defined as the square of the amplitude of the signal, reflecting the strength of the oscillation in a given frequency. Power can be derived by performing spectral analysis, which requires the Fourier transform to break down the time-domain neural signal into its constituent frequencies, with phase and amplitude of each frequency component. Commonly analyzed frequency bands include delta (1-4 Hz), theta (4-8 Hz), alpha (8-12 Hz), beta (13-30 Hz), and gamma (> 30 Hz). Using a sliding window approach, the frequency components can be decomposed over time. This way, time-frequency analysis allows for the examination of power as a function of time and frequency (reviewed by Cohen, 2014; reviewed by Gross, 2014; reviewed by Hansen et al., 2010).

1.2.2. Connectivity

In addition to local changes in brain activity, the communication patterns of larger brain networks might also be of interest. For example, one might wonder how spatially distant brain areas, like motor cortex and the BG, synchronize their activity to achieve motor control. To answer questions like that, different measures of connectivity can be considered. Essentially, these measures differ in whether they allow inferences about the directionality of the interaction of two signals (effective connectivity) or only allow a description of the statistical relationship between them (functional connectivity). Coherence, an example of functional connectivity, is a widely used measure in the field of neuroscience, including the present work. It measures the level of phase consistency between two signals from different brain regions at a given frequency, and ranges from 0 to 1 (1 meaning the signals are perfectly synchronous; 0 suggesting a random phase relationship). A high level of coherence between two signals suggests that the corresponding brain areas likely communicate in a functionally meaningful way and it is assumed that this interaction is crucial to the complex cognitive operations achieved by the brain. Coherence is calculated in the frequency domain using the normalized cross-spectral density between the two signals (reviewed by Bastos & Schoffelen, 2015; reviewed by Fries, 2015; reviewed by Friston, 2011; reviewed by Schnitzler & Gross, 2005). As a measure of effective connectivity, the present work employed Granger causality analysis. The assumption of Granger causality is that cause and effect can be determined by temporal ordering. Specifically, the effect (in signal B) should follow the cause (signal A) and past information from signal A and B can be used to predict signal B in a way superior to only using information from signal B (Haufe et al., 2012). In this case, high levels of Granger causality would suggest that signal A (Granger-) causes signal B.

1.2.3. Source analysis

In order to examine the sources of activity in the brain, it is possible to conduct analyses of power and coherence in source space. Estimating the locations of brain activity based on data recorded from sensors outside the brain bears two problems: The forward problem describes the prediction of what the sensor data would look like based on known sources of activity in the brain (Nolte, 2003). The inverse problem involves the prediction of the sources of data recorded outside the brain. The inverse problem is not easily solved, as many potential combinations of sources could produce a given topography of signals at the scalp. Therefore, advanced operations like spatial filters, which impose additional constraints to arrive at a unique solution to the inverse problem, are required. Spatial filters allow the reconstruction of sources of activity from a specific location while suppressing noise from other sources, allowing for spatial specificity (reviewed by Gross et al., 2013; reviewed by Hansen et al., 2010). In the present work, two beamformers were used to construct spatial filters: Dynamical Imaging of Coherent Sources (DICS) which calculates power and coherence in the frequency domain (Gross et al., 2001) and Linearly Constrained Minimum Variance (LCMV) which operates in the time domain (Van Veen et al., 1997). In order to solve the inverse problem using a beamformer, the forward problem must be solved first. A forward model requires the following: a head model representing the geometry, tissues, and other properties of the head, a source model which specifies where brain activity is to be estimated (typically a grid

of points either covering the whole brain or just the cortex) and a lead field matrix, relating the potential sources of activity in the source model to the measured sensor data (Gross et al., 2013).

1.3. The role of physiological neural oscillations

The present work's primary focus lies in the investigation of neural oscillations in the beta frequency range (13-30 Hz) which play a crucial role in both health (Alegre et al., 2004) and disease (Mathiopoulou et al., 2024) and have thus been investigated in thousands of scientific publications. Most research has focused on the role of beta oscillations in motor control, but more recently, beta oscillations have further been implicated in various cognitive processes (Schmidt et al., 2019). The following sections will serve as an introduction to the functional significance of beta oscillations in healthy people. It should be noted that the research presented on subcortical structures inevitably involves patients implanted with DBS systems. While this complicates the generalizability of these findings to healthy physiological neural oscillations, there is no alternative to studying neural oscillations in deep brain structures, such as the BG, in humans (reviewed by Brown & Williams, 2005).

1.3.1. Beta oscillations and movement

Beta oscillations have persistently been associated with motor control. Typically, movementrelated beta oscillations are studied using variations of the Go/NoGo task or stop signal reaction time task (Alegre et al., 2013; Aron & Poldrack, 2006; Kühn et al., 2004; Ray et al., 2012). These are simple motor tasks, involving visual cues prompting participants to perform ballistic movements, such as pressing a button, and to inhibit these movements in a pre-defined number of trials. A large body of research has led to clear associations of beta power with various movement parameters. For instance, it has been demonstrated that movement and the preparation thereof are linked with the suppression of beta oscillations in the sensorimotor cortices and the STN. Following movement, beta oscillations then reemerge and rise above baseline levels in a phenomenon known as beta rebound (Alegre et al., 2004; Fonken et al., 2016; Fry et al., 2016; Jurkiewicz et al., 2006; Ray et al., 2012) (see Figure 3). The consistent occurrence of these modulations, their prominence compared to other neural phenomena, and their sensitivity to factors such as age (Rossiter et al., 2014; Sallard et al., 2016), disease (Choi et al., 2020), and cognition (Fischer et al., 2016; Tan et al., 2016) have made them a central focus of numerous scientific studies. While still debated, it has been suggested that the post-movement beta rebound might reflect an integration of sensory feedback with predictions about upcoming movement used to either maintain or adapt current motor output (Alegre et al., 2004; Cao & Hu, 2016; Tan et al., 2016). Another interpretation states that the beta rebound reflects the clear-out of the motor program (Schmidt et al., 2019).

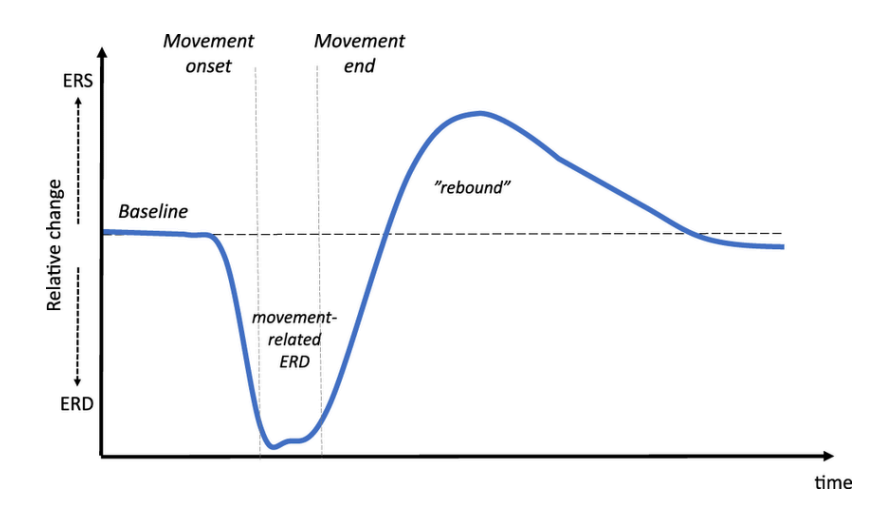


Figure 3. Movement-related beta suppression and beta rebound. The relative change in beta power in the course of a movement is illustrated. During movement preparation, beta power decreases and only rises again once movement has finished. The beta rebound involves a post-movement increase in beta power that surpasses its baseline levels. ERS: Event-related synchronization; ERD: Event-related desynchronization (reproduced from Vinding et al., 2019, under the Creative Commons Attribution 4.0 International License (CC BY 4.0)).

Besides the initiation and termination of motor programs, the inhibition of movement, i.e. withholding a prepared movement, has consistently been associated with changes in beta band activity. For example, it has been revealed that movement inhibition is associated with a shorter suppression of beta oscillations than observed during movement that is not withheld, and even with increases in beta power in motor cortical regions and the STN (Bastin, Polosan, Benis, et al., 2014; Swann et al., 2009; Wagner et al., 2018). Inhibitory success increases with higher levels of beta activity (Benis et al., 2014; W. Chen et al., 2020), clearly demonstrating the functional relevance of beta oscillations in inhibitory processes. Recent evidence indicates that the low beta band (13-21 Hz) is more strongly associated with inhibition than the high beta band (22-35 Hz), which appears to reflect cognitive functions such as attention more closely (Chandramouli et al., 2019; Oswal et al., 2021; Patai et al., 2022).

Briefly pausing a movement, rather than stopping it completely or inhibiting it, has rarely been studied. So far, studies have delivered inconclusive results, suggesting no changes in beta power on the one hand (Alegre et al., 2004; London et al., 2021), and the emergence of a beta rebound during the pause on the other (Muralidharan & Aron, 2021).

Though less frequently reported on, there is evidence that the synchronization of activity between sensorimotor cortex and the BG follows the movement-related patterns of local power within these structures, suggesting that motor control is achieved through the interactions within a wider motor network. For instance, connectivity between STN and cortex has been found to decrease prior to movement (Cassidy et al., 2002; Talakoub et al., 2016; van Wijk et al., 2017), and that decrease has been reported to be reduced when stopping a planned movement (Alegre et al., 2013). There is also some evidence of heightened beta coherence after terminating a ballistic movement (Tan et al., 2014), similar to the rebound of local beta power.

A general interpretation of the functional role of beta oscillations capturing the movementrelated dynamics described above suggests that the beta rhythm exhibits a gating function (Leventhal et al., 2012). High levels of beta might reflect a "closed gate", such that incoming stimuli do not result in action, for example when conflict is involved. Suppression of beta, on the other hand, is equivalent to an "open gate", allowing for motor or cognitive operations (information on the association of beta oscillations with cognition can be found in section 1.3.2.). This hypothesis aligns with beta reflecting the status quo of the motor or cognitive system (Engel & Fries, 2010), with high levels of beta power during consistent output or rest, and decreases in beta power when changes in current behavior are actively desired. The beta rhythm is thus thought to maintain the current motor or cognitive state (Engel & Fries, 2010), while also playing a role in monitoring sensory feedback that might suggest the requirement for a change (Cao & Hu, 2016; Tan et al., 2016).

1.3.2. Beta oscillations and cognition

While the role of beta oscillations is best established in motor control, recent evidence suggests that they may also bear functional relevance to cognitive processes. The post-movement beta rebound, for example, has been found to increase with reduced cognitive load in healthy participants (Fischer et al., 2016). In contrast, it is attenuated in both cortex and the STN in the presence of conflict and when erroneous responses have been made (Zavala et al., 2018). An interpretation explaining these observations suggests that the beta rebound reflects confidence in the future integration of behavior with sensory feedback from past actions. A high beta rebound would thus indicate that current behavioral or cognitive output/plans can be maintained. A low beta rebound implies less confidence, and possibly the need for an adaptation of behavior moving forward (Cao & Hu, 2016; Tan et al., 2016).

Beta oscillations further appear to be sensitive to the context of movement, rather than just reflecting movement itself. For instance, STN beta activity has been reported to be linked with task complexity, displaying greater movement-related suppression as complexity increases (Oswal et al., 2013). Furthermore, proactively anticipating the need to inhibit a future movement is associated with increased STN beta power, correlating with inhibitory success (Benis et al., 2014). When decisions are guided by external cues, for example when determining whether a response is required, STN beta power decreases. When no action is needed, increases in beta power have been observed (Oswal et al., 2012). These beta dynamics are not limited to physical actions but extend to purely cognitive scenarios. For example, in a task requiring decisions about encoding information into working memory, subthalamic beta power decreased when encoding occurred but was less suppressed when encoding was deemed unnecessary (Zavala, Jang, et al., 2017). Moreover, purely cognitive inhibition processes have been linked to increases in STN beta power (Brittain et al., 2012). Overall, beta oscillations demonstrate similar dynamics across motor and cognitive domains. Both movement execution and cognitive operations involve beta suppression, whereas inhibitory processes, whether motor or cognitive, are associated with increased beta activity.

Previous interpretations of the functional role of beta oscillations have claimed the beta rhythm to be "anti-kinetic" (Brown, 2003), an assumption based largely on observations made in PD patients (see section 1.4.1.), as well as the consistent finding of high levels of beta power during periods of rest or inhibition (Benis et al., 2014; Engel & Fries, 2010). Similarly, beta has been described as an "idling rhythm" (Pfurtscheller, 1992), suggesting a resting or inhibited state as the default of the beta rhythm which is only changed when action is desired. Because it is clear that beta power is not strictly movement-related but occurs even when movements are imagined (Pfurtscheller et al., 2005) or passive (Alegre et al., 2002), as well as in the context of purely cognitive tasks (Brittain et al., 2012), the interpretation of beta as merely anti-kinetic does not seem to capture its dynamics entirely.

1.3.3. The role of the cortico-basal ganglia-thalamo-cortical loop

The cortico-basal ganglia-thalamo-cortical loop generally serves to control movement. It has been associated with action selection (reviewed by Redgrave et al., 1999), invigoration of desired motor programs and the inhibition of undesired ones (reviewed by Klaus et al., 2019; reviewed by Mink, 1996). A central mechanism of the BG is to inhibit or excite the thalamus, which in turn influences motor cortex and finally motor output (reviewed by Bonnevie & Zaghloul, 2018). The status quo of BG output is the inhibition of the thalamus (reviewed by Turner & Desmurget, 2010), which means that a state of steady motor output or rest is actively favored over changes in motor output. Similarly, beta power is typically increased at rest and after the termination of motor programs but decreased during movement (see section 1.3.1.). The beta band is therefore often described as reflecting the status quo of the motor system, an interpretation that matches the tonic inhibitory function of the cortico-basal ganglia-thalamo-cortical loop (Engel & Fries, 2010). In order for motor programs to be executed, the removal of tonic inhibition of the thalamus by the BG output structures is required (reviewed by Grillner et al., 2013; reviewed by Mink, 1996). Conversely, unwanted movements can be prevented and motor programs completed by keeping the inhibition of the thalamus intact or reinstating its inhibition, respectively (reviewed by Klaus et al., 2019). The signals causing these chain reactions are sent by motor cortex (reviewed by Mink, 1996). A traditional way of conceptualizing these processes involves the direct, indirect, and hyperdirect pathways of the cortico-basal ganglia-thalamo-cortical loop (see Figure 4).

1.3.3.1. The direct pathway

Simply stated, the activation of the direct pathway allows for movement initiation and action selection. The major input structure of the BG, the striatum, receives glutamatergic inputs from cortical and thalamic areas and dopaminergic inputs via dopamine receptors D1 from the substantia nigra pars compacta (SNc). The striatum then inhibits the BG's primary output nuclei, the substantia nigra pars reticulata (SNr) and the GPi, such that the tonic inhibition of the thalamus is lifted. The result is selective motor cortical activation for movement that is desired, rather than allowing for all cortical inputs to cause movement. To accomplish this specificity in action selection, the striatum receives inputs from various cortical areas about the movement context (reviewed by Calabresi et al., 2014; reviewed by Klaus et al., 2019; reviewed by Turner & Desmurget, 2010).

Decreases in beta power are the oscillatory marker of this process and therefore reflect an active, task-attentive state of the cortex (Jurkiewicz et al., 2006).

1.3.3.2. The indirect pathway

The indirect pathway is initiated with glutamatergic stimulation of the striatum by cortex and dopaminergic inhibitory inputs via Dopamine receptors D2. The striatum then sends GABAergic inhibitory signals to the external segment of the globus pallidus (GPe), leading to reduced inhibition of the STN. This causes the STN to excite the output nuclei of the BG via glutamatergic projections, leading to thalamic inhibition and, ultimately, reduced cortical stimulation such that motor programs can be effectively inhibited. The major result of the activation of the indirect pathway is therefore preventing unwanted movements (reviewed by Calabresi et al., 2014). Postmovement increases in motor cortical and subthalamic beta power reflect this broad inhibition, or an idling state, of the motor system (Pfurtscheller, 1992; Salmelin et al., 1995; reviewed by Schmidt & Berke, 2017; Wessel et al., 2016).

1.3.3.3. The hyperdirect pathway

The hyperdirect pathway also serves to inhibit movement but acts faster than the indirect pathway. That is due to direct frontal cortical glutamatergic projections to the STN, circumventing the striatum. Once activated, the STN excites the output nuclei of the BG, increasing the inhibition of the thalamus and cortex (W. Chen et al., 2020; Oswal et al., 2021). The STN's response is known to be particularly quick, transient, and unselective - possibly serving as a broad delay or pausing signal for movement in response to stop, surprise, or conflict cues, rather than fully canceling an action (reviewed by Aron et al., 2016; reviewed by Schmidt & Berke, 2017). Rapid action halting, mediated via hyperdirect pathway fibers, has been shown to cause global motor suppression (Wessel et al., 2016), in line with the idea of the STN implementing a "hold your horses" signal (Frank, 2006). The STN is thought to function as a decision threshold, reflecting the level of concurrent conflict, with evidence in favor of a specific cortico-striatal action plan having to surpass this threshold to be executed. This way, a prepotent response can be withheld until a final action is selected (Bonnevie & Zaghloul, 2018).

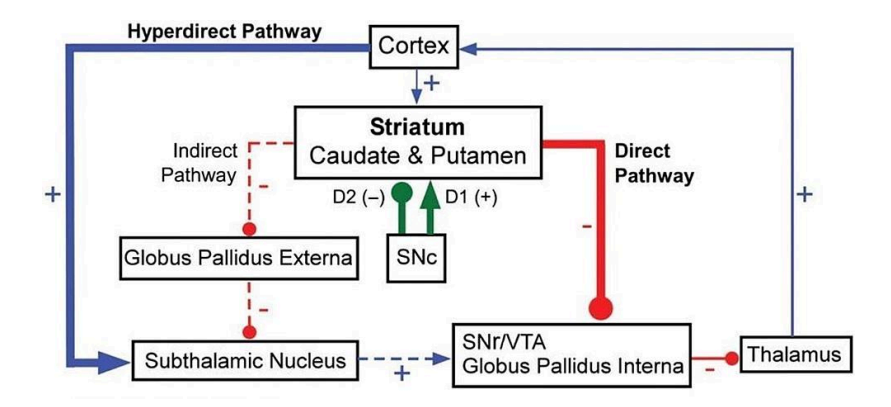


Figure 4. Pathways of the cortico-basal ganglia-thalamo-cortical loop. The direct, indirect, and hyperdirect pathways are depicted. Excitatory inputs: blue; inhibitory inputs: red; modulatory inputs: green. SNr: Substantia nigra pars reticulata; SNc: Substantia nigra pars compacta; VTA: Ventral tegmental area (reproduced from Matz & Spocter, 2022, under the Creative Commons Attribution 4.0 International License (CC BY 4.0)).

1.3.4. The role of theta and gamma oscillations

The focus of the present work is the functional role of beta oscillations in movement, cognition, and disease. Nevertheless, due to their significance in both motor and cognitive processes, this section will briefly introduce the role of physiological theta and gamma oscillations.

Gamma oscillations (> 30 Hz) are often described as pro-kinetic (Brown, 2003). Unlike beta, gamma activity increases with movement effort (Tan et al., 2013), muscle force (Anzak et al., 2012), and velocity (Lofredi et al., 2018) in the STN, and during self-paced movement in motor cortex (Cheyne et al., 2008). Similar findings apply to coherence between the STN and cortex, with increases occurring at movement initiation (Alegre et al., 2013; Litvak et al., 2012). Findings regarding gamma power dynamics during movement termination are, however, still inconclusive (Alegre et al., 2013; Fischer et al., 2017). In addition, the gamma rhythm appears to be related to various non-motor functions, such as attention to salient stimuli and monitoring of behavior and errors (in the middle frontal gyrus, Fonken et al., 2016), managing cognitive demands imposed by increased task complexity (in the STN, Oswal et al., 2013), and working memory (in the occipital cortex, Jokisch & Jensen, 2007).

Theta oscillations (3-8 Hz) have been studied less in the context of movement, though there is evidence to suggest movement-related theta synchronization in cortical sensorimotor areas in healthy individuals (Cruikshank et al., 2011; Körmendi et al., 2021). In PD patients, theta power in the primary motor cortex (M1) and the STN has revealed opposite dynamics: it decreased during hand and foot movements in the contralateral M1 but increased in the contralateral STN (Olson et al., 2022; Tan et al., 2013). The relevance of theta oscillations to healthy motor control is further highlighted by the finding that mid-frontal theta oscillations are diminished in PD patients suffering from freezing of gait (Singh et al., 2020). Additionally, mid-frontal theta has been associated with cognitive control, including navigating conflict situations and processing of recent errors (Singh et al., 2018). The STN, with its many connections to frontal regions, plays a key role in conflict-related tasks requiring the inhibition of prepotent actions. Findings confirm that STN theta power increases during tasks involving inhibition, particularly when inhibition fails (Alegre et al., 2013), and during

conflict tasks (Zavala et al., 2013; Zavala, Damera, et al., 2017), accompanied by heightened synchronization with the medial prefrontal cortex (Zavala et al., 2018).

1.4. The role of neural oscillations in disease

Beta oscillations have been implicated in the pathophysiology of movement disorders, predominantly in PD. Much evidence suggests that beta oscillations are pathologically enhanced in PD (Neumann et al., 2016) and associated with PD symptoms, such as slowness of movement (Kühn et al., 2009). Interestingly, activity in the beta band can be normalized by means of DBS and the administration of Levodopa, underscoring its pathological nature (Mathiopoulou et al., 2024). Much of what is known about the BG and beta oscillations in a diseased state originates from PD patients as DBS has become a standard treatment for PD. Other disorders, such as dystonia and essential tremor, have also contributed to this literature, but to a much lesser extent. The use of DBS in psychiatric disorders, such as Tourette syndrome and OCD, is considerably less common. However, first evidence suggests that neural oscillations are altered (Bastin, Polosan, Piallat, et al., 2014; Koh et al., 2018) and can be normalized by DBS in these disorders (Figee et al., 2013; Smolders et al., 2013), as well. The following sections will examine the oscillatory characteristics of PD and OCD, as well as their modulation by DBS.

Info box 2: Parkinson's disease (PD)

Overview

Parkinson's disease (PD) is a progressive, irreversible movement disorder and the second most common neurodegenerative disorder after Alzheimer's disease (reviewed by Aarsland et al., 2021; reviewed by DeMaagd & Philip, 2015). PD affects about 8.5 million people worldwide according to the WHO (as of 2019) with numbers expected to increase in the coming years (Dorsey et al., 2007). Men are 1.5 times more likely to suffer from PD than women (Wooten et al., 2004). While age is an important risk factor for PD and most patients have a late onset of the disease in the 6th decade, some patients first present with symptoms at much younger ages. PD can be caused by certain genetic variants and environmental factors, such as exposition to toxic agents, or secondary to drugs, but most cases of PD are idiopathic, meaning that there is no identifiable cause of the disease (reviewed by Brigo et al., 2014; reviewed by Dauer & Przedborski, 2003; reviewed by Vázquez-Vélez & Zoghbi, 2021).

Symptoms

The cardinal symptoms of PD are resting tremor, bradykinesia (slowness of movement), rigidity (stiffness), and postural instability (reviewed by Dauer & Przedborski, 2003; Höglinger & Trenkwalder, 2023; reviewed by Jankovic, 2008). Additional symptoms patients might suffer from include freezing of gait, hypophonia, and non-motor symptoms, including hypomimia, depression, sleep disturbance, sensory and autonomic dysfunction, cognitive impairment, and others (reviewed by Dauer & Przedborski, 2003; reviewed by Hariz & Blomstedt, 2022). Patients typically present with variable symptom profiles (reviewed by Vázquez-Vélez & Zoghbi, 2021) and are classified into an akinetic-rigid, tremor-dominant, or intermediary subtype depending on the dominance of symptoms (reviewed by Hariz & Blomstedt, 2022; Zhang et al., 2015).

Pathology

The pathology of PD is characterized by a depletion of dopamine in the SNp caused by a loss of dopamineproducing cells. This leads to a lack of dopaminergic inputs to the striatum. As a result, both STN and GPi/SNr neurons increase their inhibition of the thalamus, leading to reduced motor cortical activation and the core symptoms of PD. Of note, at the time of symptom manifestation, dopamine is already grossly depleted, with an estimated loss of up to 60% of dopaminergic neurons in the SNp. While it is clear that the pathology begins years before first symptom manifestation, the initial trigger remains unknown. Hypotheses for the pathogenesis of PD include oxidative stress, mitochondrial dysfunction, and the aggregation of abnormally folded protein, most evidence pointing toward the latter. Similar to other neurodegenerative diseases, PD is characterized by an accumulation of Lewy bodies - misfolded protein aggregates of alphasynuclein in brain cells, which in rare cases may be caused by a genetic mutation for alpha synuclein (reviewed by Cheng et al., 2010; reviewed by Dauer & Przedborski, 2003; reviewed by Vázquez-Vélez & Zoghbi, 2021; reviewed by Wichmann & DeLong, 1996). On an electrophysiological level, PD patients demonstrate pathologically enhanced beta activity in the STN, which has thus far been considered the neurophysiological hallmark of PD and is associated with symptom severity (Neumann et al., 2016).

Treatment

Research efforts targeting neuroprotective treatments preventing the loss of dopamine have not been successful thus far. Hence, treatment options remain focused on managing the symptoms of PD but cannot stop or reverse the disease (reviewed by Cheng et al., 2010; reviewed by Dauer & Przedborski, 2003). The first line of treatment is the dopaminergic precursor levodopa, which can be supplemented by other drugs, such as dopamine agonists. Typically, patients' quality of life initially improves greatly by the administration of dopaminergic medications. However, the effects tend to wear off after 5-10 years and so-called end-of-dose symptoms, such as hyperkinesia or hypokinesia, emerge, DBS is a treatment option for advanced PD which allows for a larger therapeutic window than achieved by medication alone (see info box 1). The procedure involves the implantation of electrodes into targets in the BG, usually the STN. While its effectiveness is undisputed, its mechanisms are still largely unknown (reviewed by Dauer & Przedborski, 2003; reviewed by Hariz & Blomstedt, 2022). Besides dopaminergic medication and DBS, exercise may positively affect motor functioning in PD (Ellis et al., 2021; reviewed by Tiihonen et al., 2021).

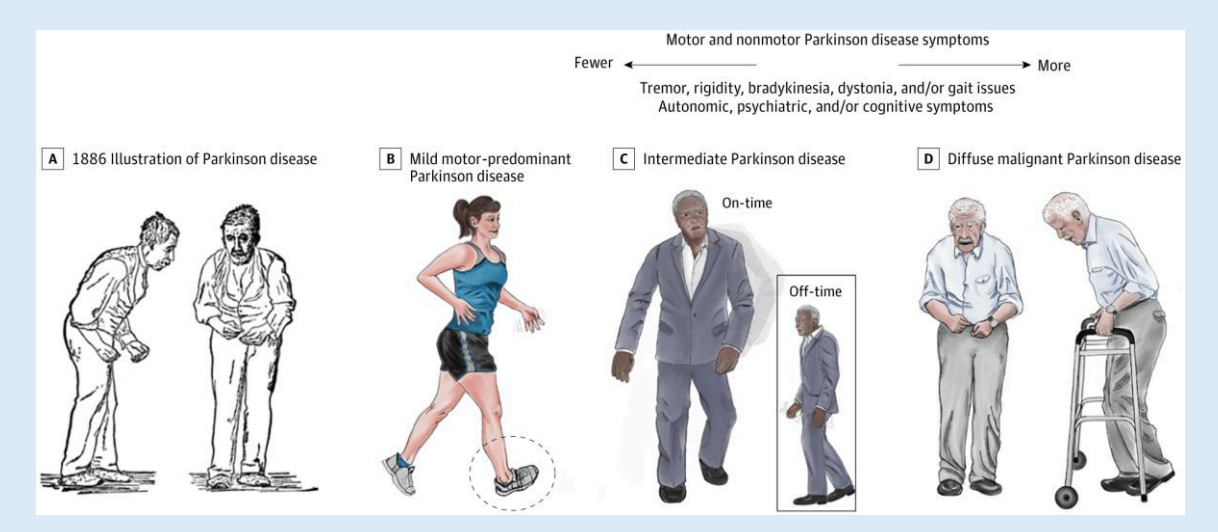


Figure 5. The symptoms of PD. The figure demonstrates an update to the conventional portrayal of PD patients (A). Patients differ in the type and severity of motor and non-motor symptoms, which affect daily life to varying degrees (B–D) (reproduced with permission from Armstrong & Okun, 2020. JAMA Neurology. © 2020 American Medical Association).

1.4.1. The role of neural oscillations in PD

The neurophysiological hallmark of PD is pathologically enhanced beta activity in the BG-cortex circuit. Untreated PD is characterized by elevated beta power within the GPi and STN, along with increased coherence between them (Brown et al., 2001), with the highest levels of beta power localizing to the dorsolateral part of STN, its sensorimotor region (Horn et al., 2017). Additionally, PD is linked with increased beta coherence between the STN and motor cortex (Hirschmann et al., 2011). Recent evidence suggests an overactivity of the hyperdirect pathway in the high beta band in PD, contributing to network changes, including the emergence of low beta power in the BG (Oswal et al., 2021). Importantly, levodopa effectively reduces elevated STN and cortical beta power and cortico-BG coherence (Brown et al., 2001; Hirschmann, Özkurt, et al., 2013). These reductions correlate with improved motor performance (Fischer et al., 2019), including normalized movement-related beta desynchronization in the supplementary motor area (SMA), enhancing movement velocity and muscle activity (Chung et al., 2018). Similarly, levodopa decreases the length, amplitude, and probability of beta bursts (G. Tinkhauser et al., 2017).

Furthermore, the beta frequency band is closely linked with PD symptoms. For instance, tremor is associated with an initial increase and a subsequent decrease in beta power in the STN (Hirschmann et al., 2019), and a reduction of beta power in cortex (Hirschmann, Hartmann, et al., 2013). Freezing of gait correlates with beta power and STN-cortex beta coherence, suggesting that BG-cortex loop dysfunction contributes to the emergence of this problematic symptom (Toledo et al., 2014). Conversely, akinesia and rigidity are negatively associated with STNcortex beta coherence in unmedicated patients (Hirschmann, Özkurt, et al., 2013), underscoring a complicated relationship between beta coherence and PD symptoms.

Although the pathophysiology of PD is most strongly associated with the beta frequency band, other frequency bands have also been explored in this context. For instance, subthalamic high frequency oscillations (> 200 Hz) are modulated by levodopa and associated with rigidity and akinesia scores (Özkurt et al., 2011). Narrowband gamma oscillations in the motor cortex, STN, and STN-cortex coherence have been connected with dyskinesias (Olaru et al., 2024; Swann et al., 2016) and correlate with medication intake in the STN (Colombo et al., 2025). Resting tremor and tremor severity are linked with increased low gamma activity (Beudel et al., 2015; Weinberger et al., 2009).

Beyond the gamma band, subcortical theta oscillations also show pathological elevations in PD patients with dystonia (Olson et al., 2022). At the cortical level, theta oscillations, typically associated with cognitive functions, are reduced in PD patients during tasks involving conflict (Singh et al., 2018). These reductions are also connected to motor symptoms, such as freezing of gait (Singh et al., 2020). Furthermore, theta and gamma rhythms in fronto-temporal-parietal regions are associated with the cognitive and emotional symptoms of PD, including cognitive impairment and anxiety (lyer et al., 2020).

1.4.2. The influence of DBS on neural oscillations in PD

Treatments of PD aim to alleviate symptoms by modulating activity within the BG-cortical loop. Stimulation is typically targeted at the dorsolateral STN, with the greatest occurrence of beta oscillations localizing to this area (Horn et al., 2017), likely preventing the spread of pathologically altered activity to other brain areas (Adam et al., 2022; Turner & Desmurget, 2010). In the STN, DBS has been found to be associated with reduced beta activity in the short-term (Y. Chen et al., 2020; Muthuraman et al., 2020). Reductions of beta power span the entire beta band, i.e. 13-35 Hz, and are distinct from the decreases in the lower beta range (~13-20 Hz) achieved by dopaminergic medication (Mathiopoulou et al., 2024). Beta oscillations in the STN can serve as a predictor of the best stimulation contact with respect to clinical outcome (di Biase et al., 2023), and, due to their clinical relevance, have been proposed as targets for sensing-capable closed loop DBS systems (Radcliffe et al., 2023). Adaptive DBS utilizing beta bursts in the STN to adapt stimulation protocols has recently demonstrated to successfully ameliorate symptoms, including freezing of gait, tremor, and bradykinesia (Wilkins et al., 2024). Cortical areas associated with DBS-induced changes include the sensorimotor cortices (Abbasi et al., 2018), and specifically the SMA (Hollunder et al., 2024). Similar to the STN, and in line with the hypothesis of DBS halting the spread of pathological oscillatory activity, DBS is known to decrease alpha and beta power in the sensorimotor cortices (Abbasi et al., 2018; Muthuraman et al., 2020) and coherence between the STN and motor cortex (Oswal et al., 2016).

While the effects of DBS in PD are best established with respect to the beta band, DBS also appears to influence neural oscillatory activity in other frequency bands. For example, DBS has been demonstrated to induce narrow-band gamma oscillations in the STN (Wiest et al., 2021). Cortical and STN DBS-entrained gamma oscillations promote the alleviation of motor symptoms (Muthuraman et al., 2020) and can be used as biomarkers for adaptive DBS to determine high and low dopaminergic states (Colombo et al., 2025; Oehrn et al., 2024), and to identify dyskinesia (Olaru et al., 2024). Some evidence further suggests an effect of DBS on lower frequencies. For instance, theta band activity increases with DBS (Giannicola et al., 2013). Biophysical modeling of the STN-striatal pathway has revealed that one of the mechanisms of DBS might be compensating for the loss of dopaminergic inputs and excessive beta activity by restoring striatal gamma and theta oscillations which are essential for healthy motor control (Adam et al., 2022).

Info Box 3: Obsessive-compulsive disorder (OCD)

Overview

Obsessive-compulsive disorder (OCD) is a psychiatric disorder, with an average lifetime prevalence of 1.3%. Women have an about 1.6 times higher risk of suffering from OCD in their lifetime (Fawcett et al., 2020). Symptoms can manifest in childhood or adulthood, with the greatest severity of symptoms in the second decade, and are often comorbid with other psychiatric disorders and symptoms (reviewed by Graybiel & Rauch, 2000). OCD is considered a hereditary disease, likely associated with several genetic alterations that are shared with other psychiatric disorders like Tourette syndrome (reviewed by Bokor & Anderson, 2014; reviewed by Graybiel & Rauch, 2000; reviewed by Nicolini et al., 2009).

Symptoms

OCD is characterized by obsessions and compulsions, that is, the presence of recurrent and persistent thoughts and urges that are unwanted and intrusive to the suffering person, causing anxiety. The individual subsequently attempts to ignore these obsessions or feels the need to perform certain stereotypical actions or mental operations to relieve anxiety and tension. Severely affected patients spend large portions of their days (at least one hour) performing ritualistic and repetitive behaviors and mental acts, such as cleaning, ordering, or praying, strictly sticking to rules pertaining to these actions, effectively keeping them from living a normal life (American Psychiatric Association, 2013; Voderholzer et al., 2022). The type of obsessions, as well as associated compulsions, can vary greatly across patients, with examples including obsessing about germs, the order of things, religion, and fear of harming others (reviewed by Bokor & Anderson, 2014). Importantly, the compulsions do not actually resolve the obsessions and are markedly excessive (American Psychiatric Association, 2013).

Pathology

The OCD pathology is hypothesized to arise from altered communication patterns across the fronto-striatal network, connecting associative limbic regions in the cortex, such as the anterior cingulate cortex (ACC) and the orbitofrontal cortex (OFC), to the BG. These structures have previously been implicated in stimulus evaluation, executive functioning, and habit learning and performance, and are therefore functionally relevant to the formation of dysfunctional habits. On a theoretical level, patients might become "stuck" in a single behavioral program due to repetitive action selection and overstabilization of current behavior, leaving them unable to shift to the next one, with these processes which normally run automatically becoming increasingly conscious. The complex pathology observed in patients likely arises from changes in both low and high frequency bands within the cortical-BG network, combining alterations in both the cognitive (intrusive thoughts) and motor (repetitive actions) functions of the BG (Bastin, Polosan, Piallat, et al., 2014; reviewed by Graybiel & Rauch, 2000), though it should be noted that oscillatory dysfunction is only one of several possible mechanisms underlying the disorder.

Treatment

Psychotherapy, such as exposure and response intervention, a type of cognitive behavioral therapy, and Serotonin reuptake inhibitors (SSRIs), are the first line of treatment of OCD (reviewed by Bokor & Anderson, 2014). The effectiveness and safety of SSRIs are established but a subset of OCD patients, approximately 40 to 60%, do not initially or satisfactorily respond to SSRIs, rendering new avenues of treatment development necessary. Examples are pharmacological treatments targeting neurotransmitters other than Serotonin, such as dopamine, as well as transcranial magnetic stimulation, electroconvulsive therapy, and DBS (reviewed by Bokor & Anderson, 2014; reviewed by van Roessel et al., 2023). The regions targeted most commonly by DBS include the anterior limb of the internal capsule, the ventral striatum and the nucleus accumbens (NAc; reviewed by Raviv et al., 2020). Due to its connections to cortical limbic/associative structures and association with repetitive cognitive operations, the STN has gained growing interest as a target for DBS in OCD (Burbaud et al., 2013; reviewed by Chabardès et al., 2013). As in PD, the mechanisms underlying the symptom-reducing effects of DBS remain poorly understood (Schwabe et al., 2021), though the effectiveness of DBS of the NAc (Denys et al., 2010) and the STN (Mallet et al., 2008) in OCD, is well-established. Of note, many patients do not receive treatment at all, possibly for fear of the stigma associated with the disease, leading to feelings of shame and reluctance to seek psychiatric help (Werner, 2019).

1.4.3. The role of neural oscillations in OCD

While progress has been made in understanding the role of neural oscillations, including beta oscillations, in the BG and cortico-BG networks in OCD, the evidence base remains relatively limited compared to PD (Horn et al., 2025). This is likely because DBS has only recently emerged as a treatment for OCD. Collectively, research suggests that OCD is characterized by overconnectivity in areas spanning the prefrontal cortex (PFC), including the OFC, as well as the STN, the putamen, and the ACC (Qing et al., 2021; Wojtecki et al., 2017), correlating with symptom severity (Beucke et al., 2013; Smith et al., 2020). Especially the theta band has been identified as a possible biomarker for OCD. Compared to healthy controls, theta and delta power have been demonstrated to be increased in OCD patients in various brain regions, including medial and lateral frontal, temporal and parietal cortices, the ACC, and other limbic structures (Desarkar et al., 2007; Kopřivová et al., 2011; Lee et al., 2023; Perera et al., 2023). In contrast, there is research suggesting that theta band activity is actually lowered in the parietal lobe, and that theta and gamma phase synchrony is decreased in limbic cortical regions, the OFC, and the insula compared to healthy controls (Koh et al., 2018). Similarly puzzling, studies have reported both increases (Bastin, Polosan, Piallat, et al., 2014) and decreases (Rappel et al., 2018) of STN theta activity during the spontaneous emergence of OCD symptoms. Thus, while changes in theta band activity are consistently detected in OCD patients, the direction of change is not yet clear.

The role of beta oscillations has not been studied extensively in OCD patients. One study reported a tendency towards reduced beta and alpha phase synchrony in cortical limbic structures (Koh et al., 2018), and another found decreased beta and gamma power in the right STN during spontaneous OCD symptoms (Bastin, Polosan, Piallat, et al., 2014). Although the precise pathological alterations of subthalamic beta activity in OCD remain unclear, beta oscillations are reliably observed in the STN of OCD patients (Accolla et al., 2016; Rappel et al., 2018; Wojtecki et al., 2017). Research suggests that in OCD, the dorsal motor region of the STN displays beta oscillations similar to those seen in PD. However, unlike PD, OCD is also characterized by elevated theta activity in the ventral cognitive-limbic region of the STN (Rappel et al., 2018). Additionally, resting-state beta coherence between the non-motor STN and the sensorimotor cortex has been documented in a single patient (the same patient as in **Study 2** of this work), suggesting that beta oscillations in cortico-BG pathways are not exclusively related to PD (Wojtecki et al., 2017).

1.4.4. The influence of DBS on neural oscillations in OCD

DBS is a new promising treatment for the symptoms of treatment-refractory OCD. Though not yet fully understood, the mechanism of DBS may lie in restoring physiological patterns of communication between structures of the cortico-striatal pathway (Figee et al., 2013; Smolders et al., 2013). Conceptually, the normalization of fronto-striatal loop activity resolves the excessive, repetitive cognitive processing style which is characteristic of OCD patients, towards goal-directed behavior (Figee et al., 2013). While this general hypothesis appears to be widely accepted, the exact neurophysiological correlates remain debated and research findings vary greatly across studies, as well as data recording and analysis methods. A recent analysis of 19 OCD patients

implanted with DBS electrodes into the STN revealed that symptom optimization through DBS specifically involved the ventromedial PFC and ACC (Hollunder et al., 2024). Some studies suggest that the normalization of the overconnectivity within the fronto-striatal loop works through a reduction of theta phase stability, which is associated with symptom reduction (Figee et al., 2013; Smolders et al., 2013). Furthermore, DBS has been demonstrated to reduce theta activity in the stria terminalis/anterior limb of the internal capsule, while activity in other frequency bands, i.e. alpha, beta and gamma, was enhanced in this area and the frontal cortex (Schwabe et al., 2021; Xiong et al., 2023).

Notably, the exact DBS-induced changes of oscillations in the theta range and other frequency bands appear to be dependent on the duration of DBS at the time of measurement. Contrary to the findings above, one study indicated that DBS acutely increased theta power and theta phase stability in lateral frontal and temporo-parietal regions, while the opposite was found for long-term stimulation (Bangel et al., 2023; Smolders et al., 2013). Similarly, theta to beta frequency band activity was increased in the NAc/internal capsule immediately after surgery, but decreased during chronic DBS (Xiong et al., 2023). In rodents, DBS of the NAc also resulted in reduced power in low frequency bands up to the beta band (Shi et al., 2022).

2. Aims

Most previous studies assessing movement-related neural oscillations in cortico-BG loops have utilized simple motor paradigms, involving discontinuous movements, such as button presses (Alegre et al., 2013; Aron & Poldrack, 2006; Cao et al., 2024; Ray et al., 2012). Additionally, most studies did not consider both cortical and subcortical structures of the motor system, although their interplay is likely the cornerstone of motor performance. Lastly, movement-related beta oscillations and their sensitivity to DBS are typically studied in PD patients, such that their dynamics in other disorders, which do not primarily involve motor dysfunction, remain elusive.

In order to address these gaps in the literature, the present thesis took advantage of simultaneous MEG and LFP recordings to study the association of beta power and coherence with complex movement in PD, as well as with motor inhibition and DBS in OCD, a disorder which is not primarily characterized by motor dysfunction.

Aims of Study 1: To investigate the role of beta oscillations across cortico-BG loops in the coordination of complex movement involving rapid changes of movement direction that were either easy to predict or unpredictable. As such, the sensitivity of beta oscillations to cognitive demands beyond mere motor processing was assessed.

Aims of Study 2: To evaluate the effect of DBS on beta oscillations in OCD, a disorder not marked by motor dysfunction. Additionally, beta dynamics during a Go/NoGo task involving the inhibition of prepotent motor responses were assessed in an OCD patient and compared to a PD control patient to pinpoint differences in motor control and inhibition across these disorders.

3. Study 1: Context-dependent modulations of subthalamo-cortical synchronization during rapid reversals of movement direction in Parkinson's Disease

Study 1 (Appendix 1) aimed at investigating beta oscillatory activity across the cortico-BG network during complex movement with varying levels of cognitive challenge. Previous research has established a role of beta oscillations in movement and the inhibition thereof (Benis et al., 2014; Jurkiewicz et al., 2006; Wessel, 2020). Specifically, paradigms involving simple movements, such as button presses, revealed that beta power decreases during movement and its preparation (Jurkiewicz et al., 2006), but increases during movement inhibition (Bastin, Polosan, Benis, et al., 2014) and rises above baseline level after movement has terminated (Fonken et al., 2016; Ray et al., 2012). Beta oscillations have thus been described as anti-kinetic (Brown, 2003), or, alternatively, as reflecting the status quo of the motor system (Engel & Fries, 2010). However, the dynamics of beta oscillations during movement scenarios which are more complicated than typically studied in simple motor paradigms, such as stop signal reaction time tasks, have rarely been investigated. The present study was intended to close this gap with a paradigm involving the continuous rotation of a wheel with occasional changes in movement direction, as well as stops of movement. Although movement-related beta suppression around movement initiation and the beta rebound after movement termination have been described in countless studies, the interaction of these processes during short breaks of movement, such as during directional changes, remain unknown. One of the major goals of the present study was therefore to assess whether short pauses of movement differ from the final termination of movement with respect to beta band activity in the motor system.

Recent evidence indicates that the beta band is not merely motor-related (Benis et al., 2014; Oswal et al., 2013). Instead, modulations of beta power have been observed during cognitive tasks in the absence of movement (Zavala, Jang, et al., 2017). How cognitive challenge in the context of a complex motor paradigm might modulate beta oscillations within cortical-BG loops has, however, not been investigated thus far. Thus, the present study aimed at revealing the sensitivity of beta oscillations to varying levels of predictability of movement instructions in the context of continuously performed movement.

Methods 3.1.

23 PD patients who remained on their regular dopaminergic medication participated in the study, 20 of whom were included in the analyses. Whole-head MEG and LFPs from the STN were recorded simultaneously peri-operatively using externalized leads. While seated in the MEG, patients performed a visually cued motor task, requiring them to start turning a wheel, change movement direction, and stop. In the so-called *predictable condition*, the timing and order of start, reversal, and stop cues were kept constant, such that the next movement prompt was easily anticipated. In a more challenging unpredictable condition, the timing of cues, as well as the

number of reversal cues (changes of movement direction) was manipulated to be unpredictable, i.e. varying between 0 and 2 reversals per trial.

The data was first segmented into trials of 4 s and centered around the movements of interest, i.e. start, reversal, and stop. For the analysis of cortical power and STN-cortex coherence, four cortical regions of interest (ROIs) were selected based on the strongest movement-related modulations of beta power and coherence: M1 and the medial sensorimotor cortex (MSMC) both contralateral and ipsilateral to the moving hand. An LCMV beamformer was used to extract the time series for these ROIs. Subsequently, the cortical ROIs and one STN LFP channel from each hemisphere per patient were included in time-resolved analyses of power and coherence for the beta and gamma frequency ranges. As baseline, the pre-event time window (-1.6 s to 0 s with respect to start, reversal, and stop) was used. The coherence analysis was supplemented with an analysis of Granger causality to determine the directionality of cortex-subcortex interaction. Beta power and coherence were additionally analyzed at the source level using DICS. For the statistical analysis of task performance, power, connectivity, and lateralization (of beta suppression and rebound), specifically with respect to the predictability of movement instructions, repeated measures analyses of covariance and cluster-based permutation tests were conducted.

3.2. Results

3.2.1. Movement-related power dynamics

First, it was confirmed that movement initiation and termination were associated with cortical and subcortical beta suppression and rebound, respectively. Gamma power showed opposite dynamics. During the re-acceleration phase after reversals of movement direction, cortical beta power decreased briefly, especially in the hemisphere ipsilateral to the moving hand. The contralateral hemisphere, in contrast, was already close to floor levels of beta power prior to reversing, such that beta power did not decrease much more. Further analyses revealed that movement-related beta oscillations were generally lateralized to the hemisphere contralateral to the moving hand, except during acceleration, which involved bilateral modulation of beta power. Surprisingly, no increases in cortical beta power occurred during reversals, even though movement was first slowed and then stopped briefly. The STN revealed dynamics that differed from those observed in cortex: Although average power changes across patients were small and not statistically significant, many patients displayed transient increases in high beta power during reversals. These brief modulations differed from the post-movement beta rebound both spectrally and in amplitude (see Figure 6).

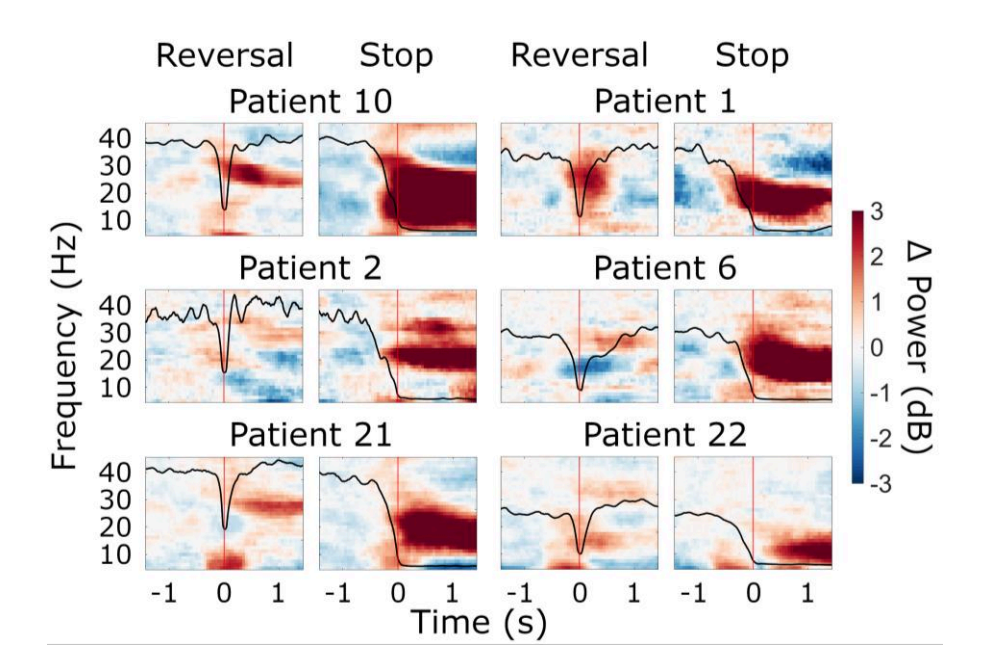


Figure 6. Reversal-related beta power modulations in the STN. Displayed are six examples of baselinecorrected STN beta power from individual patients during movement reversal and stopping (baseline: -1.6 to 0 s with respect to stop/reversal). Time point 0, marked by red lines, indicates the brief movement pause associated with reversals, and movement stop. Black lines represent the patient's trial-average turning speed (scale: 0-600 deg/s; for patient 21, adjusted to 0-750 deg/s). Patient 10: contralateral STN, predictable condition; Patient 1: contralateral STN, unpredictable condition; Patient 2: contralateral STN, predictable condition; Patient 6: ipsilateral STN, unpredictable condition; Patient 21: contralateral STN, unpredictable condition; Patient 22; ipsilateral STN, unpredictable condition (adapted and modified from Winkler, Butz, et al., 2025, under the Creative Commons Attribution 4.0 International License (CC BY 4.0)).

3.2.2. Movement-related connectivity dynamics

Coherence dynamics were similar to those of power with respect to movement-related beta suppression, post-movement beta rebound, and gamma increases at movement initiation. In contrast to cortical beta power, beta coherence was not reduced during reversals. In fact, it increased on a qualitative basis (see Figure 7a). Across all movement types and predictability conditions, a strong drive from cortex to the STN was identified.

3.2.3. The influence of predictability on power and coherence dynamics

In general, coherence modulations (i.e. differences between the pre- and post-event time windows) were more positive in the unpredictable condition, suggesting a reduced suppression following movement initiation and greater increases in coherence following stop and reversal in this condition (see Fig. 7a and b). Similarly, beta power was less reduced at movement initiation in the unpredictable compared to the predictable condition. Gamma power and coherence did not reveal any predictability-dependent changes.

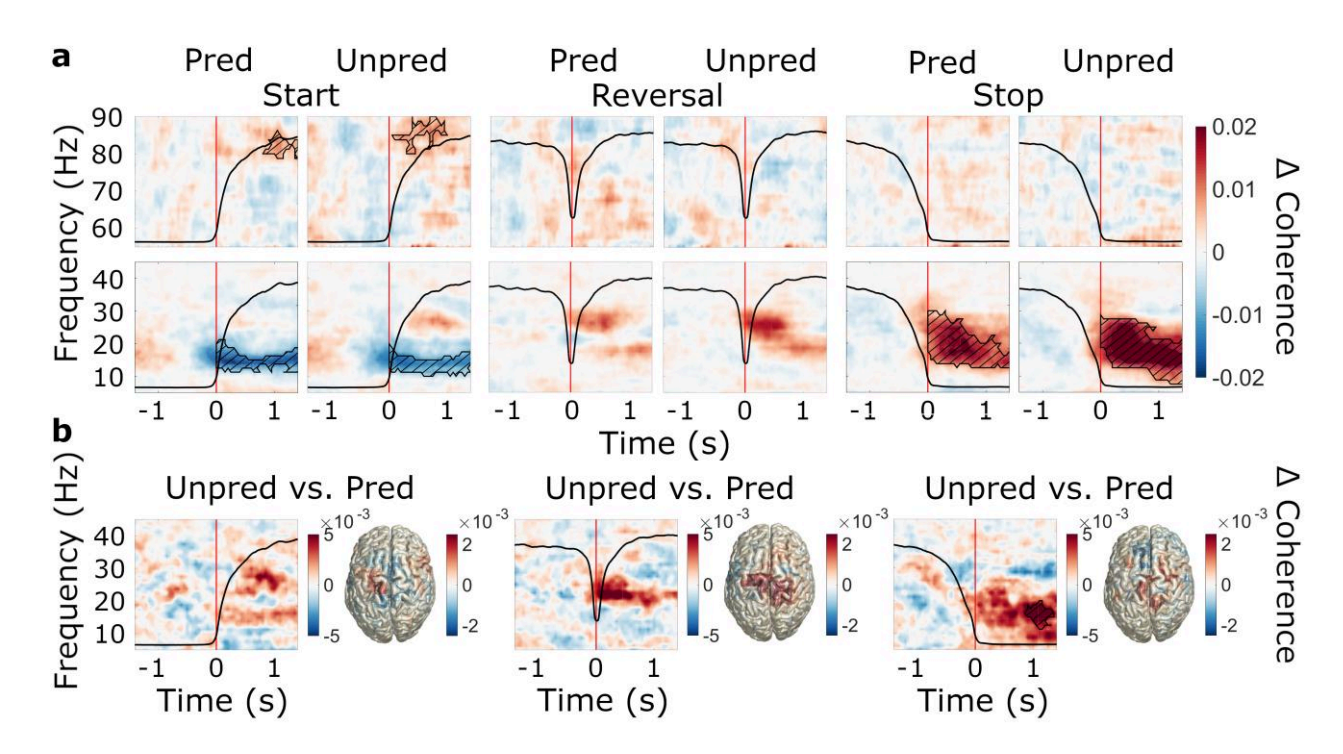


Figure 7. Movement and predictability-related modulations of STN-Cortex Coherence. (N=20) (a) Timefrequency plots illustrate group-averaged, baseline-corrected coherence between the STN and cortex (averaged across ROIs) during start, reversal, and stop of movement for both predictable and unpredictable trial types (baseline: -1.6 to 0 s with respect to start, stop, and reversal). Time point 0 indicates when the movement began, was reversed, and stopped (marked by red lines). The overlaid black lines indicate average wheel turning speed (range: 0-600 deg/s). Regions enclosed by black contours with hatched lines denote statistically significant deviations from baseline coherence. (b) Group-level comparison of coherence between the unpredictable and predictable condition. Left: time-frequency contrasts are shown, averaged across ROIs. Right: source-level differences in event-related coherence modulations within the beta frequency range are displayed (reproduced from Winkler, Butz, et al., 2025, under the Creative Commons Attribution 4.0 International License (CC BY 4.0)).

3.3. **Discussion**

Study 1 revealed the emergence of movement-related beta suppression, movement-related gamma synchronization, and a post-movement beta rebound in both power and coherence in the context of continuously performed movement. Additionally, decreases in gamma power upon movement termination were identified. Previous research has only discovered these modulations during simple, ballistic movements (Alegre et al., 2013; Litvak et al., 2012; Talakoub et al., 2016; Tan et al., 2014; van Wijk et al., 2017). The post-movement increase in beta coherence is particularly interesting, because it has rarely been described before (Tan et al., 2014). Notably, a strong cortical drive was identified across all movements. Together with the proposed role of the STN in movement inhibition (Benis et al., 2014; Ray et al., 2012) and recent evidence of monosynaptic connections between the frontal cortex and the STN (W. Chen et al., 2020; Oswal et al., 2021), it can be speculated that the increase in coherence after movement termination reflects a post-movement feedback signal from motor cortex to the STN.

Furthermore, Study 1 sheds light on the neural basis of changes of movement direction which contain a brief pause of movement. First, broadband reversal-related decreases of beta power in motor cortex were shown. The timing of these decreases, i.e. after the short pause, and the spatial

distribution involving bilateral motor cortices, strongly suggest a role of cortical beta suppression in movement acceleration after short pauses. In line with the bilateral topography of the observed beta suppression, previous research supports a more spatially diffuse organization of movementrelated beta power suppression as compared to the beta rebound (Espenhahn et al., 2017; Jurkiewicz et al., 2006; Zaepffel et al., 2013). Importantly, there was no evidence of elevations of beta power during reversals in motor cortex, suggesting that motor cortical beta power may not primarily be involved in stopping continuous movements. In contrast, the STN revealed brief increases in beta power in the STN in many patients, likely reflecting processing of the short pause that occurs during reversals. These increases were observed in the high beta band and were of rather low amplitude, therefore differing from the strong post-movement beta rebound after movement termination, which predominantly involved the low beta band. Beta oscillations have often been described as anti-kinetic (Chandramouli et al., 2019) because they may increase reaction times (Muralidharan & Aron, 2021) and decrease corticospinal excitability (Wessel et al., 2016). Therefore, avoiding a beta rebound mid-action might be vital to the recontinuation of movement after changing movement direction. In summary, it can be suggested that the beta rebound occurs only after movement has fully terminated, rendering a role in movement slowing or inhibition unlikely. The presented findings better align with the interpretation of the beta rebound as a post-movement feedback signal used to adapt or confirm a current motor program (Cao & Hu, 2016; Tan et al., 2016).

The ability to predict the next movement instruction was of particular interest to Study 1. Greater increases and smaller decreases of coherence in the unpredictable condition suggest that additional neural resources were needed to accommodate a more careful and attentive approach to the task whilst maintaining a task performance comparable to the predictable condition. This finding is in line with research positing a role of beta oscillations in cognitive processes, such as cognitive inhibition and error monitoring (Castiglione et al., 2019; Fonken et al., 2016; Schmidt et al., 2019; reviewed by Turner & Desmurget, 2010). Increased levels of beta coherence were previously demonstrated in a task involving conflict (Patai et al., 2022), which may have been associated with similar cognitive processes. The reduced beta power suppression observed during unexpected movement initiation may indicate that patients were less prepared to move, which is supported by research reporting similar reductions of beta suppression in the face of uncertainty and unpredictability in simpler motor paradigms (Alegre et al., 2003; Tzagarakis et al., 2010).

3.4. Conclusion

In summary, **Study 1** revealed distinct changes in local power and STN-cortex connectivity during complex movement and changes thereof. Briefly stopping a movement mid-action appears to involve different oscillatory processes than fully terminating a motor sequence. When effective preparation and anticipation of motor commands is hampered, STN-cortex synchronization increases, suggesting a role of cortico-subcortical motor pathways in coordinating movements in response to unpredictable events.

4. Study 2: Deep brain stimulation-responsive subthalamocortical coupling in obsessive-compulsive disorder

Study 2 (Appendix 2) aimed at evaluating the sensitivity of beta oscillations to DBS in OCD, a psychiatric disorder not characterized by motor dysfunction. Brain alterations in OCD include hyperconnectivity within fronto-BG circuits (Beucke et al., 2013; Smith et al., 2020), with elevated theta activity serving as a possible biomarker (Bastin, Polosan, Piallat, et al., 2014; Lee et al., 2023; Perera et al., 2023; Rappel et al., 2018). DBS has been reported to reduce theta activity in OCD (Figee et al., 2013; Schwabe et al., 2021). In contrast, pathologically enhanced beta oscillations are often described as the hallmark of PD (Brown et al., 2001; Hirschmann et al., 2011; Oswal et al., 2021) and have been linked with various PD-specific motor symptoms, including bradykinesia and rigidity (Kühn et al., 2009; Lofredi et al., 2019). DBS has been found to normalize excessive beta activity in cortico-BG loops in PD, which is associated with a reduction of symptom severity (Abbasi et al., 2018; Y. Chen et al., 2020; Mathiopoulou et al., 2024; Muthuraman et al., 2020; Wilkins et al., 2024), suggesting a direct link between STN beta oscillations and motor slowing.

However, beta oscillations and the influence of DBS on oscillatory activity are typically studied in PD patients, as DBS is a standard treatment for PD. In OCD, the role of beta oscillations remains poorly understood. Some studies have identified beta abnormalities in the STN (Bastin, Polosan, Piallat, et al., 2014) and cortex (Koh et al., 2018), and DBS has been reported to increase (Schwabe et al., 2021) and diminish (Xiong et al., 2023) beta oscillations across the stria terminalis, anterior limb of the internal capsule, and frontal cortex. However, the effect of DBS on beta activity in the STN, despite its documented presence (Rappel et al., 2018; Wojtecki et al., 2017), remains elusive in OCD, a gap in the literature that Study 2 was intended to fill.

The focus on PD patients in most prior studies on motor control further presents a significant limitation for understanding the dynamics of beta oscillations in cortico-BG loops during movement and motor inhibition. Previous research has revealed that the beta band is modulated by various movement-related parameters (Benis et al., 2014; Fischer et al., 2019; Fischer et al., 2016), as well as by movement initiation, termination, and inhibition (Alegre et al., 2004; Bastin, Polosan, Benis, et al., 2014). Study 2 was intended to assess the effect of movement and the inhibition thereof on neural oscillations in motor cortex and the STN in a rare case of an OCD patient receiving DBS, and to compare these patterns to a PD patient to pinpoint possible disease-specific differences in these modulations.

4.1. Methods

Study 2 involved a single case of severe OCD: a 53-year-old female patient implanted with DBS electrodes targeting the STN 12 years ago. At that time, she participated in a research study in which LFPs were recorded using externalized leads (Wojtecki et al., 2017). She took part in Study 2 following the replacement of her original stimulator with a new device. The Medtronic Percept PC (Medtronic Inc., Minneapolis, MN, USA) is capable of recording LFPs from the implanted electrodes. LFPs and whole-head MEG were measured simultaneously. 5-minute resting-state recordings were performed in DBS OFF and during unilateral stimulation at 130 Hz in each hemisphere (amplitude: 1.2 mA; pulse width: 60 µs).

Additionally, the patient performed a visually cued Go/NoGo task that assesses the ability to inhibit prepotent responses. In this task, each trial was initiated with a fixation cross presented on screen. Next, a cue appeared indicating whether the target stimulus was more likely to be Go or NoGo, followed by the Go or NoGo stimulus, and feedback. In case of a Go stimulus, the patient had to push a button with the right index finger. In case of a NoGo stimulus, any response had to be withheld. Trials were labeled as congruent if the cue matched the target, and incongruent, if it did not. No stimulation was applied during the task. One 60-year-old female tremor-dominant PD patient implanted with the same DBS system targeting the STN participated in the Go/NoGo task as a control.

To analyze the resting-state data, the data was segmented into non-overlapping trials of 1 s, and spectral power, LFP-MEG coherence and STN-cortex source-level coherence using DICS were computed. To obtain an unbiased estimate of STN power, oscillatory components were first separated from the aperiodic background as it can obscure or inflate power estimates by contributing non-rhythmic activity (Donoghue et al., 2020). For the analysis of the Go/NoGo task data, trials were centered on the Go/NoGo target stimulus. Time-frequency analysis was performed considering the STN and activity extracted from bilateral M1 using an LCMV beamformer. Averaged power over all trial types and time points was used as baseline. Congruent and incongruent trials were pooled given a lack of statistically significant differences between them. Statistical comparisons between DBS ON vs. DBS OFF and Go vs. NoGo trials were performed using cluster-based permutation tests.

4.2. Results

4.2.1. The influence of DBS on beta power and coherence in OCD

Prominent peaks of resting-state beta power in the right STN and coherence between the right STN and the sensorimotor cortex were observed in the OCD patient. These peaks were significantly reduced by DBS of both the left and right STN (see Figure 8).

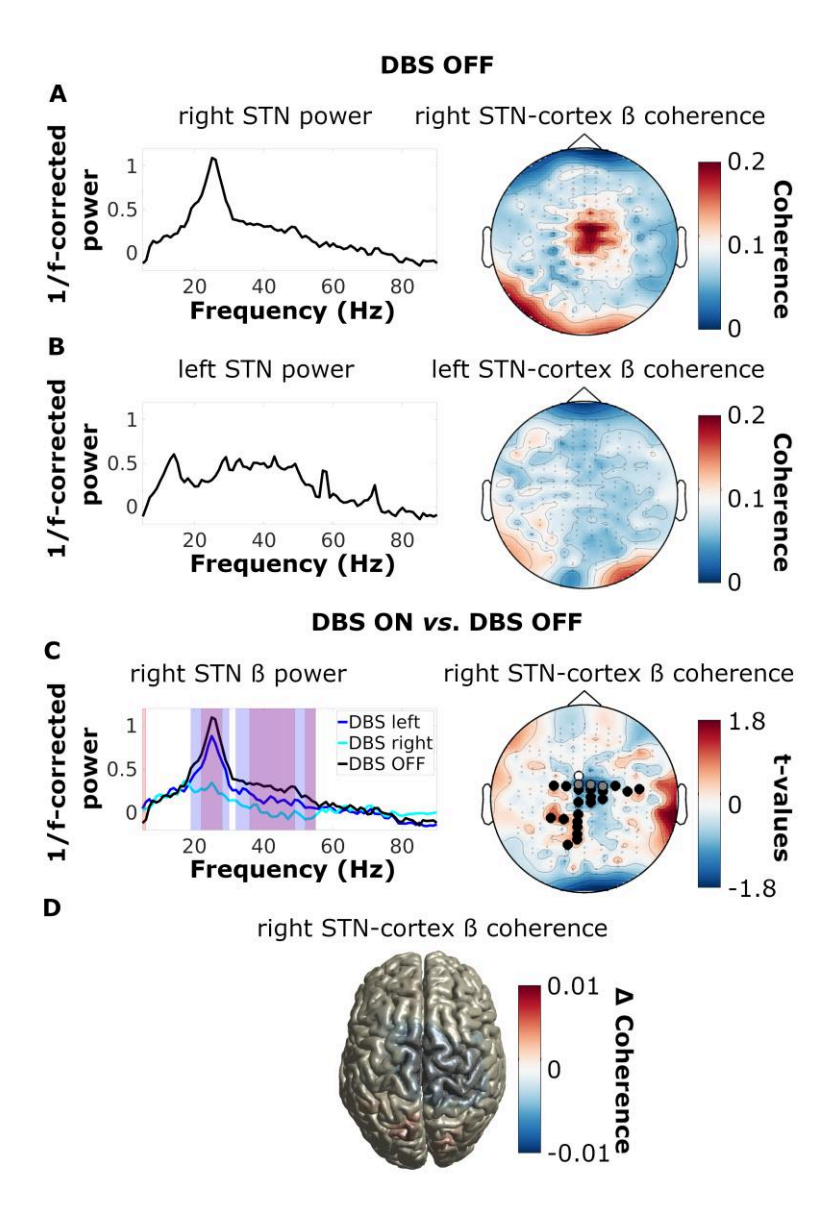


Figure 8. DBS attenuates beta power and coherence in the OCD patient. Shown are the log10-transformed resting-state power spectra (with aperiodic fit removed) and the topographical distribution of STN-MEG sensor coherence in the beta range (13-30 Hz) for the right (A) and left (B) STN, respectively. (C, left) Log10-transformed resting-state power spectra (with aperiodic fit removed) are depicted for the right STN across three conditions: DBS OFF, right DBS ON, and left DBS ON. Shaded areas indicate significant differences: right DBS ON vs. OFF: blue; left DBS ON vs. OFF: red; overlapping clusters: purple. (C, right) Topography of right STN-MEG sensor coherence during right DBS ON vs. OFF and left DBS ON vs. OFF. Channels that are significantly modulated are highlighted: right DBS: black; left DBS: white; overlap: grey. (D) The bottom panel represents the source-reconstructed contrast between DBS ON (averaged over left and right DBS) and DBS OFF conditions (reproduced from Winkler, Werner, et al., 2025, under the Creative Commons Attribution 4.0 International License (CC BY 4.0)).

4.2.2. Modulations of beta and theta power during a Go/NoGo task

In both the OCD and PD patient, Go-trials were associated with beta power suppression and a beta rebound in M1. In the OCD patient, the movement-related suppression of cortical beta power was interrupted by an early beta power increase during NoGo trials, clearly distinguishing response execution from inhibition. Patterns of cortical beta power modulation were generally rather similar across patients. However, on the level of the STN, power modulations differentiated PD and OCD: The PD patient revealed modulations of the beta frequency band only. Specifically, Go-trials were associated with similar power changes as observed in M1. NoGo trials were linked with increases in beta power. In the OCD patient, a different picture emerged: Differences between Go and NoGo trials were limited to the theta band, with NoGo trials revealing higher theta power than Go-trials (see Figure 9).

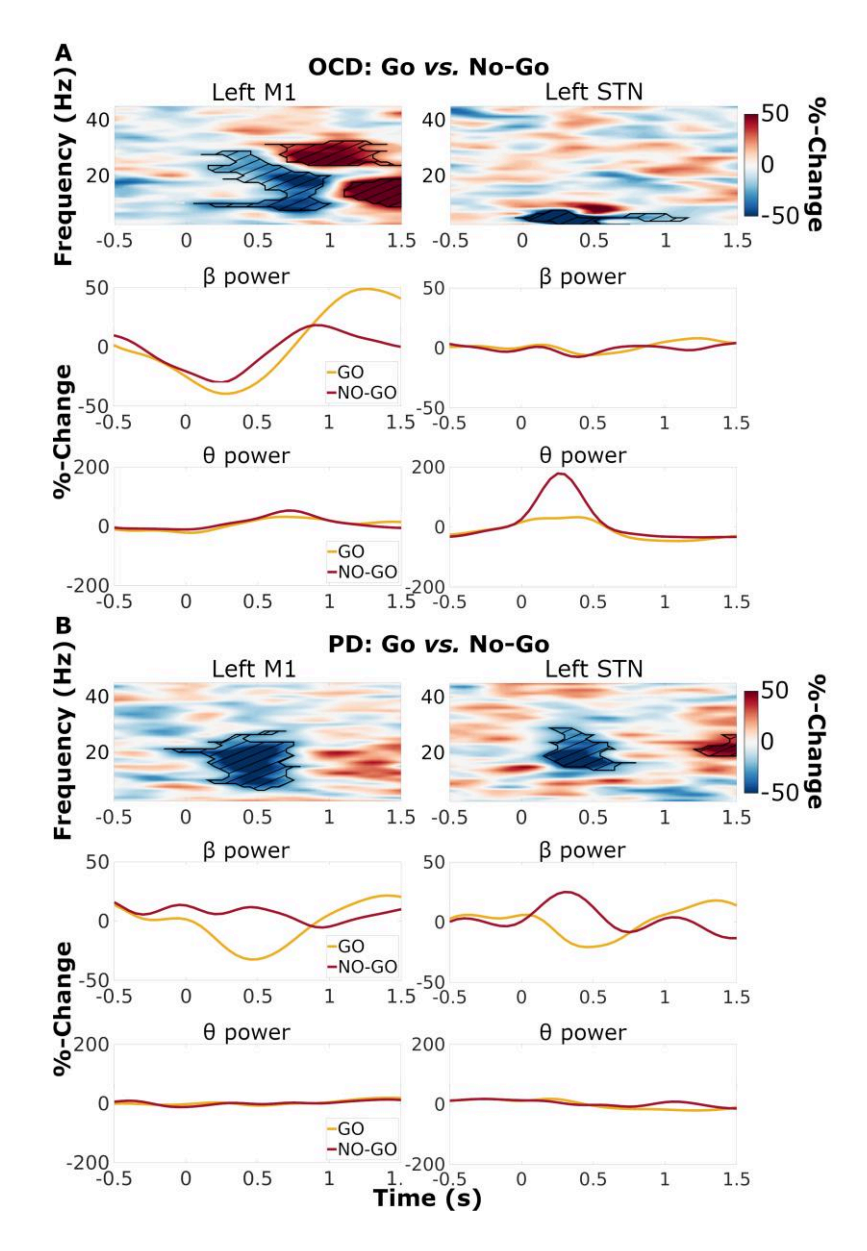


Figure 9. Distinct patterns of left STN power modulation during response inhibition in OCD and PD. Trials are centered on the Go/NoGo target stimulus. Left-sided modulations are shown as both patients used the right hand for the task. Top: Time-frequency representations show the difference in power between baselinecorrected Go (% change) and baseline-corrected NoGo (% change) trials (pooled over congruent and incongruent trials) for the OCD (A) and the PD (B) patients. Hatched lines within contours reflect statistically significant differences. Bottom: Time-resolved band-average power changes in the beta (13-30 Hz) and theta (3–8 Hz) ranges (reproduced from Winkler, Werner, et al., 2025, under the Creative Commons Attribution 4.0 International License (CC BY 4.0)).

4.3. Discussion

While DBS-induced reductions of beta power and coherence have consistently been associated with motor symptom improvement in PD (Abbasi et al., 2018; Y. Chen et al., 2020; Mathiopoulou et al., 2024; Muthuraman et al., 2020; Wilkins et al., 2024), Study 2 revealed similar effects of DBS on power and coherence in a single case of OCD in the absence of motor impairment. These findings challenge the assumption that a decrease in beta oscillations associated with DBS is exclusively linked with the alleviation of motor symptoms. In fact, DBS-responsive resting-state peaks of STN beta power and STN-cortex beta coherence are not necessarily markers of PD or motor dysfunction. Instead, they may reflect broader physiological functions of the STN (Accolla et al., 2017), such as somatosensory processing (reviewed by Barone & Rossiter, 2021). Alternatively, given that the STN integrates cognitive, limbic, and motor processes (Accolla et al., 2017) and exhibits beta oscillations in both motor (Rappel et al., 2018) and non-motor (Accolla et al., 2016; Wojtecki et al., 2017) regions, DBS-responsive beta oscillations might reflect a shared characteristic of PD and OCD, possibly related to high levels of inhibition due to neurodegeneration in the case of PD, and to cognitive processes linked with the inhibition of compulsions in OCD.

Although resting-state beta oscillations and their modulation by DBS in OCD did not markedly differ from what is known from PD patients, motor task-based modulations of neural oscillations revealed possible disease-specific differences. Modulations of STN power during NoGo trials peaked in the beta band for the PD patient, and in the theta band for the OCD patient. Altered theta band activity has previously been connected with OCD (Bastin, Polosan, Piallat, et al., 2014; Rappel et al., 2018). Additionally, the theta band has been implicated in cognitive processes related to conflict (Zavala et al., 2013). Enhanced theta activity during NoGo trials could therefore reflect OCD-specific symptoms, such as the inability to inhibit actions and manage conflict. In contrast, modulations within the beta band in PD could be associated with the PD-specific overactivity of STN-cortex loops, possibly resulting from an over-activation of the STN by cortex (Oswal et al., 2021).

4.4. Conclusion

In summary, Study 2 suggests that resting-state beta oscillations across cortico-BG loops and their modulation by DBS are not specific to PD or motor dysfunction. Motor task-related modulations of STN power might be more suited to reveal differences between diseases: trials involving the inhibition of a prepotent response were associated with modulations of beta power in PD, and theta power in OCD, possibly reflecting disease-specific neurophysiological alterations.

5. General discussion

The present thesis aimed at assessing the association of neural oscillations, particularly within the beta range, with movement scenarios marked by complex motor and cognitive demands. Moreover, the goal was to evaluate the modulation of beta oscillations by both DBS and movement execution vs. inhibition in OCD, a disease not marked by motor impairment. The following sections will discuss the merits and limitations of the presented studies. Recommendations to address the limitations will be outlined in the **Outlook**.

5.1. Merits

Both presented studies capitalized on the rare opportunity to simultaneously record cortical and subcortical oscillatory activity, which is only possible in humans undergoing DBS surgery. As such, this thesis delivers important contributions to the study of motor network-wide neural signals. Beyond their scientific value, the presented findings may aid the development of closed-loop DBS systems which rely on the identification of oscillatory markers of specific movement parameters. Finally, a thorough understanding of the effects of DBS across different disorders can ultimately help disentangle its underlying mechanisms and contribute to characterizing the pathological oscillatory changes associated with these diseases.

One of the main merits of Study 1 was revealing the specialized dynamics of neural oscillations within the STN, motor cortical areas, and the interaction between these structures during ongoing movement and the adaptation of these mechanisms to a changing environment. The motor task in Study 1 differed from paradigms typically employed when studying motor control in two ways: First, movement was performed in a continuous fashion, involving rapid mid-action changes of the movement. Second, patients had to adapt to contexts of varying cognitive complexity. This way, Study 1 could illuminate some of the more intricate aspects of motor control and might more closely reflect behavior as it occurs in everyday life.

Study 2 had one key strength: it presented a rare incident of a psychiatric patient receiving DBS, allowing for comparison with a PD control patient and the PD literature. As such, Study 2 revealed that beta oscillations in OCD are decreased by DBS, a phenomenon known from the PD literature. Additionally, Study 2 demonstrated that task-based neural oscillations distinguished better between diseases than resting-state oscillations. Study 2 was further noteworthy in that sensingcapable DBS devices were used to record STN LFPs, such that DBS leads did not have to be externalized. The reported findings are therefore more likely to reflect naturalistic patterns of neural oscillatory activity.

5.1.1. Beta synchronization during cognitive challenge

Critically, this thesis demonstrates that beta oscillations are sensitive to the predictability of sequential movement prompts. Study 1 revealed that synchrony between the sensorimotor cortex and the STN was increased when movement instructions became less predictable, calling for more attentive behavior. Additionally, the beta power suppression at movement initiation was reduced in this condition. With that, existing evidence positing a role of beta oscillations in cognitive processes (Brittain et al., 2012; Castiglione et al., 2019) can be extended to a context of complex movement that involves the active anticipation of the next movement instruction. Importantly, simultaneous measurements of STN LFPs and whole-head MEG allowed the consideration of several hubs of the cortico-BG network and identifying changes in the synchronization between them. While local changes in motor-related beta oscillations have been observed in response to cognitive processes (Fischer et al., 2016; Tan et al., 2016), complex behavior involves the entire cortico-subcortical motor loop, and likely greater inputs from cortical structures, possibly via hyperdirect pathway fibers. Similarly to the results of Study 1, STN-cortex beta coherence has been found to be up-modulated after conflict cues in a judgement task (Patai et al., 2022). Together with these results, Study 1 suggests that cortico-subcortical beta synchronization might be engaged during cognitive processes arising in situations of surprise and uncertainty. Notably, the reported effect of cue predictability fits with the idea of beta oscillations reflecting a closed gate in situations involving conflict or uncertainty (Leventhal et al., 2012), and supporting action inhibition (Benis et al., 2014), thereby avoiding hasty behavioral output in scenarios requiring caution.

5.1.2. Beta rebound signals sequence completion, not temporary halts

Importantly, this thesis revealed that brief stops of movement, as occurring during a change of movement direction, and the termination of a motor sequence have distinct electrophysiological profiles. The post-movement beta rebound has previously been reported in simple motor paradigms (Alegre et al., 2004; Fonken et al., 2016; Fry et al., 2016; Jurkiewicz et al., 2006; Ray et al., 2012), which **Study 1** confirmed with a paradigm of continuously performed movement. A postmovement rebound of coherence was also observed, which has only been reported in a single study following ballistic movements (Tan et al., 2014), and might reflect a post-movement feedback signal from cortex communicated via the hyperdirect pathway. In contrast, mid-action changes and short pauses of movement have rarely been studied before. The few studies which have been conducted presented inconsistent results: Two studies documented no beta rebound in between successive movements (Alegre et al., 2004; London et al., 2021) and one did find a beta rebound (Muralidharan & Aron, 2021). In Study 1, no beta rebound was observed in the STN or motor cortex. Instead, bilateral cortical beta power reductions reflected the re-acceleration of movement, STN power changes were variable, occurring mainly in the high beta range and in lower amplitude, and changes in cortico-subcortical synchrony involved elevations on merely a qualitative level, which were not compatible with a post-movement beta rebound of coherence.

Based on these findings, important suggestions on both the functions of the much-discussed beta rebound and the role of beta oscillations during movement in general, can be made. The results of **Study 1** are mostly in line with the beta rebound reflecting a post-movement feedback signal used to either maintain or update a current motor plan (Cao & Hu, 2016). Importantly, it only emerges once a motor program is fully terminated. It appears to be involved neither in actively stopping an ongoing motion, as this would require its emergence while movement is still in progress, nor in updating current motor programs, such as during reversals of movement direction. The post-movement beta rebound peaked in the low beta band and was strong in amplitude both of these characteristics distinguished it from the modulations of beta power and coherence observed during reversals. First, these were much lower in amplitude and variable across patients. Second, reversal-related beta power increases in the STN peaked in the high beta band. These brief increases in beta activity could be reflective of processing linked with the short pause of movement during reversals. The lack of a modulation in the low beta range suggests that low beta oscillations, in contrast to high beta oscillations, only re-emerge once movement is fully terminated. This observation supports recent research suggesting that high and low beta oscillations subserve distinct functions (Chandramouli et al., 2019; Oswal et al., 2021; Patai et al., 2022). Specifically, the low beta band better reflects the anti-kinetic characteristics often discussed in the context of beta oscillations (Brown, 2003; Muralidharan & Aron, 2021; Wessel et al., 2016). Previous research suggests that beta power must be reduced for movement to start (Heinrichs-Graham & Wilson, 2016; Khanna & Carmena, 2017). Thus, the lower range of the beta spectrum might have to be avoided during movement breaks, particularly when a quick recontinuation of movement is desired.

5.1.3. Beta oscillations are modulated by DBS in OCD

One of the major merits of Study 2 was that LFPs from the STN were measured in a patient not suffering from PD or any other movement disorder. Given that DBS is a standard treatment for PD and PD is a relatively common disorder, most studies reporting on the synchronization dynamics within BG targets and interactions with cortical structures recruited from this patient group only. This complicates the generalizability of findings regarding the mechanisms of DBS, and the role of cortico-BG synchronization in movement and cognition, to patients without motor dysfunction. DBS is still rarely used outside the realm of movement disorders, but OCD is one disease for which DBS has recently been applied. However, the comparability of research on DBS in OCD with studies on PD is limited by the fact that DBS is targeted at various deep brain structures in OCD (reviewed by Raviv et al., 2020), and not primarily at the STN. Even though efforts have been made to compile the results of studies measuring the effects of DBS on neural oscillations in OCD, findings, especially in the beta range, are variable (Horn et al., 2025). Therefore, Study 2 delivers valuable insights into the role of neural oscillations in movement, and the effects of DBS on neural oscillations in cortex and the STN, in OCD. As the STN was the target of DBS in the OCD patient in **Study 2**, direct comparisons with PD were possible.

Study 2 importantly revealed that DBS-responsive resting-state beta oscillations occur in OCD, even though it was demonstrated that the patient did not present with any motor impairment. DBSrelated reductions of STN beta power and STN-cortex beta coherence have thus far been reported for PD only (Oswal et al., 2016), which led to the suspicion that these effects might be specific to PD. The simultaneous improvement in PD-specific motor symptoms further suggested that beta oscillations in STN-cortex loops might be a sign of motor pathology (Abbasi et al., 2018; Y. Chen et al., 2020; Mathiopoulou et al., 2024; Muthuraman et al., 2020; Wilkins et al., 2024). Based on Study 2, these assumptions should be updated: DBS-responsive beta power and coherence are not solely a sign of PD or motor pathology but could indicate physiological processes (Accolla et al., 2017), such as maintaining the current state of cognition and movement (Engel & Fries, 2010). Alternatively, they could reflect overlaps in the PD and OCD pathologies, such as elevated inhibition, stemming from neurodegeneration in the case of PD or deliberate efforts to resist compulsions in the case of OCD.

5.1.4. Beta and theta oscillations distinguish PD and OCD

An important suggestion made by this thesis is that disease-specific modulations of STN power are more readily observed during a task than at rest. In Study 2, trials requiring inhibition were associated with STN power changes in the theta band in OCD, and with changes in the beta band in PD. Several suggestions follow from these observations. First, the theta band might be critically involved in the OCD pathophysiology. Trials involving the inhibition of a prepotent response might be particularly challenging to OCD patients as they tend to present with an over-stabilization of behavior (Bastin, Polosan, Piallat, et al., 2014). The theta band has been implicated in the OCD pathophysiology in previous works (Perera et al., 2023; Rappel et al., 2018) and has been shown to be related to cognitive processes associated with conflict (Zavala et al., 2013). Its involvement in a task requiring behavioral inhibition after the presentation of possibly conflicting cues is therefore not surprising. Second, given that the OCD patient did not reveal any modulations of STN beta band activity during trials requiring inhibition, it is unlikely that this signal represents a physiological mechanism, but rather reflects the pathological overactivity of beta oscillations in PD. Lastly, Study 2 suggests that task-based modulations may be better suited to distinguish different diseases at the oscillatory level than resting-state oscillations. Possibly, disease-related behavioral impairments (i.e. compromised motor control, difficulties with conflict resolution etc.) have to be actively engaged during a task in order to reveal the underlying pathologically altered neural activity and the brain areas involved. This is consistent with findings from functional MRI studies indicating that task-based connectivity captures more behaviorally relevant information than resting-state connectivity (Elliott et al., 2019; Zhao et al., 2023).

5.2. Limitations

While both studies presented in this thesis demonstrate significant advancements in the field, limitations, including reduced generalizability of the presented findings resulting from the specific patient sample, as well as small sample sizes, should be considered.

5.2.1. Generalizability beyond Parkinson's disease

Study 1 bears the obvious limitation that neural oscillations were recorded in PD patients, possibly limiting the generalizability of its results to healthy individuals. Given that one of the main goals of Study 1 was to understand complex movement under cognitive challenge in general, rather than just in PD patients, its results have to be interpreted with caution. Even though patients were on their usual medication regimen, which should normalize oscillatory activity (Brown et al., 2001; Hirschmann, Özkurt, et al., 2013), and well-capable of performing the motor task, oscillatory dynamics might still have been pathologically altered. On the other hand, the observed effect of increased cortex-subcortex interaction during unpredictable trials aligns well with the notion of the frontal cortex performing high-level cognitive operations (Altamura et al., 2010). Additionally, the beta rebound and movement-related beta suppression have previously been observed in healthy individuals (Alegre et al., 2004). Movement-related beta coherence dynamics, however, cannot be assessed in healthy participants non-invasively. Another limitation inherent to studying PD is the clinical variability across patients and their advanced age. In Study 1, this issue was accounted for by controlling for age and other clinical variables in statistical analyses. Further suggestions for addressing this issue and increasing generalizability can be found in Recommendation 1 of the Outlook.

5.2.2. Sample size

Even though Study 2 involved a patient not suffering from PD, bringing about important insights into the disease-specific and DBS-dependent neural dynamics of PD and OCD, it bears one major limitation: the sample size. Given that DBS remains rare among OCD patients (Abdelnaim et al., 2023; Gadot et al., 2022; Mar-Barrutia et al., 2021), acquiring larger sample sizes will be the main challenge for future studies in the field. Furthermore, the evidence base for the mechanisms of DBS in OCD patients is still limited compared to PD, which complicated the comparability of the findings of Study 2 with established research results. Another drawback was that the PD patient was not measured at rest with DBS ON vs. DBS OFF, further limiting comparability. While Study 1 had a sample size of 20, which is noteworthy considering the research methods used, the inclusion of further patients could have allowed for a clearer picture of STN beta dynamics during reversals of movement direction. Possibilities to address the issue of sample size in future research are discussed in **Recommendations 1 and 2** of the **Outlook**.

5.2.3. Stun effect

Patients with externalized DBS leads are typically recorded one day after electrode placement. The so-called stun effect resulting from the trauma caused by the implantation of DBS electrodes involves a temporary improvement of motor symptoms (Mann et al., 2009), which might be beneficial when wanting to study healthy movement as in Study 1. However, it might still alter neural oscillatory activity and thereby limit the generalizability of research findings. Sensingcapable DBS devices, which do not require the externalization of leads to record LFPs from deep brain targets and thus offer a solution to this issue (Attilio et al., 2025; Soh et al., 2025), were not yet available at the time of data collection of Study 1 but were used in Study 2. **Recommendation 2** of the **Outlook** presents further benefits of this new technology.

5.2.4. Ecological validity

While the motor task in Study 1 involved movements which are more complex than in previous research, merely turning a wheel does not capture the complexity of everyday behavior. It should be acknowledged that the reported beta dynamics may not apply to movements which are more complicated or simply differ from the ones studied here (Kennedy et al., 2011; London et al., 2021; Muralidharan & Aron, 2021). The Go/NoGo task employed in **Study 2** is a simple motor paradigm assessing the inhibition of a prepotent response. In **Study 2**, it was possible to distinguish between OCD and PD with this task. Whether the observed spectral differences are specific to the paradigm at hand or can be reproduced with other tasks remains elusive. Recommendations 2 and 3 of the Outlook present specific suggestions for future experimental setups that allow for a more naturalistic behavior of participants.

5.2.5. Scope of analysis

Unraveling the neural mechanisms of complex movement and cognition is unlikely to be achieved in a single study. The focus of Study 1 on the beta frequency band was chosen due to its association with various movement parameters (Benis et al., 2014; Fischer et al., 2019; Fischer et al., 2016) and emerging evidence of an involvement of this frequency band in cognitive processes (Zavala, Jang, et al., 2017). In Study 2, the focus on low frequencies, i.e. theta and beta, was due to their established implications in the OCD (Bastin, Polosan, Piallat, et al., 2014) and PD (Brown et al., 2001) pathophysiologies. However, including other frequency bands in the analyses could have led to further important results in both studies.

The analyses performed in this thesis were intended to cover both local and long-range changes in neural oscillatory activity. However, a description of the directionality of cortico-subcortical signaling is lacking for Study 2. Furthermore, the analyses in both studies are limited to local power and coherence between the sensorimotor cortex and STN. Recommendation 5 of the Outlook outlines possibilities for further analysis of the data. MEG and LFP recordings were the chosen methods of data collection in both studies. While these approaches have many advantages, such as excellent temporal resolution, other tools could have been employed.

Examples include tools that offer a higher spatial resolution or do not rely on neural oscillations, which have been proposed by some to be epiphenomenal rather than underlying neural processing (Jones, 2016). Thus, research methods which can be used to supplement the present thesis' findings are detailed in **Recommendation 4** of the **Outlook**.

5.2.6. The role of the STN in changes of movement direction

Although the results of **Study 1** suggest that the STN exhibits low-amplitude changes in high beta power, as well as elevations in coherence during reversals, group-average beta power and coherence were not modulated significantly. Patients differed in their movement speed and in the length of movement breaks during reversals. The resulting heterogeneity across patients might be the reason why the question of how the STN's oscillatory dynamics relate to short movement breaks cannot be answered conclusively. The employed analysis methods further do not allow pinpointing the exact pathways giving rise to the changes that were observed on the singlesubject level. Recommendations for future research which would address these issues are outlined in Recommendations 4 and 5 of the Outlook.

5.2.7. Electrode locations

Study 2 identified distinct oscillatory patterns within the STN in the OCD and PD patients during a Go/NoGo task. The reported dominance of theta oscillations in OCD and beta oscillations in PD may partly reflect slight differences in electrode placement, with a more anteromedial location in OCD and a dorsolateral location in PD. However, it should be noted that beta oscillations have been documented in the non-motor area of the STN in OCD (Accolla et al., 2016), and theta oscillations in the dorsolateral motor area of the STN in PD (Olson et al., 2022), suggesting that task-related modulations of these signals would have been possible regardless of electrode positioning.

Variations in electrode placement represent a general limitation for studies investigating LFPs from deep brain structures. Nevertheless, because the motor region of the STN is typically the DBS target in PD patients (Horn et al., 2017), which was confirmed for each patient in **Study 1**, variability in electrode placement is less likely to have influenced the findings of this study. Recommendation 1 of the Outlook presents possibilities for demonstrating more clearly whether the observed differences in Study 2 truly reflect disease-specific patterns rather than differences in electrode placement.

6. Outlook

Both studies presented in this thesis reflect substantial contributions to the field of neuroscience, specifically to the understanding of the role of neural (beta) oscillations in the control of complex movement and their modulation by DBS in disorders not typically studied in this context, such as OCD. Various recommendations for future research can be made based on these studies and their unique limitations. These recommendations may further be used to answer some of the remaining open scientific questions presented below.

With respect to **Study 1**, it will be important to determine the specific time point at which a beta rebound emerges during short breaks of movement, given its absence during reversals in this study. Do slightly longer pauses of movement differ from reversals in their electrophysiological profiles? Additionally, it remains to be clarified which structural pathways are activated during reversals of movement direction compared to full stops. Similarly, beyond the STN, M1, and MSMC, which additional cortical and subcortical motor structures are engaged in directional movement changes vs. full terminations of continuous movement and what is the temporal sequence of their activation? Finally, it should be tested whether cortex-subcortex interaction increases with cognitive challenge in a linear fashion.

In relation to **Study 2**, future research should seek to disentangle whether the dampening of STN beta oscillations is a general effect of DBS, which can be observed across diseases within and outside the domain of movement disorders, and how these oscillatory changes evolve with chronic DBS. Though suggested by Study 2, future research should attempt to more conclusively determine whether motor task-based STN beta oscillations are specific to PD or also occur in other disorders.

6.1. Recommendation 1: Extend research to disorders other than Parkinson's disease and to healthy participants.

Currently, there remain various challenges to studying the neural oscillatory basis of motor control. The complexity of everyday behavior likely requires an intricate interplay of cortical and subcortical structures. Such dynamics cannot be captured in healthy individuals and even when considering patients with movement disorders other than PD, such as essential tremor or dystonia, the generalizability to the healthy population remains limited due to disease-specific neural alterations. Still, future research should extend the study of complex movement, as done in Study 1, to other patient populations (Steina et al., 2025; van Wijk et al., 2017), to at least rule out the possibility of research findings only applying to PD specifically. Since DBS electrodes are often not targeted at the STN in disorders other than PD, it will be possible to compare the oscillatory dynamics of the STN to these other structures, possibly leading to further insights into how motor control is achieved in the BG. Additionally, cortical activity can be recorded in healthy controls to confirm the findings of this thesis in the healthy sensorimotor cortex (Alegre et al., 2004).

Study 2 presented a single case of OCD and one PD control patient. The conclusions drawn from Study 2 should be re-evaluated in the light of future research. As more patients with treatmentrefractory OCD can be offered DBS, study sample sizes will rise. Furthermore, it will likely be possible to compare the effects of DBS on neural oscillations in PD with other disorders, such as depression, in the near future. Future research drawing on different patient populations and electrode placements will help tremendously in differentiating diseases at the oscillatory level, as well as identifying both disease-specific mechanisms of DBS and those that are shared across conditions. It would be important, for example, to elucidate whether beta oscillations decrease as a response to DBS in diseases across the board. Additionally, a wider pool of pathologies to draw from would allow studying the cortico-subcortical underpinnings of motor control in a less biased fashion.

6.2. Recommendation 2: Take advantage of sensing-capable deep brain stimulation systems.

While largely unavailable at the time the data for **Study 1** was collected, sensing-capable DBS devices will help circumvent the stun effect (see section 5.2.3) in future research as they allow recording LFPs from the implanted electrode at any point in time after surgery. This new technology eliminates the need for patients to undergo two separate surgeries to allow for the externalization of DBS leads in a first step and the implantation of the stimulator in a second step, resulting in improved comfort for the patients and, possibly, larger sample sizes. Furthermore, the association of neural oscillations with behavior/symptoms may be studied in more naturalistic environments by taking experiments outside the lab (Soh et al., 2025), possibly using portable EEG systems in combination with LFP recordings, or taking advantage of virtual or augmented reality settings. Lastly, longitudinal study designs could be used to demonstrate more clearly how local and long-range brain activity is impacted by DBS in the long run across diseases (Y. Chen et al., 2020). It should be noted, however, that a major challenge with sensing-capable devices is their limited use in research and the need for further technological advancements to ease data processing. For instance, at this point, the synchronization of the LFP signal with other signals, such as MEG, is complicated, and there is no consensus on how this can be achieved best (Hnazaee et al., 2023; Soh et al., 2025).

6.3. Recommendation 3: Develop complex motor tasks.

While Study 1 was advantageous compared to previous studies with respect to the complexity of the behavioral task, future research might consider using designs which pose even greater or entirely different demands on participants. For example, instead of a turning motion, other continuous movements could be chosen, possibly involving the legs rather than the hands (Khawaldeh et al., 2020; Thenaisie et al., 2022). The cognitive challenge in Study 1 could be adapted by systematically increasing the unpredictability of movement prompts to determine whether this leads to even greater adjustments of cortico-subcortical synchronization. Furthermore, the breaks in between successive movements could be manipulated to determine the time point at which a beta rebound would arise. This could either be done by looking at fast

vs. slow reversals or using a different movement which involves more deliberate pausing (Alegre et al., 2004; Muralidharan & Aron, 2021).

Study 2 suggests that task-based neural oscillations capture the disease-specific pathophysiological alterations of PD and OCD better than resting-state oscillations. This hypothesis could be tested in future studies using paradigms other than the Go/NoGo Task (Alegre et al., 2013; Benis et al., 2014; Patai et al., 2022). This would help elucidate the extent to which movement-related beta oscillations, particularly in the STN, are truly pathological in PD and how they compare to oscillatory activity in other disorders. One possibility is that motor-related STN beta activity is inherently pathological, reflecting a PD-specific spread of activity from cortical regions to the STN (Oswal et al., 2021). Alternatively, movement-related STN beta oscillations during movement initiation, inhibition, and stopping might be part of the healthy motor system.

6.4. Recommendation 4: Expand research methods beyond magnetoencephalography and local field potentials.

While MEG and LFP recordings using externalized leads provide various advantages over other methods, it will be important for future research to utilize other tools to complement the findings presented in this work. Even though it is possible to reconstruct the sources of activity in MEG research, activity of deeper structures of the brain, which are likely relevant to complex motor control, is better captured with functional MRI due to its exceptional spatial resolution. Additional possibilities include the use of diffusion MRI and fiber tracking to, for example, correlate STNcortex beta coherence during reversals and movement stops with the strength of structural pathways, such as the hyperdirect pathway (Oswal et al., 2021), which was assumed to be activated during terminations of continuous movements in Study 1. The findings from Study 2 could be supplemented by testing whether differences in behavior on task or oscillatory profiles across diseases relate to specific tracts (e.g. hyperdirect and frontostriatal pathways in PD and OCD, respectively) or to assess which tracts are modulated by DBS. Finally, correlating oscillatory activity during complex movement with action potentials by means of microelectrode recordings or electrocorticography could provide deeper insights into the dynamics of movement encoding within the motor system (Fischer et al., 2020; Igarashi et al., 2013).

6.5. Recommendation 5: Expand data analysis beyond oscillatory power and coherence.

Spectral power across canonical frequency bands (i.e. delta, theta, alpha, beta, and gamma) is a much-studied parameter of neural oscillations providing valuable insights into the oscillatory dynamics associated with various diseases, as well as behavioral and cognitive processes. However, focusing solely on the periodic properties of neural oscillations might lead to overlooking the characteristics of aperiodic components, which have been demonstrated to have functional significance, as well. Disregarding the aperiodic component of oscillations might further lead to false conclusions in spectral analyses (Donoghue et al., 2020). Future research could explore the aperiodic activity associated with complex movement, similar to **Study 1**, possibly revealing deeper insights into how cortical and subcortical motor areas coordinate motor control. Aperiodic activity could also provide an additional means of comparing diseases and their responses to DBS, potentially extending the findings of **Study 2**.

Further exploration of the data from **Study 1 and 2** could entail the consideration of additional frequency bands, such as delta and high frequency oscillations (Özkurt et al., 2011; Perera et al., 2023), and the characterization of beta bursts. It has been suggested that beta band activity occurs in bursts varying in amplitude and duration. Such bursts have been shown to change with the dopaminergic state (G. Tinkhauser et al., 2017) and adaptive DBS (Gerd Tinkhauser et al., 2017). Future research extending Study 2 could perform an analysis of beta bursts to confirm or possibly refine the conclusion that PD and OCD exhibit comparable patterns of DBS-responsive beta activity in the resting state. Furthermore, beta bursts have previously been investigated in the context of movement stopping (Diesburg et al., 2021). Given their brief nature, the temporal order of beta bursts occurring across different regions of the cortico-BG motor system can offer insights into which areas may be driving activity in others. Coherence analyses, as performed in Study 1, can be complemented with this approach in future research. Such an analysis could, for example, help clarify the role of the STN in briefly halting an action compared to terminating it. Here, the consideration of further cortical areas (e.g. the inferior frontal gyrus or the supplementary motor area) (Swann et al., 2009) would allow for a better understanding of the interactions and the sequential activation of cortical and subcortical motor areas.

Lastly, computational modeling can be used in future studies to simulate cortico-BG loop dynamics (Oswal et al., 2021) and test the effects of DBS or specific task demands on beta oscillations across diseases. Analyses expanding upon Study 1 could further determine whether the ongoing modulation of spectral power relates to various movement-related parameters, such as movement speed. Another possibility would be simulating long vs. short breaks during reversals, so as to more conclusively differentiate the oscillatory basis of short breaks of ongoing behavior from full stops.

7. Conclusion

In summary, this thesis makes important contributions to our understanding of the role of STNcortex beta oscillations in the control of complex movement. Long-range synchronization between the sensorimotor cortex and the STN appears essential in situations involving heightened levels of uncertainty. Additionally, this work advances the ongoing discussion surrounding the postmovement beta rebound by demonstrating that this phenomenon occurs only after complete movement termination, and not during brief pauses of movement. Notably, this thesis contributes valuable insights into the effects of DBS beyond PD by demonstrating DBS-responsive beta oscillations synchronized across the cortico-BG motor loop in an OCD patient. Finally, it highlights the value of task-based neural oscillations for distinguishing between PD and OCD, with PD being primarily associated with beta-range modulations and OCD with theta-range modulations.

8. References

- Aarsland, D., Batzu, L., Halliday, G. M., Geurtsen, G. J., Ballard, C., Ray Chaudhuri, K., & Weintraub, D. (2021). Parkinson disease-associated cognitive impairment. Nature Reviews Disease Primers, 7(1), 47. https://doi.org/10.1038/s41572-021-00280-3
- Abbasi, O., Hirschmann, J., Storzer, L., Özkurt, T. E., Elben, S., Vesper, J., Wojtecki, L., Schmitz, G., Schnitzler, A., & Butz, M. (2018). Unilateral deep brain stimulation suppresses alpha and beta oscillations in sensorimotor cortices. *Neuroimage*, 174, 201-207. https://doi.org/https://doi.org/10.1016/j.neuroimage.2018.03.026
- Abdelnaim, M. A., Lang-Hambauer, V., Hebel, T., Schoisswohl, S., Schecklmann, M., Deuter, D., Schlaier, J., & Langguth, B. (2023). Deep brain stimulation for treatment resistant obsessive compulsive disorder; an observational study with ten patients under real-life conditions. Frontiers in Psychiatry, 14, 1242566. https://doi.org/10.3389/fpsyt.2023.1242566
- Accolla, E. A., Herrojo Ruiz, M., Horn, A., Schneider, G. H., Schmitz-Hübsch, T., Draganski, B., & Kühn, A. A. (2016). Brain networks modulated by subthalamic nucleus deep brain stimulation. Brain, 139(Pt 9), 2503-2515. https://doi.org/10.1093/brain/aww182
- Accolla, E. A., Horn, A., Herrojo-Ruiz, M., Neumann, W.-J., & Kühn, A. A. (2017). Reply: Oscillatory coupling of the subthalamic nucleus in obsessive compulsive disorder. Brain, 140(9), e57-e57. https://doi.org/10.1093/brain/awx165
- Adam, E. M., Brown, E. N., Kopell, N., & McCarthy, M. M. (2022). Deep brain stimulation in the subthalamic nucleus for Parkinson's disease can restore dynamics of striatal networks. Proceedings of the National Academy of Sciences, 119(19), e2120808119. https://doi.org/10.1073/pnas.2120808119
- Adamantidis, A. R., Gutierrez Herrera, C., & Gent, T. C. (2019). Oscillating circuitries in the sleeping brain. Nature Reviews Neuroscience, 20(12), 746-762. https://doi.org/10.1038/s41583-019-0223-4
- Alegre, M., Gurtubay, I. G., Labarga, A., Iriarte, J., Malanda, A., & Artieda, J. (2003). Alpha and beta oscillatory changes during stimulus-induced movement paradigms: Effect of stimulus predictability. Neuroreport, 14(3), 381-385. https://doi.org/10.1097/00001756-200303030-00017
- Alegre, M., Gurtubay, I. G., Labarga, A., Iriarte, J., Malanda, A., & Artieda, J. (2004). Alpha and beta oscillatory activity during a sequence of two movements. Clinical Neurophysiology, 115(1), 124-130. https://doi.org/10.1016/S1388-2457(03)00311-0
- Alegre, M., Labarga, A., Gurtubay, I. G., Iriarte, J., Malanda, A., & Artieda, J. (2002). Beta electroencephalograph changes during passive movements: Sensory afferences contribute to beta event-related desynchronization in humans. *Neuroscience Letters*, 331(1), 29-32. https://doi.org/10.1016/s0304-3940(02)00825-x
- Alegre, M., Lopez-Azcarate, J., Obeso, I., Wilkinson, L., Rodriguez-Oroz, M. C., Valencia, M., Garcia-Garcia, D., Guridi, J., Artieda, J., Jahanshahi, M., & Obeso, J. A. (2013). The subthalamic nucleus is involved in successful inhibition in the stop-signal task: A local field potential study in Parkinson's disease. Experimental Neurology, 239, 1-12. https://doi.org/10.1016/j.expneurol.2012.08.027
- Altamura, M., Goldberg, T. E., Elvevåg, B., Holroyd, T., Carver, F. W., Weinberger, D. R., & Coppola, R. (2010). Prefrontal cortex modulation during anticipation of working memory demands as revealed by magnetoencephalography. International Journal of Biomedical Imaging, 2010, 840416. https://doi.org/10.1155/2010/840416
- American Psychiatric Association. (2013). Diagnostic and statistical manual of mental disorders (5 ed.). American Psychiatric Publishing.
- Anzak, A., Tan, H., Pogosyan, A., Foltynie, T., Limousin, P., Zrinzo, L., Hariz, M., Ashkan, K., Bogdanovic, M., Green, A. L., Aziz, T., & Brown, P. (2012). Subthalamic nucleus activity

- optimizes maximal effort motor responses in Parkinson's disease. *Brain*, 135(9), 2766-2778. https://doi.org/10.1093/brain/aws183
- Armstrong, M. J., & Okun, M. S. (2020). Time for a new image of Parkinson disease. *JAMA Neurology*, 77(11), 1345-1346. https://doi.org/10.1001/jamaneurol.2020.2412
- Aron, A. R., Herz, D. M., Brown, P., Forstmann, B. U., & Zaghloul, K. (2016). Frontosubthalamic circuits for control of action and cognition. *The Journal of Neuroscience*, *36*(45), 11489-11495. https://doi.org/10.1523/JNEUROSCI.2348-16.2016
- Aron, A. R., & Poldrack, R. A. (2006). Cortical and subcortical contributions to stop signal response inhibition: Role of the subthalamic nucleus. *The Journal of Neuroscience*, 26(9), 2424-2433. https://doi.org/10.1523/jneurosci.4682-05.2006
- Attilio, D. T., Domenico, L. T., Giusy, G., Giorgio, V., & Angelo, L. (2025). Innovative developments in deep brain stimulation devices. *Interdisciplinary Neurosurgery*, *40*, 102035. https://doi.org/https://doi.org/10.1016/j.inat.2025.102035
- Baillet, S., Mosher, J. C., & Leahy, R. M. (2001). Electromagnetic brain mapping. *IEEE Signal Processing Magazine*, *18*(6), 14-30. https://doi.org/10.1109/79.962275
- Bangel, K. A., Bais, M., Eijsker, N., Schuurman, P. R., van den Munckhof, P., Figee, M., Smit, D. J. A., & Denys, D. (2023). Acute effects of deep brain stimulation on brain function in obsessive—compulsive disorder. *Clinical Neurophysiology*, *148*, 109-117. https://doi.org/https://doi.org/10.1016/j.clinph.2022.12.012
- Barone, J., & Rossiter, H. E. (2021). Understanding the role of sensorimotor beta oscillations [Mini Review]. *Frontiers in Systems Neuroscience*, *15*(51). https://doi.org/10.3389/fnsys.2021.655886
- Bastin, J., Polosan, M., Benis, D., Goetz, L., Bhattacharjee, M., Piallat, B., Krainik, A., Bougerol, T., Chabardès, S., & David, O. (2014). Inhibitory control and error monitoring by human subthalamic neurons. *Translational Psychiatry*, *4*(9), e439. https://doi.org/10.1038/tp.2014.73
- Bastin, J., Polosan, M., Piallat, B., Krack, P., Bougerol, T., Chabardès, S., & David, O. (2014). Changes of oscillatory activity in the subthalamic nucleus during obsessive-compulsive disorder symptoms: Two case reports. *Cortex*, *60*, 145-150. https://doi.org/https://doi.org/10.1016/j.cortex.2013.12.007
- Bastos, A. M., & Schoffelen, J. M. (2015). A tutorial review of functional connectivity analysis methods and their interpretational pitfalls. *Frontiers in Systems Neuroscience*, *9*, 175. https://doi.org/10.3389/fnsys.2015.00175
- Benis, D., David, O., Lachaux, J.-P., Seigneuret, E., Krack, P., Fraix, V., Chabardès, S., & Bastin, J. (2014). Subthalamic nucleus activity dissociates proactive and reactive inhibition in patients with Parkinson's disease. *Neuroimage*, *91*, 273-281. https://doi.org/10.1016/j.neuroimage.2013.10.070
- Berger, H. (1929). Über das Elektrenkephalogramm des Menschen. *Archiv für Psychiatrie und Nervenkrankheiten*, 87(1), 527-570. https://doi.org/10.1007/BF01797193
- Beucke, J. C., Sepulcre, J., Talukdar, T., Linnman, C., Zschenderlein, K., Endrass, T., Kaufmann, C., & Kathmann, N. (2013). Abnormally high degree connectivity of the orbitofrontal cortex in obsessive-compulsive disorder. *JAMA Psychiatry*, *70*(6), 619-629. https://doi.org/10.1001/jamapsychiatry.2013.173
- Beudel, M., Little, S., Pogosyan, A., Ashkan, K., Foltynie, T., Limousin, P., Zrinzo, L., Hariz, M., Bogdanovic, M., Cheeran, B., Green, A. L., Aziz, T., Thevathasan, W., & Brown, P. (2015). Tremor reduction by deep brain stimulation is associated with gamma power suppression in Parkinson's disease. *Neuromodulation: Technology at the Neural Interface*, *18*(5), 349-354. https://doi.org/https://doi.org/10.1111/ner.12297
- Bokor, G., & Anderson, P. D. (2014). Obsessive-compulsive disorder. *Journal of Pharmacy Practice*, 27(2), 116-130. https://doi.org/10.1177/0897190014521996

- Bonnevie, T., & Zaghloul, K. A. (2018). The subthalamic nucleus: Unravelling new roles and mechanisms in the control of action. The Neuroscientist, 25(1), 48-64. https://doi.org/10.1177/1073858418763594
- Brigo, F., Erro, R., Marangi, A., Bhatia, K., & Tinazzi, M. (2014). Differentiating drug-induced parkinsonism from Parkinson's disease: An update on non-motor symptoms and investigations. Parkinsonism & Related Disorders, 20(8), 808-814. https://doi.org/10.1016/j.parkreldis.2014.05.011
- Brittain, J. S., Watkins, K. E., Joundi, R. A., Ray, N. J., Holland, P., Green, A. L., Aziz, T. Z., & Jenkinson, N. (2012). A role for the subthalamic nucleus in response inhibition during conflict. The Journal of Neuroscience, 32(39), 13396-13401. https://doi.org/10.1523/jneurosci.2259-12.2012
- Brown, P. (2003). Oscillatory nature of human basal ganglia activity: Relationship to the pathophysiology of Parkinson's disease. Movement Disorders, 18(4), 357-363. https://doi.org/10.1002/mds.10358
- Brown, P., Oliviero, A., Mazzone, P., Insola, A., Tonali, P., & Di Lazzaro, V. (2001). Dopamine dependency of oscillations between subthalamic nucleus and pallidum in Parkinson's disease. The Journal of Neuroscience, 21(3), 1033-1038. https://doi.org/10.1523/jneurosci.21-03-01033.2001
- Brown, P., & Williams, D. (2005). Basal ganglia local field potential activity: Character and functional significance in the human. Clinical Neurophysiology, 116(11), 2510-2519. https://doi.org/https://doi.org/10.1016/j.clinph.2005.05.009
- Burbaud, P., Clair, A. H., Langbour, N., Fernandez-Vidal, S., Goillandeau, M., Michelet, T., Bardinet, E., Chéreau, I., Durif, F., Polosan, M., Chabardès, S., Fontaine, D., Magnié-Mauro, M. N., Houeto, J. L., Bataille, B., Millet, B., Vérin, M., Baup, N., Krebs, M. O., Cornu, P., Pelissolo, A., Arbus, C., Simonetta-Moreau, M., Yelnik, J., Welter, M. L., & Mallet, L. (2013). Neuronal activity correlated with checking behaviour in the subthalamic nucleus of patients with obsessive-compulsive disorder. Brain, 136(1), 304-317. https://doi.org/10.1093/brain/aws306
- Calabresi, P., Picconi, B., Tozzi, A., Ghiglieri, V., & Di Filippo, M. (2014). Direct and indirect pathways of basal ganglia: A critical reappraisal. Nature Neuroscience, 17(8), 1022-1030. https://doi.org/10.1038/nn.3743
- Cao, C., Litvak, V., Zhan, S., Liu, W., Zhang, C., Sun, B., Li, D., & van Wijk, B. C. M. (2024). Low-beta versus high-beta band cortico-subcortical coherence in movement inhibition and expectation. Neurobiology of Disease, 201, 106689. https://doi.org/https://doi.org/10.1016/j.nbd.2024.106689
- Cao, L., & Hu, Y.-M. (2016). Beta rebound in visuomotor adaptation: Still the status quo? The Journal of Neuroscience, 36(24), 6365-6367. https://doi.org/10.1523/JNEUROSCI.1007-16.2016
- Cassidy, M., Mazzone, P., Oliviero, A., Insola, A., Tonali, P., Lazzaro, V. D., & Brown, P. (2002). Movement-related changes in synchronization in the human basal ganglia. Brain, 125(6), 1235-1246. https://doi.org/10.1093/brain/awf135
- Castiglione, A., Wagner, J., Anderson, M., & Aron, A. R. (2019). Preventing a thought from coming to mind elicits increased right frontal beta just as stopping action does. Cerebral Cortex, 29(5), 2160-2172. https://doi.org/10.1093/cercor/bhz017
- Chabardès, S., Polosan, M., Krack, P., Bastin, J., Krainik, A., David, O., Bougerol, T., & Benabid, A. L. (2013). Deep brain stimulation for obsessive-compulsive disorder: Subthalamic nucleus target. World Neurosurgery, 80(3), S31.e31-S31.e38. https://doi.org/https://doi.org/10.1016/j.wneu.2012.03.010
- Chandramouli, C., Iliana, E. B., & Krishna, V. S. (2019). Frequency shifts and depth dependence of premotor beta band activity during perceptual cecision-making. The Journal of Neuroscience, 39(8), 1420-1435. https://doi.org/10.1523/JNEUROSCI.1066-18.2018

- Chen, W., de Hemptinne, C., Miller, A. M., Leibbrand, M., Little, S. J., Lim, D. A., Larson, P. S., & Starr, P. A. (2020). Prefrontal-subthalamic hyperdirect pathway modulates movement inhibition in humans. Neuron, 106(4), 579-588. https://doi.org/10.1016/j.neuron.2020.02.012
- Chen, Y., Gong, C., Tian, Y., Orlov, N., Zhang, J., Guo, Y., Xu, S., Jiang, C., Hao, H., Neumann, W.-J., Kühn, A. A., Liu, H., & Li, L. (2020). Neuromodulation effects of deep brain stimulation on beta rhythm: A longitudinal local field potential study. Brain Stimulation, 13(6), 1784-1792. https://doi.org/https://doi.org/10.1016/j.brs.2020.09.027
- Cheng, H. C., Ulane, C. M., & Burke, R. E. (2010). Clinical progression in Parkinson disease and the neurobiology of axons. Annals of Neurology, 67(6), 715-725. https://doi.org/10.1002/ana.21995
- Cheyne, D., Bells, S., Ferrari, P., Gaetz, W., & Bostan, A. C. (2008). Self-paced movements induce high-frequency gamma oscillations in primary motor cortex. Neuroimage, 42(1), 332-342. https://doi.org/https://doi.org/10.1016/j.neuroimage.2008.04.178
- Choi, J. W., Malekmohammadi, M., Sparks, H., Kashanian, A., Cross, K. A., Bordelon, Y., & Pouratian, N. (2020). Altered pallidocortical low-beta oscillations during self-initiated movements in Parkinson disease. Frontiers in Systems Neuroscience, 14, 54. https://doi.org/10.3389/fnsys.2020.00054
- Chung, J. W., Burciu, R. G., Ofori, E., Coombes, S. A., Christou, E. A., Okun, M. S., Hess, C. W., & Vaillancourt, D. E. (2018). Beta-band oscillations in the supplementary motor cortex are modulated by levodopa and associated with functional activity in the basal ganglia. Neurolmage: Clinical, 19, 559-571. https://doi.org/10.1016/j.nicl.2018.05.021
- Cohen, M. X. (2014). Analyzing neural time series data: Theory and practice. The MIT Press.
- Colombo, A., Bernasconi, E., Alva, L., Sousa, M., Debove, I., Nowacki, A., Serquet, C., Petermann, K., Nguyen, T. A. K., Magalhães, A. D., Lachenmayer, L., Waskönig, J., Nef, T., Schuepbach, M., Pollo, C., Krack, P., Averna, A., & Tinkhauser, G. (2025). Finely tuned y tracks medication cycles in Parkinson's disease: An ambulatory brain-sense study. Movement Disorders, 40(5). https://doi.org/10.1002/mds.30160
- Cruikshank, L. C., Singhal, A., Hueppelsheuser, M., & Caplan, J. B. (2011). Theta oscillations reflect a putative neural mechanism for human sensorimotor integration. Journal of Neurophysiology, 107(1), 65-77. https://doi.org/10.1152/jn.00893.2010
- Dauer, W., & Przedborski, S. (2003). Parkinson's disease: Mechanisms and models. Neuron, 39(6), 889-909. https://doi.org/10.1016/S0896-6273(03)00568-3
- DeMaagd, G., & Philip, A. (2015). Parkinson's disease and its management: Part 1: Disease entity, risk factors, pathophysiology, clinical presentation, and diagnosis. Pharmacy & Therapeutics, 40(8), 504-532.
- Denys, D., Mantione, M., Figee, M., van den Munckhof, P., Koerselman, F., Westenberg, H., Bosch, A., & Schuurman, R. (2010). Deep brain stimulation of the nucleus accumbens for treatment-refractory obsessive-compulsive disorder. Archives of General Psychiatry, 67(10), 1061-1068. https://doi.org/10.1001/archgenpsychiatry.2010.122
- Desarkar, P., Sinha, V. K., Jagadheesan, K., & Nizamie, S. H. (2007). Subcortical functioning in obsessive-compulsive disorder: an exploratory EEG coherence study. The World Journal of Biological Psychiatry, 8(3), 196-200. https://doi.org/10.1080/15622970601148547
- di Biase, L., Piano, C., Bove, F., Ricci, L., Caminiti, M. L., Stefani, A., Viselli, F., Modugno, N., Cerroni, R., Calabresi, P., Bentivoglio, A. R., Tufo, T., & Di Lazzaro, V. (2023). Intraoperative local field potential beta power and three-dimensional neuroimaging mapping predict long-term clinical response to deep brain stimulation in Parkinson disease: A retrospective study. Neuromodulation, 26(8), 1724-1732. https://doi.org/10.1016/j.neurom.2022.12.013
- Diesburg, D. A., Greenlee, J. D. W., & Wessel, J. R. (2021). Cortico-subcortical β burst dynamics underlying movement cancellation in humans. eLife, 10, e70270. https://doi.org/10.7554/eLife.70270

- Donoghue, T., Haller, M., Peterson, E. J., Varma, P., Sebastian, P., Gao, R., Noto, T., Lara, A. H., Wallis, J. D., Knight, R. T., Shestyuk, A., & Voytek, B. (2020). Parameterizing neural power spectra into periodic and aperiodic components. Nature Neuroscience, 23(12), 1655-1665. https://doi.org/10.1038/s41593-020-00744-x
- Dorsey, E. R., Constantinescu, R., Thompson, J. P., Biglan, K. M., Holloway, R. G., Kieburtz, K., Marshall, F. J., Ravina, B. M., Schifitto, G., Siderowf, A., & Tanner, C. M. (2007). Projected number of people with Parkinson disease in the most populous nations, 2005 through 2030. Neurology, 68(5), 384-386. https://doi.org/doi:10.1212/01.wnl.0000247740.47667.03
- Elliott, M. L., Knodt, A. R., Cooke, M., Kim, M. J., Melzer, T. R., Keenan, R., Ireland, D., Ramrakha, S., Poulton, R., Caspi, A., Moffitt, T. E., & Hariri, A. R. (2019). General functional connectivity: Shared features of resting-state and task fMRI drive reliable and heritable individual differences in functional brain networks. Neuroimage, 189, 516-532. https://doi.org/https://doi.org/10.1016/j.neuroimage.2019.01.068
- Ellis, T. D., Colón-Semenza, C., DeAngelis, T. R., Thomas, C. A., Hilaire, M. S., Earhart, G. M., & Dibble, L. E. (2021). Evidence for early and regular physical therapy and exercise in Parkinson's disease. Seminars in Neurology, 41(2), 189-205. https://doi.org/10.1055/s-0041-1725133
- Engel, A., & Fries, P. (2010). Beta-band oscillation signalling the status quo? Current Opinion in Neurobiology, 20(2), 156-165. https://doi.org/10.1016/j.conb.2010.02.015
- Espenhahn, S., de Berker, A. O., van Wijk, B. C. M., Rossiter, H. E., & Ward, N. S. (2017). Movement-related beta oscillations show high intra-individual reliability. *Neuroimage*, 147, 175-185. https://doi.org/10.1016/j.neuroimage.2016.12.025
- Fawcett, E. J., Power, H., & Fawcett, J. M. (2020). Women are at greater risk of ocd than men: A meta-analytic review of OCD prevalence worldwide. Journal of Clinical Psychiatry, 81(4). https://doi.org/10.4088/JCP.19r13085
- Figee, M., Luigies, J., Smolders, R., Valencia-Alfonso, C.-E., van Wingen, G., de Kwaasteniet, B., Mantione, M., Ooms, P., de Koning, P., Vulink, N., Levar, N., Droge, L., van den Munckhof, P., Schuurman, P. R., Nederveen, A., van den Brink, W., Mazaheri, A., Vink, M., & Denys, D. (2013). Deep brain stimulation restores frontostriatal network activity in obsessive-compulsive disorder. Nature Neuroscience, 16(4), 386-387. https://doi.org/10.1038/nn.3344
- Fischer, P., Lipski, W., Neumann, W.-J., Turner, R., Fries, P., Brown, P., & Richardson, R. (2020). Movement-related coupling of human subthalamic nucleus spikes to cortical gamma. eLife, 9, e51956. https://doi.org/10.7554/elife.51956.sa1
- Fischer, P., Pogosyan, A., Green, A. L., Aziz, T. Z., Hyam, J., Foltynie, T., Limousin, P., Zrinzo, L., Samuel, M., Ashkan, K., Da Lio, M., De Cecco, M., Fornaser, A., Brown, P., & Tan, H. (2019). Beta synchrony in the cortico-basal ganglia network during regulation of force control on and off dopamine. Neurobiology of Disease, 127, 253-263. https://doi.org/10.1016/j.nbd.2019.03.004
- Fischer, P., Pogosyan, A., Herz, D. M., Cheeran, B., Green, A. L., Fitzgerald, J., Aziz, T. Z., Hyam, J., Little, S., Foltynie, T., Limousin, P., Zrinzo, L., Brown, P., & Tan, H. (2017). Subthalamic nucleus gamma activity increases not only during movement but also during movement inhibition. eLife, 6, e23947. https://doi.org/10.7554/eLife.23947
- Fischer, P., Tan, H., Pogosyan, A., & Brown, P. (2016). High post-movement parietal low-beta power during rhythmic tapping facilitates performance in a stop task. European Journal of Neuroscience, 44(5), 2202-2213. https://doi.org/10.1111/ejn.13328
- Földi, T., Lőrincz, M. L., & Berényi, A. (2021). Temporally targeted interactions with pathologic oscillations as therapeutical targets in epilepsy and beyond. Frontiers in Neural Circuits, 15, 784085. https://doi.org/10.3389/fncir.2021.784085
- Fonken, Y. M., Rieger, J. W., Tzvi, E., Crone, N. E., Chang, E., Parvizi, J., Knight, R. T., & Krämer, U. M. (2016). Frontal and motor cortex contributions to response inhibition:

- Evidence from electrocorticography. *Journal of Neurophysiology*, *115*(4), 2224-2236. https://doi.org/10.1152/jn.00708.2015
- Frank, M. J. (2006). Hold your horses: A dynamic computational role for the subthalamic nucleus in decision making. *Neural Networks*, *19*(8), 1120-1136. https://doi.org/10.1016/j.neunet.2006.03.006
- Fries, P. (2015). Rhythms for cognition: Communication through coherence. *Neuron*, 88(1), 220-235. https://doi.org/10.1016/j.neuron.2015.09.034
- Friston, K. J. (2011). Functional and effective connectivity: A review. *Brain Connectivity*, 1(1), 13-36. https://doi.org/10.1089/brain.2011.0008
- Fry, A., Mullinger, K. J., O'Neill, G. C., Barratt, E. L., Morris, P. G., Bauer, M., Folland, J. P., & Brookes, M. J. (2016). Modulation of post-movement beta rebound by contraction force and rate of force development. *Human Brain Mapping*, *37*(7), 2493-2511. https://doi.org/https://doi.org/10.1002/hbm.23189
- Gadot, R., Najera, R., Hirani, S., Anand, A., Storch, E., Goodman, W. K., Shofty, B., & Sheth, S. A. (2022). Efficacy of deep brain stimulation for treatment-resistant obsessive-compulsive disorder: Systematic review and meta-analysis. *Journal of Neurology, Neurosurgery, and Psychiatry*, 93,1166-1173. https://doi.org/10.1136/jnnp-2021-328738
- Giannicola, G., Rosa, M., Marceglia, S., Scelzo, E., Rossi, L., Servello, D., Menghetti, C., Pacchetti, C., Zangaglia, R., Locatelli, M., Caputo, E., Cogiamanian, F., Ardolino, G., Barbieri, S., & Priori, A. (2013). The effects of levodopa and deep brain stimulation on subthalamic local field low-frequency oscillations in Parkinson's disease. *Neurosignals*, 21(1-2), 89-98. https://doi.org/10.1159/000336543
- Graybiel, A. M., & Rauch, S. L. (2000). Toward a neurobiology of obsessive-compulsive disorder. *Neuron*, 28(2), 343-347. https://doi.org/10.1016/S0896-6273(00)00113-6
- Grillner, S., Robertson, B., & Stephenson-Jones, M. (2013). The evolutionary origin of the vertebrate basal ganglia and its role in action selection. The *Journal of Physiology*, 591(22), 5425-5431. https://doi.org/10.1113/jphysiol.2012.246660
- Gross, J. (2014). Analytical methods and experimental approaches for electrophysiological studies of brain oscillations. *Journal of Neuroscience Methods*, 228(100), 57-66. https://doi.org/10.1016/j.jneumeth.2014.03.007
- Gross, J., Baillet, S., Barnes, G. R., Henson, R. N., Hillebrand, A., Jensen, O., Jerbi, K., Litvak, V., Maess, B., Oostenveld, R., Parkkonen, L., Taylor, J. R., van Wassenhove, V., Wibral, M., & Schoffelen, J.-M. (2013). Good practice for conducting and reporting MEG research. *Neuroimage*, 65, 349-363. https://doi.org/https://doi.org/10.1016/j.neuroimage.2012.10.001
- Gross, J., Kujala, J., Hämäläinen, M., Timmermann, L., Schnitzler, A., & Salmelin, R. (2001). Dynamic imaging of coherent sources: Studying neural interactions in the human brain. *Proceedings of the National Academy of Sciences*, *98*(2), 694-699. https://doi.org/10.1073/pnas.98.2.694
- Hansen, P. C., Kringelbach, M. L., & Salmelin, R. (2010). *MEG: An Introduction to Methods*. Oxford University Press. https://doi.org/10.1093/acprof:oso/9780195307238.001.0001
- Hariz, M., & Blomstedt, P. (2022). Deep brain stimulation for Parkinson's disease. *Journal of Internal Medicine*, 292(5), 764-778. https://doi.org/10.1111/joim.13541
- Haufe, S., Nikulin, V., & Nolte, G. (2012). Alleviating the influence of weak data asymmetries on Granger-causal analyses. In F. Theis, A. Cichocki, A. Yeredor, & M. Zibulevski (Eds.), Latent variable analysis and signal separation (Vol. 7191, pp. 25-33), Springer. https://doi.org/10.1007/978-3-642-28551-6 4
- Heinrichs-Graham, E., & Wilson, T. W. (2016). Is an absolute level of cortical beta suppression required for proper movement? Magnetoencephalographic evidence from healthy aging. *Neuroimage*, *134*, 514-521. https://doi.org/10.1016/j.neuroimage.2016.04.032
- Herrington, T. M., Cheng, J. J., & Eskandar, E. N. (2016). Mechanisms of deep brain stimulation. *Journal of Neurophysiology*, *115*(1), 19-38. https://doi.org/10.1152/jn.00281.2015

- Hirschmann, J., Abbasi, O., Storzer, L., Butz, M., Hartmann, C. J., Wojtecki, L., & Schnitzler, A. (2019). Longitudinal recordings reveal transient increase of alpha/low-beta power in the subthalamic nucleus associated with the onset of parkinsonian rest tremor. Frontiers in Neurology, 10, 145. https://doi.org/10.3389/fneur.2019.00145
- Hirschmann, J., Hartmann, C. J., Butz, M., Hoogenboom, N., Ozkurt, T. E., Elben, S., Vesper, J., Wojtecki, L., & Schnitzler, A. (2013). A direct relationship between oscillatory subthalamic nucleus-cortex coupling and rest tremor in Parkinson's disease. Brain, 136(12), 3659-3670. https://doi.org/10.1093/brain/awt271
- Hirschmann, J., Özkurt, T. E., Butz, M., Homburger, M., Elben, S., Hartmann, C. J., Vesper, J., Wojtecki, L., & Schnitzler, A. (2011). Distinct oscillatory STN-cortical loops revealed by simultaneous MEG and local field potential recordings in patients with Parkinson's disease. Neuroimage, 55(3), 1159-1168. https://doi.org/10.1016/j.neuroimage.2010.11.063
- Hirschmann, J., Özkurt, T. E., Butz, M., Homburger, M., Elben, S., Hartmann, C. J., Vesper, J., Wojtecki, L., & Schnitzler, A. (2013). Differential modulation of STN-cortical and corticomuscular coherence by movement and levodopa in Parkinson's disease. Neuroimage. 68, 203-213. https://doi.org/10.1016/j.neuroimage.2012.11.036
- Hnazaee, M. F., Sure, M., O'Neill, G. C., Leogrande, G., Schnitzler, A., Florin, E., & Litvak, V. (2023). Combining magnetoencephalography with telemetric streaming of intracranial recordings and deep brain stimulation—A feasibility study. Imaging Neuroscience, 1, 1-22. https://doi.org/10.1162/imag a 00029
- Höglinger G., Trenkwalder C. et al., Parkinson-Krankheit, S2k-Leitlinie, 2023, in: Deutsche Gesellschaft für Neurologie (Hrsq.), Leitlinien für Diagnostik und Therapie in der Neurologie. Online: www.dgn.org/leitlinien (abgerufen am 13.04.2025).
- Hollunder, B., Ostrem, J. L., Sahin, I. A., Rajamani, N., Oxenford, S., Butenko, K., Neudorfer, C., Reinhardt, P., Zvarova, P., Polosan, M., Akram, H., Vissani, M., Zhang, C., Sun, B., Navratil, P., Reich, M. M., Volkmann, J., Yeh, F.-C., Baldermann, J. C., Dembek, T. A., Visser-Vandewalle, V., Alho, E. J. L., Franceschini, P. R., Nanda, P., Finke, C., Kühn, A. A., Dougherty, D. D., Richardson, R. M., Bergman, H., DeLong, M. R., Mazzoni, A., Romito, L. M., Tyagi, H., Zrinzo, L., Joyce, E. M., Chabardes, S., Starr, P. A., Li, N., & Horn, A. (2024). Mapping dysfunctional circuits in the frontal cortex using deep brain stimulation. Nature Neuroscience, 27, 573-586. https://doi.org/10.1038/s41593-024-01570-1
- Horn, A., Li, N., Meyer, G. M., Gadot, R., Provenza, N. R., & Sheth, S. A. (2025). Deep brain stimulation response circuits in obsessive compulsive disorder. Biological Psychiatry. https://doi.org/10.1016/j.biopsych.2025.03.008
- Horn, A., Neumann, W. J., Degen, K., Schneider, G. H., & Kühn, A. A. (2017). Toward an electrophysiological "sweet spot" for deep brain stimulation in the subthalamic nucleus. Human Brain Mapping, 38(7), 3377-3390. https://doi.org/10.1002/hbm.23594
- Igarashi, J., Isomura, Y., Arai, K., Harukuni, R., & Fukai, T. (2013). A θ-γ oscillation code for neuronal coordination during motor behavior. The Journal of Neuroscience, 33(47), 18515-18530. https://doi.org/10.1523/jneurosci.2126-13.2013
- Iyer, K. K., Au, T. R., Angwin, A. J., Copland, D. A., & Dissanayaka, N. N. (2020). Theta and gamma connectivity is linked with affective and cognitive symptoms in Parkinson's disease. Journal of Affective Disorders, 277, 875-884. https://doi.org/https://doi.org/10.1016/j.jad.2020.08.086
- Jankovic, J. (2008). Parkinson's disease: clinical features and diagnosis. Journal of Neurology, Neurosurgery and Psychiatry, 79(4), 368-376. https://doi.org/10.1136/jnnp.2007.131045
- Jokisch, D., & Jensen, O. (2007). Modulation of gamma and alpha activity during a working memory task engaging the dorsal or ventral stream. The Journal of Neuroscience, 27(12), 3244-3251. https://doi.org/10.1523/jneurosci.5399-06.2007

- Jones, S. R. (2016). When brain rhythms aren't 'rhythmic': Implication for their mechanisms and meaning. Current Opinion in Neurobiology, 40, 72-80. https://doi.org/10.1016/j.conb.2016.06.010
- Jurkiewicz, M., Gaetz, W., Bostan, A., & Cheyne, D. (2006). Post-movement beta rebound is generated in motor cortex: Evidence from neuromagnetic recordings. Neuroimage, 32, 1281-1289. https://doi.org/10.1016/j.neuroimage.2006.06.005
- Kennedy, J. S., Singh, K. D., & Muthukumaraswamy, S. D. (2011). An MEG investigation of the neural mechanisms subserving complex visuomotor coordination. International Journal of Psychophysiology, 79(2), 296-304. https://doi.org/https://doi.org/10.1016/j.ijpsycho.2010.11.003
- Khanna, P., & Carmena, J. M. (2017). Beta band oscillations in motor cortex reflect neural population signals that delay movement onset. *eLife*, 6, e24573. https://doi.org/10.7554/eLife.24573
- Khawaldeh, S., Tinkhauser, G., Shah, S. A., Peterman, K., Debove, I., Nguyen, T. A. K., Nowacki, A., Lachenmayer, M. L., Schuepbach, M., Pollo, C., Krack, P., Woolrich, M., & Brown, P. (2020). Subthalamic nucleus activity dynamics and limb movement prediction in Parkinson's disease. Brain, 143(2), 582-596. https://doi.org/10.1093/brain/awz417
- Klaus, A., Alves da Silva, J., & Costa, R. M. (2019). What, if, and when to move: Basal ganglia circuits and self-paced action initiation. Annual Review of Neuroscience, 42(1), 459-483. https://doi.org/10.1146/annurev-neuro-072116-031033
- Koh, M. J., Seol, J., Kang, J. I., Kim, B. S., Namkoong, K., Chang, J. W., & Kim, S. J. (2018). Altered resting-state functional connectivity in patients with obsessive-compulsive disorder: A magnetoencephalography study. International Journal of Psychophysiology, 123, 80-87. https://doi.org/https://doi.org/10.1016/j.ijpsycho.2017.10.012
- Kopřivová, J., Congedo, M., Horáček, J., Praško, J., Raszka, M., Brunovský, M., Kohútová, B., & Höschl, C. (2011). EEG source analysis in obsessive-compulsive disorder. Clinical Neurophysiology, 122(9), 1735-1743. https://doi.org/https://doi.org/10.1016/j.clinph.2011.01.051
- Körmendi, J., Ferentzi, E., Weiss, B., & Nagy, Z. (2021). Topography of movement-related delta and theta brain oscillations. *Brain Topography*, *34*(5), 608-617. https://doi.org/10.1007/s10548-021-00854-0
- Kühn, A. A., Tsui, A., Aziz, T., Ray, N., Brücke, C., Kupsch, A., Schneider, G. H., & Brown, P. (2009). Pathological synchronisation in the subthalamic nucleus of patients with Parkinson's disease relates to both bradykinesia and rigidity. Experimental Neurology, 215(2), 380-387. https://doi.org/10.1016/j.expneurol.2008.11.008
- Kühn, A. A., Williams, D., Kupsch, A., Limousin, P., Hariz, M., Schneider, G. H., Yarrow, K., & Brown, P. (2004). Event-related beta desynchronization in human subthalamic nucleus correlates with motor performance. Brain, 127(4), 735-746. https://doi.org/10.1093/brain/awh106
- Lee, I., Kim, K. M., & Lim, M. H. (2023). Theta and gamma activity differences in obsessivecompulsive disorder and panic disorder: Insights from resting-state eeg with eLORETA. Brain Sciences, 13(10). https://doi.org/10.3390/brainsci13101440
- Leventhal, Daniel K., Gage, Gregory J., Schmidt, R., Pettibone, Jeffrey R., Case, Alaina C., & Berke, Joshua D. (2012). Basal ganglia beta oscillations accompany cue utilization. Neuron, 73(3), 523-536. https://doi.org/10.1016/j.neuron.2011.11.032
- Litvak, V., Eusebio, A., Jha, A., Oostenveld, R., Barnes, G., Foltynie, T., Limousin, P., Zrinzo, L., Hariz, M. I., Friston, K., & Brown, P. (2012). Movement-related changes in local and longrange synchronization in Parkinson's disease revealed by simultaneous magnetoencephalography and intracranial recordings. The Journal of Neuroscience, 32(31), 10541. https://doi.org/10.1523/JNEUROSCI.0767-12.2012
- Lofredi, R., Neumann, W.-J., Bock, A., Horn, A., Huebl, J., Siegert, S., Schneider, G.-H., Krauss, J. K., & Kühn, A. A. (2018). Dopamine-dependent scaling of subthalamic gamma bursts

- with movement velocity in patients with Parkinson's disease. eLife, 7, e31895. https://doi.org/10.7554/eLife.31895
- Lofredi, R., Tan, H., Neumann, W.-J., Yeh, C.-H., Schneider, G.-H., Kühn, A. A., & Brown, P. (2019). Beta bursts during continuous movements accompany the velocity decrement in Parkinson's disease patients. *Neurobiology of Disease*, 127, 462-471. https://doi.org/https://doi.org/10.1016/j.nbd.2019.03.013
- London, D., Fazl, A., Katlowitz, K., Soula, M., Pourfar, M. H., Mogilner, A. Y., & Kiani, R. (2021). Distinct population code for movement kinematics and changes of ongoing movements in human subthalamic nucleus. eLife, 10, e64893. https://doi.org/10.7554/eLife.64893
- Mallet, L., Polosan, M., Jaafari, N., Baup, N., Welter, M. L., Fontaine, D., du Montcel, S. T., Yelnik, J., Chéreau, I., Arbus, C., Raoul, S., Aouizerate, B., Damier, P., Chabardès, S., Czernecki, V., Ardouin, C., Krebs, M. O., Bardinet, E., Chaynes, P., Burbaud, P., Cornu, P., Derost, P., Bougerol, T., Bataille, B., Mattei, V., Dormont, D., Devaux, B., Vérin, M., Houeto, J. L., Pollak, P., Benabid, A. L., Agid, Y., Krack, P., Millet, B., & Pelissolo, A. (2008). Subthalamic nucleus stimulation in severe obsessive-compulsive disorder. The New England Journal of Medicine, 359(20), 2121-2134. https://doi.org/10.1056/NEJMoa0708514
- Mann, J. M., Foote, K. D., Garvan, C. W., Fernandez, H. H., Jacobson, C. E. t., Rodriguez, R. L., Haq, I. U., Siddiqui, M. S., Malaty, I. A., Morishita, T., Hass, C. J., & Okun, M. S. (2009). Brain penetration effects of microelectrodes and DBS leads in STN or GPi. Journal of Neurology, Neurosurgery and Psychiatry, 80(7), 794-797. https://doi.org/10.1136/jnnp.2008.159558
- Mar-Barrutia, L., Real, E., Segalás, C., Bertolín, S., Menchón, J. M., & Alonso, P. (2021). Deep brain stimulation for obsessive-compulsive disorder: A systematic review of worldwide experience after 20 years. World Journal of Psychiatry, 11(9), 659-680. https://doi.org/10.5498/wjp.v11.i9.659
- Mathiopoulou, V., Lofredi, R., Feldmann, L. K., Habets, J., Darcy, N., Neumann, W. J., Faust, K., Schneider, G. H., & Kühn, A. A. (2024). Modulation of subthalamic beta oscillations by movement, dopamine, and deep brain stimulation in Parkinson's disease. npj Parkinson's Disease, 10(1), 77. https://doi.org/10.1038/s41531-024-00693-3
- Matz, O. C., & Spocter, M. (2022). The effect of Huntington's disease on the basal nuclei: A review. Cureus. 14(4), e24473, https://doi.org/10.7759/cureus.24473
- Mink, J. W. (1996). The basal ganglia: Focused selection and inhibition of competing motor programs. Progress in Neurobiology, 50(4), 381-425. https://doi.org/https://doi.org/10.1016/S0301-0082(96)00042-1
- Mostofi, A., Baig, F., Bourlogiannis, F., Uberti, M., Morgante, F., & Pereira, E. A. C. (2021). Postoperative externalization of deep brain stimulation leads does not increase infection risk. Neuromodulation: Technology at the Neural Interface, 24(2), 265-271. https://doi.org/https://doi.org/10.1111/ner.13331
- Muralidharan, V., & Aron, A. R. (2021). Behavioral induction of a high beta state in sensorimotor cortex leads to movement slowing. Journal of Cognitive Neuroscience, 33(7), 1311-1328. https://doi.org/10.1162/jocn a 01717
- Muthuraman, M., Bange, M., Koirala, N., Ciolac, D., Pintea, B., Glaser, M., Tinkhauser, G., Brown, P., Deuschl, G., & Groppa, S. (2020). Cross-frequency coupling between gamma oscillations and deep brain stimulation frequency in Parkinson's disease. Brain, 143(11), 3393-3407. https://doi.org/10.1093/brain/awaa297
- Neumann, W. J., Degen, K., Schneider, G. H., Brücke, C., Huebl, J., Brown, P., & Kühn, A. A. (2016). Subthalamic synchronized oscillatory activity correlates with motor impairment in patients with Parkinson's disease. Movement Disorders, 31(11), 1748-1751. https://doi.org/10.1002/mds.26759

- Neumann, W. J., Köhler, R. M., & Kühn, A. A. (2022). A practical guide to invasive neurophysiology in patients with deep brain stimulation. Clinical Neurophysiology, 140, 171-180. https://doi.org/https://doi.org/10.1016/j.clinph.2022.05.004
- Neumann, W. J., Steiner, L. A., & Milosevic, L. (2023). Neurophysiological mechanisms of deep brain stimulation across spatiotemporal resolutions. Brain, 146(11), 4456-4468. https://doi.org/10.1093/brain/awad239
- Nicolini, H., Arnold, P., Nestadt, G., Lanzagorta, N., & Kennedy, J. L. (2009). Overview of genetics and obsessive-compulsive disorder. Psychiatry Research, 170(1), 7-14. https://doi.org/https://doi.org/10.1016/j.psychres.2008.10.011
- Nolte, G. (2003). The magnetic lead field theorem in the quasi-static approximation and its use for magnetoencephalography forward calculation in realistic volume conductors. *Physics* in Medicine and Biology, 48(22), 3637-3652. https://doi.org/10.1088/0031-9155/48/22/002
- Oehrn, C. R., Cernera, S., Hammer, L. H., Shcherbakova, M., Yao, J., Hahn, A., Wang, S., Ostrem, J. L., Little, S., & Starr, P. A. (2024). Chronic adaptive deep brain stimulation versus conventional stimulation in Parkinson's disease: A blinded randomized feasibility trial. Nature Medicine. https://doi.org/10.1038/s41591-024-03196-z
- Olaru, M., Cernera, S., Hahn, A., Wozny, T. A., Anso, J., de Hemptinne, C., Little, S., Neumann, W.-J., Abbasi-Asl, R., & Starr, P. A. (2024). Motor network gamma oscillations in chronic home recordings predict dyskinesia in Parkinson's disease. Brain, 147(6), 2038-2052. https://doi.org/10.1093/brain/awae004
- Olson, J. W., Nakhmani, A., Irwin, Z. T., Edwards, L. J., Gonzalez, C. L., Wade, M. H., Black, S. D., Awad, M. Z., Kuhman, D. J., Hurt, C. P., Guthrie, B. L., & Walker, H. C. (2022). Cortical and subthalamic nucleus spectral changes during limb movements in Parkinson's disease patients with and without dystonia. Movement Disorders, 37(8), 1683-1692. https://doi.org/https://doi.org/10.1002/mds.29057
- Olson, M. C., Shill, H., Ponce, F., & Aslam, S. (2023). Deep brain stimulation in PD: Risk of complications, morbidity, and hospitalizations: A systematic review. Frontiers in Aging Neuroscience, 15, 1258190. https://doi.org/10.3389/fnagi.2023.1258190
- Oswal, A., Beudel, M., Zrinzo, L., Limousin, P., Hariz, M., Foltynie, T., Litvak, V., & Brown, P. (2016). Deep brain stimulation modulates synchrony within spatially and spectrally distinct resting state networks in Parkinson's disease. Brain, 139(5), 1482-1496. https://doi.org/10.1093/brain/aww048
- Oswal, A., Cao, C., Yeh, C.-H., Neumann, W.-J., Gratwicke, J., Akram, H., Horn, A., Li, D., Zhan, S., Zhang, C., Wang, Q., Zrinzo, L., Foltynie, T., Limousin, P., Bogacz, R., Sun, B., Husain, M., Brown, P., & Litvak, V. (2021). Neural signatures of hyperdirect pathway activity in Parkinson's disease. Nature Communications, 12(1), 5185. https://doi.org/10.1038/s41467-021-25366-0
- Oswal, A., Litvak, V., Brücke, C., Huebl, J., Schneider, G. H., Kühn, A. A., & Brown, P. (2013). Cognitive factors modulate activity within the human subthalamic nucleus during voluntary movement in Parkinson's disease. The Journal of Neuroscience, 33(40), 15815-15826. https://doi.org/10.1523/JNEUROSCI.1790-13.2013
- Oswal, A., Litvak, V., Sauleau, P., & Brown, P. (2012). Beta reactivity, prospective facilitation of executive processing, and its dependence on dopaminergic therapy in Parkinson's disease. The Journal of Neuroscience, 32(29), 9909-9916. https://doi.org/10.1523/JNEUROSCI.0275-12.2012
- Özkurt, T. E., Butz, M., Homburger, M., Elben, S., Vesper, J., Wojtecki, L., & Schnitzler, A. (2011). High frequency oscillations in the subthalamic nucleus: A neurophysiological marker of the motor state in Parkinson's disease. Experimental Neurology, 229(2), 324-331. https://doi.org/10.1016/j.expneurol.2011.02.015

- Parastarfeizabadi, M., & Kouzani, A. Z. (2017). Advances in closed-loop deep brain stimulation devices. Journal of NeuroEngineering and Rehabilitation, 14(1), 79. https://doi.org/10.1186/s12984-017-0295-1
- Parrino, L., Ferrillo, F., Smerieri, A., Spaggiari, M. C., Palomba, V., Rossi, M., & Terzano, M. G. (2004). Is insomnia a neurophysiological disorder? The role of sleep EEG microstructure. Brain Research Bulletin, 63(5), 377-383. https://doi.org/https://doi.org/10.1016/j.brainresbull.2003.12.010
- Patai, E. Z., Foltynie, T., Limousin, P., Akram, H., Zrinzo, L., Bogacz, R., & Litvak, V. (2022). Conflict detection in a sequential decision task is associated with increased corticosubthalamic coherence and prolonged subthalamic oscillatory response in the β band. The Journal of Neuroscience, 42(23), 4681. https://doi.org/10.1523/JNEUROSCI.0572-21.2022
- Perera, M. P. N., Mallawaarachchi, S., Bailey, N. W., Murphy, O. W., & Fitzgerald, P. B. (2023). Obsessive-compulsive disorder (OCD) is associated with increased electroencephalographic (EEG) delta and theta oscillatory power but reduced delta connectivity. Journal of Psychiatric Research, 163, 310-317. https://doi.org/https://doi.org/10.1016/j.jpsychires.2023.05.026
- Pfurtscheller, G. (1992). Event-related synchronization (ERS): An electrophysiological correlate of cortical areas at rest. Electroencephalography and Clinical Neurophysiology, 83(1), 62-69. https://doi.org/10.1016/0013-4694(92)90133-3
- Pfurtscheller, G., Neuper, C., Brunner, C., & da Silva, F. L. (2005). Beta rebound after different types of motor imagery in man. Neuroscience Letters, 378(3), 156-159. https://doi.org/10.1016/j.neulet.2004.12.034
- Piña-Fuentes, D., van Dijk, J. M. C., van Zijl, J. C., Moes, H. R., van Laar, T., Oterdoom, D. L. M., Little, S., Brown, P., & Beudel, M. (2020). Acute effects of adaptive deep brain stimulation in Parkinson's disease. Brain Stimulation, 13(6), 1507-1516. https://doi.org/10.1016/j.brs.2020.07.016
- Pouratian, N., Thakkar, S., Kim, W., & Bronstein, J. M. (2012). Deep brain stimulation for the treatment of Parkinson's disease: Efficacy and safety. Degenerative Neurological and Neuromuscular Disease, 2, 107-117. https://doi.org/10.2147/DNND.S25750
- Qing, X., Gu, L., & Li, D. (2021). Abnormalities of localized connectivity in obsessive-compulsive disorder: A voxel-wise meta-analysis. Frontiers in Human Neuroscience. 15, 739175. https://doi.org/10.3389/fnhum.2021.739175
- Radcliffe, E. M., Baumgartner, A. J., Kern, D. S., Al Borno, M., Ojemann, S., Kramer, D. R., & Thompson, J. A. (2023). Oscillatory beta dynamics inform biomarker-driven treatment optimization for Parkinson's disease. Journal of Neurophysiology, 129(6), 1492-1504. https://doi.org/10.1152/jn.00055.2023
- Rappel, P., Marmor, O., Bick, A. S., Arkadir, D., Linetsky, E., Castrioto, A., Tamir, I., Freedman, S. A., Mevorach, T., Gilad, M., Bergman, H., Israel, Z., & Eitan, R. (2018). Subthalamic theta activity: A novel human subcortical biomarker for obsessive compulsive disorder. Translational Psychiatry, 8(1), 118. https://doi.org/10.1038/s41398-018-0165-z
- Raviv, N., Staudt, M. D., Rock, A. K., MacDonell, J., Slyer, J., & Pilitsis, J. G. (2020). A systematic review of deep brain stimulation targets for obsessive compulsive disorder. Neurosurgery, 87(6). https://doi.org/10.1093/neuros/nyaa249
- Ray, N. J., Brittain, J.-S., Holland, P., Joundi, R. A., Stein, J. F., Aziz, T. Z., & Jenkinson, N. (2012). The role of the subthalamic nucleus in response inhibition: Evidence from local field potential recordings in the human subthalamic nucleus. Neuroimage, 60(1), 271-278. https://doi.org/10.1016/j.neuroimage.2011.12.035
- Redgrave, P., Prescott, T. J., & Gurney, K. (1999). The basal ganglia: A vertebrate solution to the selection problem? Neuroscience, 89(4), 1009-1023. https://doi.org/10.1016/s0306-4522(98)00319-4

- Rossiter, H. E., Davis, E. M., Clark, E. V., Boudrias, M.-H., & Ward, N. S. (2014). Beta oscillations reflect changes in motor cortex inhibition in healthy ageing. Neuroimage, 91, 360-365. https://doi.org/https://doi.org/10.1016/j.neuroimage.2014.01.012
- Sallard, E., Tallet, J., Thut, G., Deiber, M.-P., & Barral, J. (2016). Age-related changes in postmovement beta synchronization during a selective inhibition task. Experimental Brain Research, 234(12), 3543-3553. https://doi.org/10.1007/s00221-016-4753-v
- Salmelin, R., Hämäläinen, M., Kajola, M., & Hari, R. (1995). Functional segregation of movement-related rhythmic activity in the human brain. *Neuroimage*, 2(4), 237-243. https://doi.org/10.1006/nimg.1995.1031
- Schmidt, R., & Berke, J. D. (2017). A pause-then-cancel model of stopping: Evidence from basal ganglia neurophysiology. Philosophical Transactions of the Royal Society B: Biological Sciences, 372(1718). https://doi.org/10.1098/rstb.2016.0202
- Schmidt, R., Herrojo Ruiz, M., Kilavik, B. E., Lundqvist, M., Starr, P. A., & Aron, A. R. (2019). Beta oscillations in working memory, executive control of movement and thought, and sensorimotor function. The Journal of Neuroscience, 39(42), 8231-8238. https://doi.org/10.1523/JNEUROSCI.1163-19.2019
- Schnitzler, A., & Gross, J. (2005). Normal and pathological oscillatory communication in the brain. Nature Reviews Neuroscience, 6(4), 285-296. https://doi.org/10.1038/nrn1650
- Schwabe, K., Alam, M., Saryyeva, A., Lütjens, G., Heissler, H. E., Winter, L., Heitland, I., Krauss, J. K., & Kahl, K. G. (2021). Oscillatory activity in the BNST/ALIC and the frontal cortex in OCD: Acute effects of DBS. Journal of Neural Transmission, 128(2), 215-224. https://doi.org/10.1007/s00702-020-02297-6
- Shi, Y., Wang, M., Xiao, L., Gui, L., Zheng, W., Bai, L., Su, B., Li, B., Xu, Y., Pan, W., Zhang, J., & Wang, W. (2022). Potential therapeutic mechanism of deep brain stimulation of the nucleus accumbens in obsessive-compulsive disorder. Frontiers in Cellular Neuroscience, 16, 1057887. https://doi.org/10.3389/fncel.2022.1057887
- Singh, A., Cole, R. C., Espinoza, A. I., Brown, D., Cavanagh, J. F., & Narayanan, N. S. (2020). Frontal theta and beta oscillations during lower-limb movement in Parkinson's disease. Clinical Neurophysiology, 131(3), 694-702. https://doi.org/https://doi.org/10.1016/j.clinph.2019.12.399
- Singh, A., Richardson, S. P., Narayanan, N., & Cavanagh, J. F. (2018). Mid-frontal theta activity is diminished during cognitive control in Parkinson's disease. Neuropsychologia, 117. 113-122. https://doi.org/https://doi.org/10.1016/j.neuropsychologia.2018.05.020
- Smith, E. E., Schüller, T., Huys, D., Baldermann, J. C., Andrade, P., Allen, J. J. B., Visser-Vandewalle, V., Ullsperger, M., Gruendler, T. O. J., & Kuhn, J. (2020). A brief demonstration of frontostriatal connectivity in OCD patients with intracranial electrodes. Neuroimage, 220, 117138. https://doi.org/https://doi.org/10.1016/j.neuroimage.2020.117138
- Smolders, R., Mazaheri, A., van Wingen, G., Figee, M., de Koning, P. P., & Denys, D. (2013). Deep brain stimulation targeted at the nucleus accumbens decreases the potential for pathologic network communication. *Biological Psychiatry*, 74(10), e27-e28. https://doi.org/10.1016/j.biopsych.2013.03.012
- Soh, C., Hervault, M., Rohl, A. H., Greenlee, J. D. W., & Wessel, J. R. (2025). Precisely-timed outpatient recordings of subcortical local field potentials from wireless streaming-capable deep-brain stimulators: A method and toolbox. Journal of Neuroscience Methods, 418, 110448. https://doi.org/https://doi.org/10.1016/j.jneumeth.2025.110448
- Steina, A., Sure, S., Butz, M., Vesper, J., Schnitzler, A., & Hirschmann, J. (2025). Oscillatory coupling between thalamus, cerebellum, and motor cortex in essential tremor. Movement Disorders, 40(5), 896-905. https://doi.org/https://doi.org/10.1002/mds.30165
- Swann, N., de Hemptinne, C., Miocinovic, S., Qasim, S., Wang, S. S., Ziman, N., Ostrem, J. L., San Luciano, M., Galifianakis, N. B., & Starr, P. A. (2016). Gamma oscillations in the hyperkinetic state detected with chronic human brain recordings in Parkinson's disease.

- The Journal of Neuroscience, 36(24), 6445. https://doi.org/10.1523/JNEUROSCI.1128-16.2016
- Swann, N., Tandon, N., Canolty, R., Ellmore, T. M., McEvoy, L. K., Dreyer, S., DiSano, M., & Aron, A. R. (2009). Intracranial EEG reveals a time- and frequency-specific role for the right inferior frontal gyrus and primary motor cortex in stopping initiated responses. The Journal of Neuroscience, 29(40), 12675. https://doi.org/10.1523/JNEUROSCI.3359-09.2009
- Talakoub, O., Neagu, B., Udupa, K., Tsang, E., Chen, R., Popovic, M. R., & Wong, W. (2016). Time-course of coherence in the human basal ganglia during voluntary movements. Scientific Reports, 6(1), 34930. https://doi.org/10.1038/srep34930
- Tan, H., Pogosyan, A., Anzak, A., Ashkan, K., Bogdanovic, M., Green, A. L., Aziz, T., Foltynie, T., Limousin, P., Zrinzo, L., & Brown, P. (2013). Complementary roles of different oscillatory activities in the subthalamic nucleus in coding motor effort in Parkinsonism. Experimental Neurology, 248, 187-195. https://doi.org/https://doi.org/10.1016/j.expneurol.2013.06.010
- Tan, H., Wade, C., & Brown, P. (2016). Post-movement beta activity in sensorimotor cortex indexes confidence in the estimations from internal models. The Journal of Neuroscience, 36(5), 1516. https://doi.org/10.1523/JNEUROSCI.3204-15.2016
- Tan, H., Zavala, B., Pogosyan, A., Ashkan, K., Zrinzo, L., Foltynie, T., Limousin, P., & Brown, P. (2014). Human subthalamic nucleus in movement error detection and its evaluation during visuomotor adaptation. The Journal of Neuroscience, 34(50), 16744. https://doi.org/10.1523/JNEUROSCI.3414-14.2014
- Thenaisie, Y., Lee, K., Moerman, C., Scafa, S., Gálvez, A., Pirondini, E., Burri, M., Ravier, J., Puiatti, A., Accolla, E., Wicki, B., Zacharia, A., Castro Jiménez, M., Bally, J. F., Courtine, G., Bloch, J., & Moraud, E. M. (2022). Principles of gait encoding in the subthalamic nucleus of people with Parkinson's disease. Science Translational Medicine, 14(661), eabo1800. https://doi.org/10.1126/scitranslmed.abo1800
- Tiihonen, M., Westner, B. U., Butz, M., & Dalal, S. S. (2021). Parkinson's disease patients benefit from bicycling - a systematic review and meta-analysis. npj Parkinson's Disease, 7(1), 86. https://doi.org/10.1038/s41531-021-00222-6
- Tinkhauser, G., Pogosyan, A., Little, S., Beudel, M., Herz, D. M., Tan, H., & Brown, P. (2017). The modulatory effect of adaptive deep brain stimulation on beta bursts in Parkinson's disease. Brain, 140(4), 1053-1067. https://doi.org/10.1093/brain/awx010
- Tinkhauser, G., Pogosyan, A., Tan, H., Herz, D. M., Kühn, A. A., & Brown, P. (2017). Beta burst dynamics in Parkinson's disease OFF and ON dopaminergic medication. Brain, 140(11), 2968-2981. https://doi.org/10.1093/brain/awx252
- Toledo, J. B., López-Azcárate, J., Garcia-Garcia, D., Guridi, J., Valencia, M., Artieda, J., Obeso, J., Alegre, M., & Rodriguez-Oroz, M. (2014). High beta activity in the subthalamic nucleus and freezing of gait in Parkinson's disease. Neurobiology of Disease, 64, 60-65. https://doi.org/https://doi.org/10.1016/j.nbd.2013.12.005
- Turner, R. S., & Desmurget, M. (2010). Basal ganglia contributions to motor control: A vigorous tutor. Current Opinion in Neurobiology, 20(6), 704-716. https://doi.org/10.1016/j.conb.2010.08.022
- Tzagarakis, C., Ince, N. F., Leuthold, A. C., & Pellizzer, G. (2010). Beta-band activity during motor planning reflects response uncertainty. The Journal of Neuroscience, 30(34), 11270-11277. https://doi.org/10.1523/jneurosci.6026-09.2010
- van Roessel, P. J., Grassi, G., Aboujaoude, E. N., Menchón, J. M., Van Ameringen, M., & Rodríguez, C. I. (2023). Treatment-resistant OCD: Pharmacotherapies in adults. Comprehensive Psychiatry, 120, 152352. https://doi.org/https://doi.org/10.1016/j.comppsych.2022.152352
- Van Veen, B. D., van Drongelen, W., Yuchtman, M., & Suzuki, A. (1997). Localization of brain electrical activity via linearly constrained minimum variance spatial filtering. IEEE

- Transactions on Biomedical Engineering, 44(9), 867-880. https://doi.org/10.1109/10.623056
- van Wijk, B. C. M., Neumann, W.-J., Schneider, G.-H., Sander, T. H., Litvak, V., & Kühn, A. A. (2017). Low-beta cortico-pallidal coherence decreases during movement and correlates with overall reaction time. Neuroimage, 159, 1-8. https://doi.org/10.1016/j.neuroimage.2017.07.024
- Vázquez-Vélez, G. E., & Zoghbi, H. Y. (2021). Parkinson's disease genetics and pathophysiology. Annual Review of Neuroscience, 44, 87-108. https://doi.org/10.1146/annurev-neuro-100720-034518
- Vinding, M. C., Tsitsi, P., Piitulainen, H., Waldthaler, J., Jousmäki, V., Ingvar, M., Svenningsson, P., & Lundqvist, D. (2019). Attenuated beta rebound to proprioceptive afferent feedback in Parkinson's disease. Scientific Reports, 9(1), 2604. https://doi.org/10.1038/s41598-019-39204-3
- Voderholzer, U., Rubart, A., Favreau, M., Kathmann, N., Staniloiu, A., Wahl-Kordon, A., & Zurowski, B. S3-Leitlinie Zwangsstörungen – Langversion, 2022, in: Deutsche Gesellschaft für Psychiatrie und Psychotherapie, Psychosomatik und Nervenheilkunde (Hrsg.) Online: https://register.awmf.org/assets/quidelines/038 017I S3 Zwangsst%C3%B6rungen 202 2-07.pdf (abgerufen am 15.04.2025).
- Wagner, J., Wessel, J. R., Ghahremani, A., & Aron, A. R. (2018). Establishing a right frontal beta signature for stopping action in scalp eeg: Implications for testing inhibitory control in other task contexts. Journal of Cognitive Neuroscience, 30(1), 107-118. https://doi.org/10.1162/jocn a 01183
- Ward, L. M. (2003). Synchronous neural oscillations and cognitive processes. Trends in Cognitive Sciences, 7(12), 553-559. https://doi.org/https://doi.org/10.1016/j.tics.2003.10.012
- Weinberger, M., Hutchison, W. D., Lozano, A. M., Hodaie, M., & Dostrovsky, J. O. (2009). Increased gamma oscillatory activity in the subthalamic nucleus during tremor in Parkinson's disease patients. *Journal of Neurophysiology*, 101(2), 789-802. https://doi.org/10.1152/jn.90837.2008
- Werner, C. (2019). Demographics of OCD and effective treatment: Brief report. Biomedical Journal of Scientific & Technical Research, 22. https://doi.org/10.26717/BJSTR.2019.22.003761
- Wessel, J. R. (2020). β-bursts reveal the trial-to-trial dynamics of movement initiation and cancellation. The Journal of Neuroscience, 40(2), 411. https://doi.org/10.1523/JNEUROSCI.1887-19.2019
- Wessel, J. R., Ghahremani, A., Udupa, K., Saha, U., Kalia, S. K., Hodaie, M., Lozano, A. M., Aron, A. R., & Chen, R. (2016). Stop-related subthalamic beta activity indexes global motor suppression in Parkinson's disease. Movement Disorders, 31(12), 1846-1853. https://doi.org/10.1002/mds.26732
- Wichmann, T., & DeLong, M. R. (1996). Functional and pathophysiological models of the basal ganglia. Current Opinion in Neurobiology, 6(6), 751-758. https://doi.org/https://doi.org/10.1016/S0959-4388(96)80024-9
- Wiest, C., Tinkhauser, G., Pogosyan, A., He, S., Baig, F., Morgante, F., Mostofi, A., Pereira, E. A., Tan, H., Brown, P., & Torrecillos, F. (2021). Subthalamic deep brain stimulation induces finely-tuned gamma oscillations in the absence of levodopa. Neurobiology of Disease, 152, 105287. https://doi.org/https://doi.org/10.1016/j.nbd.2021.105287
- Wilkins, K. B., Petrucci, M. N., Lambert, E. F., Melbourne, J. A., Gala, A. S., Akella, P., Parisi, L., Cui, C., Kehnemouyi, Y. M., Hoffman, S. L., Aditham, S., Diep, C., Dorris, H. J., Parker, J. E., Herron, J. A., & Bronte-Stewart, H. M. (2024). Beta burst-driven adaptive deep brain stimulation improves gait impairment and freezing of gait in Parkinson's disease. medRxiv. https://doi.org/10.1101/2024.06.26.24309418

- Winkler, L., Butz, M., Sharma, A., Vesper, J., Schnitzler, A., Fischer, P., & Hirschmann, J. (2025). Context-dependent modulations of subthalamo-cortical synchronization during rapid reversals of movement direction in Parkinson's disease. eLife. 13. RP101769. https://doi.org/10.7554/eLife.101769
- Winkler, L., Werner, L. M., Butz, M., Hartmann, C. J., Schnitzler, A., & Hirschmann, J. (2025). Deep brain stimulation-responsive subthalamo-cortical coupling in obsessive-compulsive disorder. *medRvix*. https://doi.org/10.1101/2025.06.12.25329123
- Wojtecki, L., Hirschmann, J., Elben, S., Boschheidgen, M., Trenado, C., Vesper, J., & Schnitzler, A. (2017). Oscillatory coupling of the subthalamic nucleus in obsessive compulsive disorder. Brain, 140(9), e56. https://doi.org/10.1093/brain/awx164
- Wooten, G. F., Currie, L. J., Bovbjerg, V. E., Lee, J. K., & Patrie, J. (2004). Are men at greater risk for Parkinson's disease than women? Journal of Neurology, Neurosurgery and Psychiatry, 75(4), 637-639. https://doi.org/10.1136/jnnp.2003.020982
- Xiong, B., Wen, R., Gao, Y., & Wang, W. (2023). Longitudinal changes of local field potential oscillations in nucleus accumbens and anterior limb of the internal capsule in obsessivecompulsive disorder. Biological Psychiatry, 93(11), e39-e41. https://doi.org/10.1016/j.biopsych.2021.06.004
- Zaepffel, M., Trachel, R., Kilavik, B. E., & Brochier, T. (2013). Modulations of EEG beta power during planning and execution of grasping movements. PLOS ONE, 8(3), e60060. https://doi.org/10.1371/journal.pone.0060060
- Zavala, B., Brittain, J.-S., Jenkinson, N., Ashkan, K., Foltynie, T., Limousin, P., Zrinzo, L., Green, A. L., Aziz, T., Zaghloul, K., & Brown, P. (2013). Subthalamic nucleus local field potential activity during the Eriksen Flanker Task reveals a novel role for theta phase during conflict monitoring. The Journal of Neuroscience, 33(37), 14758. https://doi.org/10.1523/JNEUROSCI.1036-13.2013
- Zavala, B., Damera, S., Dong, J. W., Lungu, C., Brown, P., & Zaghloul, K. A. (2017). Human subthalamic nucleus theta and beta oscillations entrain neuronal firing during sensorimotor conflict. Cerebral Cortex, 27(1), 496-508. https://doi.org/10.1093/cercor/bhv244
- Zavala, B., Jang, A., Trotta, M., Lungu, C. I., Brown, P., & Zaghloul, K. A. (2018). Cognitive control involves theta power within trials and beta power across trials in the prefrontalsubthalamic network. Brain, 141(12), 3361-3376. https://doi.org/10.1093/brain/awy266
- Zavala, B., Jang, A. I., & Zaghloul, K. A. (2017). Human subthalamic nucleus activity during nonmotor decision making. eLife, 6, e31007. https://doi.org/10.7554/eLife.31007
- Zhang, J., Wei, L., Hu, X., Xie, B., Zhang, Y., Wu, G.-R., & Wang, J. (2015). Akinetic-rigid and tremor-dominant Parkinson's disease patients show different patterns of intrinsic brain activity. Parkinsonism & Related Disorders, 21(1), 23-30. https://doi.org/https://doi.org/10.1016/j.parkreldis.2014.10.017
- Zhao, W., Makowski, C., Hagler, D. J., Garavan, H. P., Thompson, W. K., Greene, D. J., Jernigan, T. L., & Dale, A. M. (2023). Task fMRI paradigms may capture more behaviorally relevant information than resting-state functional connectivity. Neuroimage, 270, 119946. https://doi.org/https://doi.org/10.1016/j.neuroimage.2023.119946

9. Erklärung

Ich versichere an Eides Statt, dass die Dissertation von mir selbständig und ohne unzulässige fremde Hilfe unter Beachtung der "Grundsätze zur Sicherung guter wissenschaftlicher Praxis an der Heinrich-Heine-Universität Düsseldorf" erstellt worden ist. Die Dissertation wurde in der vorliegenden oder in ähnlicher Form noch bei keiner anderen Institution eingereicht. Ich habe bisher keine erfolglosen Promotionsversuche unternommen.

Düsseldorf, den

Lucie Winkler

10. Danksagung

Zunächst möchte ich Herrn Prof. Dr. Schnitzler herzlich danken, dass er mir die Möglichkeit gegeben hat, an seinem Institut zu promovieren und an spannenden Projekten mitzuarbeiten.

Mein besonderer Dank gilt meinem Doktorvater, Herrn Prof. Dr. Markus Butz, für die hervorragende Betreuung, die motivierenden Worte, die Aufmunterung in herausfordernden Momenten und die vielen netten und wertvollen Gespräche.

Ebenso danke ich Herrn Dr. Jan Hirschmann für die großartige Zusammenarbeit über all die Jahre, sein Verständnis, seine Geduld und dafür, dass ich mich stets als Teil seiner Arbeitsgruppe fühlen durfte. Mein Dank gilt auch Frau Dr. Petra Fischer für die inspirierende und freundliche Zusammenarbeit am "Reverse"-Projekt.

Herrn Prof. Dr. Gerhard Jocham danke ich für die Zweitbetreuung meiner Doktorarbeit und die angenehme Zusammenarbeit.

Ohne die Patientinnen und Patienten, die an meinen Studien teilgenommen haben, wäre diese Arbeit nicht möglich gewesen. Ihnen gebührt mein tiefster Dank. An dieser Stelle möchte ich auch Herrn Prof. Dr. Jan Vesper für die neurochirurgische Unterstützung danken.

Mein herzliches Dankeschön richte ich an meine Kolleginnen und Kollegen am Institut für Klinische Neurowissenschaften und Medizinische Psychologie. Danke für die schöne Zeit, sowohl während der Arbeit als auch darüber hinaus. Ein besonderer Dank gilt Lucy. Es war schön, über die Jahre das Büro mit dir zu teilen, Höhen und Tiefen zusammen zu meistern und dabei nie den Spaß zu verlieren. Meiner Kollegin Alex danke ich ebenso herzlich - zusammen mit Lucy habe ich mit ihr spannende Konferenzen in Washington D.C. und Kopenhagen erleben dürfen. Nicht zuletzt danke ich allen Kolleginnen und Kollegen, mit denen ich in der Lehre tätig sein durfte, insbesondere Herrn Prof. Dr. Markus Butz und Frau Dr. Katja Biermann-Ruben. Ebenso bedanke ich mich bei allen, die diese Arbeit sorgfältig Korrektur gelesen haben.

Von Herzen danke ich meiner Familie und meinen Freunden für ihre anhaltende Unterstützung in den vergangenen Jahren. Besonderer Dank gilt dabei meinen Schwestern, Amelie und Leonie, und meiner Schwiegerfamilie.

Abschließend möchte ich drei Menschen meinen tiefsten Dank aussprechen:

Meinen Eltern danke ich von Herzen dafür, dass sie immer an mich geglaubt, mich unterstützt und mich auch manchmal davon überzeugt haben, den Laptop beiseitezulegen. Ihr habt euch stets für meine Arbeit interessiert und mich auf diesem Weg begleitet. Ohne euch wäre all dies nicht möglich gewesen. Meinem Mann und besten Freund, Dijan, danke ich für seine unermüdliche Unterstützung, seine Aufmunterung und die geteilte Freude. Danke, dass du mich auf drei Konferenzen begleitet hast und nun mehr über das Beta-Frequenzband weißt, als dir lieb ist. Ich weiß nicht, wie ich das alles ohne dich geschafft hätte. Am schönsten ist es, diese Freude nun mit dir und unserer kleinen Nayla teilen zu dürfen.

11. Appendix

This work is based on the following:

Appendix 1:

Winkler, L., Butz, M., Sharma, A., Vesper, J., Schnitzler, A., Fischer, P., & Hirschmann, J. (2025). Context-dependent modulations of subthalamo-cortical synchronization during rapid reversals of movement direction in Parkinson's disease. eLife, 13, RP101769. https://doi.org/10.7554/eLife.101769

Statement of contribution

J.H., P.F. and M.B. planned this research project. The data recordings started before I began my PhD, but most of the data was recorded by me with the support of J.H. and M.B. I conducted the analysis of the behavioral data with P.F. The analysis of the electrophysiological data, including the preprocessing, was performed by me. I prepared the figures for this manuscript and wrote the manuscript. All authors discussed the results and edited the manuscript.

Copyright and license notice

This article is licensed under a Creative Commons Attribution 4.0 International License, which permits use, sharing, adaptation, distribution and reproduction in any medium or format, as long as you give appropriate credit to the original author(s) and the source, provide a link to the Creative Commons license, and indicate if changes were made. To view a copy of this license, visit http://creativecommons.org/licenses/by/4.0

Appendix 2:

Winkler, L., Werner, L. M., Butz, M., Hartmann, C. J., Schnitzler, A., & Hirschmann, J. (2025). Deep brain stimulation-responsive subthalamo-cortical coupling in obsessive-compulsive disorder. medRxiv. https://doi.org/10.1101/2025.06.12.25329123

Statement of contribution

J.H., A.S. and L.M.W. planned this research project. The data recordings were performed by J.H. and L.M.W. I conducted the analysis, including the preprocessing, of the data. I prepared all figures for this manuscript and wrote the manuscript. All authors discussed the results and edited the manuscript.

Copyright and license notice

This article is licensed under a Creative Commons Attribution 4.0 International License, which permits use, sharing, adaptation, distribution and reproduction in any medium or format, as long as you give appropriate credit to the original author(s) and the source, provide a link to the Creative Commons license, and indicate if changes were made. To view a copy of this license, visit http://creativecommons.org/licenses/by/4.0



Context-dependent modulations of subthalamo-cortical synchronization during rapid reversals of movement direction in Parkinson's disease

Lucie Winkler¹, Markus Butz¹, Abhinav Sharma^{2,3}, Jan Vesper⁴, Alfons Schnitzler¹, Petra Fischer^{5*}, Jan Hirschmann¹

¹Institute of Clinical Neuroscience and Medical Psychology, Medical Faculty and University Hospital Düsseldorf, Heinrich Heine University Düsseldorf, Duesseldorf, Germany; ²Medical Research Council Brain Network Dynamics Unit, University of Oxford, Oxford, United Kingdom; ³Nuffield Department of Clinical Neurosciences, University of Oxford, Oxford, United Kingdom; ⁴Department of Functional Neurosurgery and Stereotaxy, Medical Faculty and University Hospital Düsseldorf, Düsseldorf, Germany; ⁵School of Physiology, Pharmacology & Neuroscience, University of Bristol, Bristol, United Kingdom

*For correspondence: petra.fischer@bristol.ac.uk

Competing interest: The authors declare that no competing interests exist.

Funding: See page 16

Sent for Review 09 August 2024 Preprint posted 21 August 2024

Reviewed preprint posted 11 November 2024

Reviewed preprint revised 14 February 2025

Version of Record published 05 June 2025

Reviewing Editor: Laura L Colgin, University of Texas at Austin, United States

© Copyright Winkler et al. This article is distributed under the terms of the Creative Commons Attribution License, which permits unrestricted use and redistribution provided that the original author and source are credited.

eLife Assessment

This **valuable** study combined whole-head magnetoencephalography (MEG) and subthalamic (STN) local field potential (LFP) recordings in patients with Parkinson's disease undergoing deep brain stimulation surgery. The paper provides **convincing** evidence that cortical and STN beta oscillations are sensitive to movement context.

Abstract The role of beta band activity in cortico-basal ganglia interactions during motor control has been studied extensively in resting-state and for simple movements, such as button pressing. However, little is known about how beta oscillations change and interact in more complex situations involving rapid changes of movement in various contexts. To close this knowledge gap, we combined magnetoencephalography (MEG) and local field potential recordings from the subthalamic nucleus (STN) in Parkinson's disease patients to study beta dynamics during initiation, stopping, and rapid reversal of rotational movements. The action prompts were manipulated to be predictable vs. unpredictable. We observed movement-related beta suppression at motor sequence start, and a beta rebound after motor sequence stop in STN power, motor cortical power, and STN-cortex coherence. Despite involving a brief stop of movement, no clear rebound was observed during reversals of turning direction. At the cortical level, beta power decreased bilaterally following reversals, but more so in the hemisphere ipsilateral to movement, due to a floor effect on the contralateral side. In the STN, power modulations varied across patients, with patients displaying brief increases or decreases of high-beta power. Importantly, cue predictability affected these modulations. Event-related increases of STNcortex beta coherence were generally stronger in the unpredictable than in the predictable condition. In summary, this study reveals the influence of movement context on beta oscillations in basal gangliacortex loops when humans change ongoing movements according to external cues. We find that movement scenarios requiring higher levels of caution involve enhanced modulations of subthalamocortical beta synchronization. Furthermore, our results confirm that beta oscillations reflect the start and end of motor sequences better than movement changes within a sequence.



Introduction

Beta oscillations within cortical sensorimotor areas and the basal ganglia have been proposed to play a role in movement initiation, termination, and inhibition (Benis et al., 2014; Jurkiewicz et al., 2006; Wessel, 2020). Altered beta band activity has been strongly linked to motor impairment in Parkinson's disease (PD), demonstrating its relevance to proper motor performance (Brown et al., 2001; Cassidy et al., 2002; Tinkhauser et al., 2017). The beta rhythm is often interpreted as reflecting the status quo (Engel and Fries, 2010), that is, active maintenance or stabilization of current motor or cognitive output to attenuate alternatives and distractions (Espenhahn et al., 2017; Fischer et al., 2019). The basal ganglia keep cortex under inhibitory control (Bonnevie and Zaghloul, 2019) which, similarly to releasing a break in a car, must be removed to change the current motor state (Alegre et al., 2013).

Starting and stopping of movement have mostly been studied with variations of the Stop Signal Task and the Go/No-Go Task (Alegre et al., 2013; Aron and Poldrack, 2006; Ray et al., 2012) that require participants to perform simple, ballistic movements and inhibit them occasionally. Shortly before and during movement, beta oscillations are suppressed (beta suppression), reflecting a task-related active state of the motor network (Jurkiewicz et al., 2006). In contrast, beta power transiently increases above baseline levels after movement termination (beta rebound) (Fonken et al., 2016; Ray et al., 2012), indicating inhibition (Salmelin et al., 1995; Schmidt and Berke, 2017) and motor adaptation processes (Struber et al., 2021; Tan et al., 2014). Whether these modulations are causally involved in motor control is still under debate (Pfurtscheller et al., 2005; Toledo et al., 2016).

Response inhibition has been associated with increased beta power or reduced suppression thereof in prefrontal cortical areas (*Swann et al., 2009*; *Wagner et al., 2018*), and in the subthalamic nucleus (STN) (*Bastin et al., 2014*), with some studies reporting correlations with inhibitory success (*Benis et al., 2014*; *Chen et al., 2020*). Besides playing a critical role in stopping movement (*Mosher et al., 2021*), the STN seems to be involved in delaying or pausing movement until sufficient evidence in favor of a motor program has accumulated (*Ray et al., 2012*). Recent evidence demonstrated that the STN is recruited by the prefrontal cortex via the hyperdirect pathway to implement its pausing function (*Chen et al., 2020*; *Lofredi et al., 2021*; *Oswal et al., 2021*; *Wessel et al., 2019*). However, the role of cortico-subcortical beta synchronization in coordinating movements that are already ongoing remains elusive.

Communication between STN and cortex might become particularly important in tasks involving cognitive factors, such as anticipation. STN beta power has been found to index task complexity and behavioral control (*Oswal et al., 2013*), proactive inhibition and planning (*Benis et al., 2014*), non-motor decision making, and working memory (*Zavala et al., 2017*), and cue evaluation with respect to behavioral goals (*Oswal et al., 2012*). Yet, the extent to which modulation of beta oscillations in basal-ganglia cortex networks depends on expectation remains unknown.

In the present study, we address these research gaps with a paradigm that involves a rotational movement performed in a continuous fashion with occasional rapid changes in movement direction (reversals), as well as movement initiations and terminations. Accounting for the relevance of basal ganglia-cortical loops in motor control, we recorded cortical and STN oscillatory activity simultaneously in PD patients who had undergone implantation of deep brain stimulation (DBS) electrodes the day before. Patients performed the rotational movements according to visual instructions which were manipulated such that their identity and time of appearance was either predictable or unpredictable. With this design, we aimed (1) to investigate the dynamics of STN and STN-cortex beta synchronization during movement reversal compared to those of starting and stopping and (2) to assess the effect of the temporal predictability of movement instructions on the coordination of beta synchronization for starting, stopping, and reversing.

Results

Behavior

Patients turned a wheel (*Figure 1b*) with their index finger at their preferred speed and were prompted by visual cues to start, reverse, or stop rotational movement (*Figure 1a*) while we simultaneously measured MEG and STN local field potentials (LFPs). We considered an average of 60.1 (SD = 14.8) predictable start trials, 59.3 (SD = 17.8) unpredictable start trials, 59.9 (SD = 14.2) predictable reversal trials, 58.6 (SD = 15.5) unpredictable reversal trials, 61.3 (SD = 15.3) predictable stop trials and 60.2



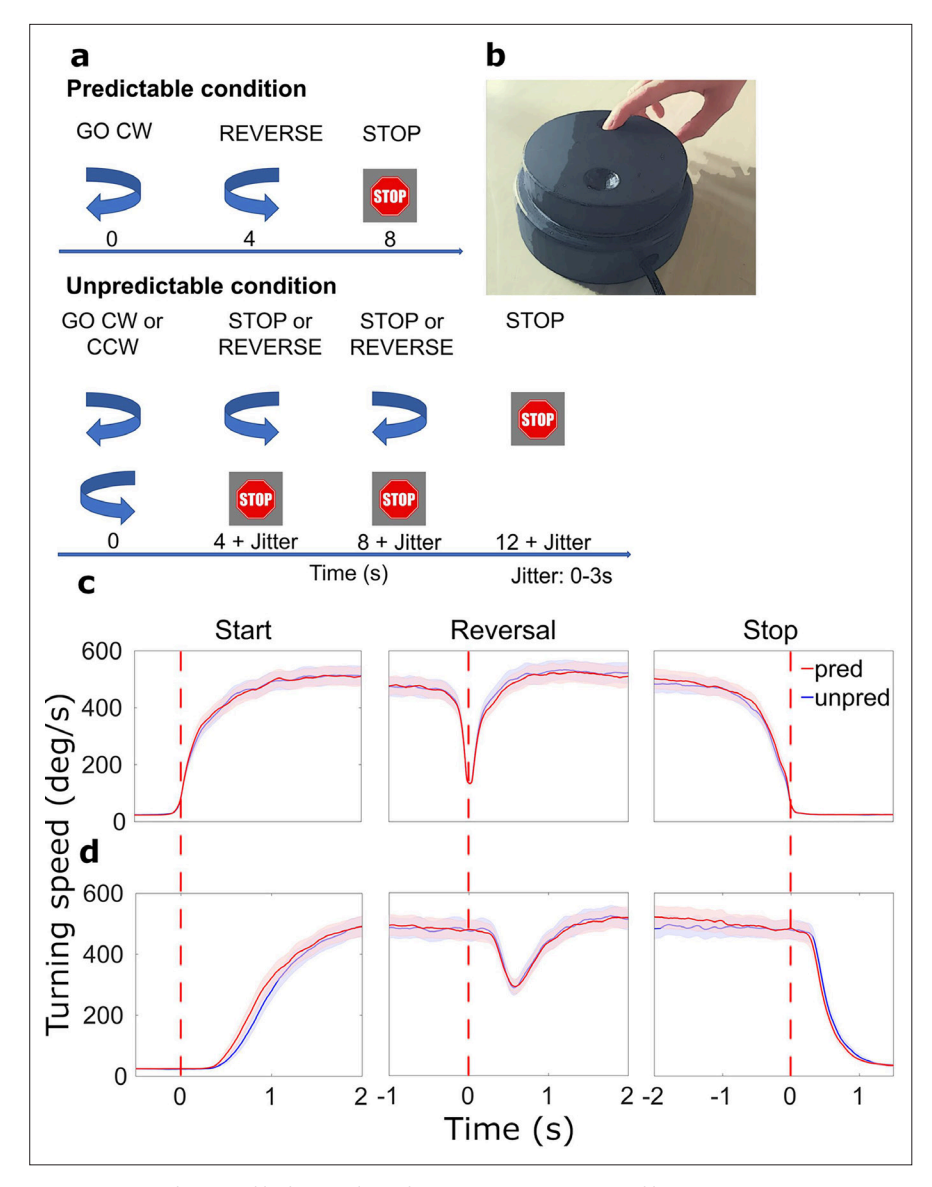


Figure 1. Paradigm and behavioral results. (a) Patients were cued by arrows to start turning or reverse movement direction. Stop cues were presented at the end of each sequence. The timing of cues varied with the condition: in the predictable condition, the start cue was always followed by a reverse cue after 4 s and a stop cue after another 4 s (no jitter). In the unpredictable condition, there were either 0, 1, or 2 reversals (equal probability). Cue onset was jittered. CW: clockwise, CCW: counterclockwise. (b) Turning device for motor paradigm. (c) Average movement-aligned wheel speed. Red dotted lines indicate when turning began, was reversed in direction, and halted. (d) Average cue-aligned wheel speed. Red dotted lines indicate when the start, reversal, and stop cues appeared, respectively. N=20.

(SD = 17.4) unpredictable stop trials per patient for analysis. To assess whether the predictability of movement prompts had an effect on behavior, we analyzed its effect on movement speed and reaction times. Angular speed changes in start, reversal, and stop trials were similar in the predictable and the unpredictable condition when the data was aligned to action onset (*Figure 1c*, $F_{cond}(1,16) = 0.037$, $p_{cond} = 0.850$, $\eta p^2 = 0.002$; see *Supplementary file 1* for the complete results of the ANOVA). Aligning trials to cue onsets revealed that starting and stopping occurred slightly later in the unpredictable condition (*Figure 1d*). This was reflected by a main effect of *condition* ($F_{cond}(1,16) = 6.698$, $p_{cond} = 0.020$, $\eta p^2 = 0.295$) and a *condition*movement type* interaction effect ($F_{cond*mov}(2,15) = 4.916$, $p_{cond*mov} = 0.023$, $\eta p^2 = 0.396$) on reaction times. Post-hoc t-tests revealed that reaction times to predictable start cues (M = 0.757, SD = 0.154) and stop cues (M = 0.824, SD = 0.202) were significantly shorter



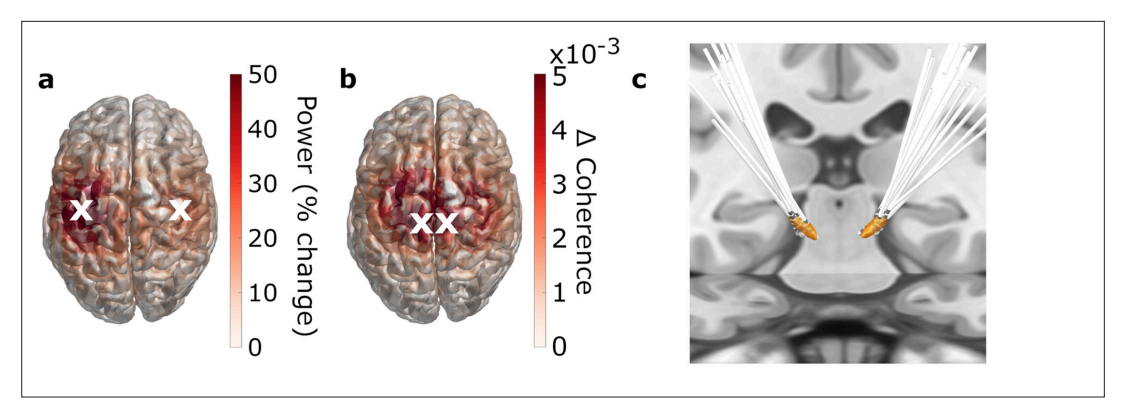


Figure 2. Regions of interest. (**a, b**) 3D source-reconstruction in MNI space. N=20. White crosses mark the cortical regions of interests (ROIs) selected for further analysis based on the strongest relative change in power (**a**) and the strongest absolute change in coherence (**b**). (**c**) All patients' deep brain stimulation (DBS) electrodes, localized with Lead-DBS.

than reaction times to unpredictable start (M=0.840, SD = 0.160) and stop (M=.889, SD = 0.233) cues (start: t=-3.469, one-sided p=0.001, d=-0.776, stop: t=-2.213, one-sided p=0.020, d=-0.495). Thus, starting and stopping were not performed at different speeds across conditions, but were initialized earlier in the predictable condition.

Power

Modulations of beta power associated with starting and stopping

In order to assess whether beta power modulations associated with reversals were distinct from beta suppression and rebound (research aim 1), we centered the trials on movement initiation, reversal, and termination, respectively, and assessed beta power dynamics. Besides the STN, this was done for two motor cortical regions of interest (ROIs): primary motor cortex (M1, hand knob region) and medial sensorimotor cortex (MSMC). This choice was based on the strongest movement-related modulations of beta power and coherence (*Figure 2*, see Regions of interest in the Methods section for further detail). For comparison, we also present group average time-frequency spectra for the gamma frequency band.

As expected, starting to turn the wheel was associated with a prominent beta suppression (contralateral STN: $t_{clustersum} = -2128.9$, p<0.001; ipsilateral STN: $t_{clustersum} = -2062.8$, p<0.001; contralateral M1: $t_{clustersum} = -8199.5$, p<0.001), whereas stopping resulted in a beta rebound (contralateral STN: $t_{clustersum} = 2843.0$, p<0.001; ipsilateral STN: $t_{clustersum} = 1488.8$, p=0.003; contralateral M1: $t_{clustersum} = 5958.9$, p<0.001, ipsilateral M1: $t_{clustersum} = 3834.7$, p<0.001) in both motor cortex and STN (*Figures 3a, 4a and b*). The beta suppression occurred bilaterally while the beta rebound was more lateralized to the hemisphere contralateral to movement, as corroborated by a statistical analysis of the lateralization index (*Figure 4c* and *Supplementary file 2*). Power changes in MSMC were generally similar to those in M1.

Modulations of gamma power associated with starting and stopping

Significant increases in gamma power at movement start were only observed in the contralateral STN ($t_{clustersum} = 2216.5$, p=0.003, *Figure 3a*). At movement stop, there was a decrease in gamma power in contralateral STN ($t_{clustersum} = -734.8$, p=0.016, *Figure 3a*) and contralateral M1 ($t_{clustersum} = -1447.4$, p=0.002, *Figure 4b*). However, changes in gamma power were overall much smaller in magnitude compared to the beta suppression and rebound.

Modulation of STN beta power associated with reversals

Modulations of beta oscillations associated with reversals of movement direction were of particular interest to this study (research aim 1). When reversing, one first needs to stop the ongoing movement before accelerating again in the opposite direction. Stopping is followed by the beta rebound, whereas starting is preceded by beta suppression. To the best of our knowledge, no study has investigated the



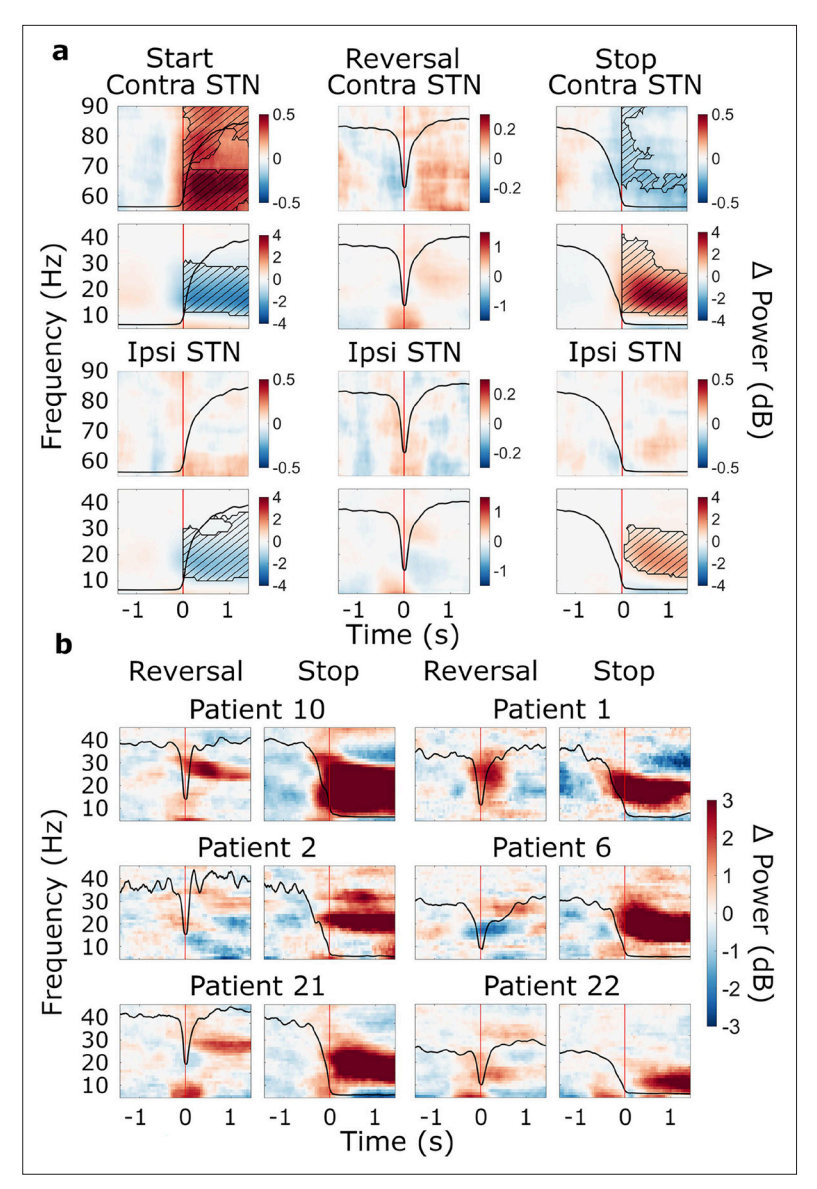


Figure 3. Movement-related beta power modulations in the subthalamic nucleus (STN). (a) Time-frequency spectra of start, reversal, and stop trials for the STN (group average, trials averaged across predictability conditions). Time 0 marks the moment turning began, was reversed in direction, and halted (red lines). The black line in each plot represents the average wheel turning speed (scale: 0–600 deg/s). Power was baseline-corrected (baseline: –1.6–0 s). Hatched lines within black contours indicate significant changes relative to baseline. N=20. (b) Six examples of individual patients at reversal and stop. Power was baseline-corrected (baseline: –1.6–0 s). Time 0 marks the brief pause of movement occurring during reversals, and movement stop, respectively (red lines). The black line in each plot represents each patient's trial-average wheel turning speed (scale: 0–600 deg/s; for patient 21, the scale was adapted to 0–750 deg/s). Patient 10: contralateral, predictable; Patient 1: contralateral, unpredictable; Patient 22: contralateral, unpredictable; Patient 22: posilateral, unpredictable; Patient 22: contralateral, unpredictable; Patient 22: posilateral, unpredictable.

The online version of this article includes the following figure supplement(s) for figure 3:

Figure supplement 1. Cue-aligned beta power modulations in the subthalamic nucleus (STN).

neural signals underlying acceleration that immediately follows stopping. In the STN, reversals were associated with a brief modulation of beta power, which was weak in the group-average spectrum and did not reach significance (*Figure 3a*). Reversal-related beta power modulations of individual patients were variable. Some patients revealed brief increases, whereas others showed decreases in STN beta power upon reaching the turning point (*Figure 3b*). Reversal-related increases of beta power differed



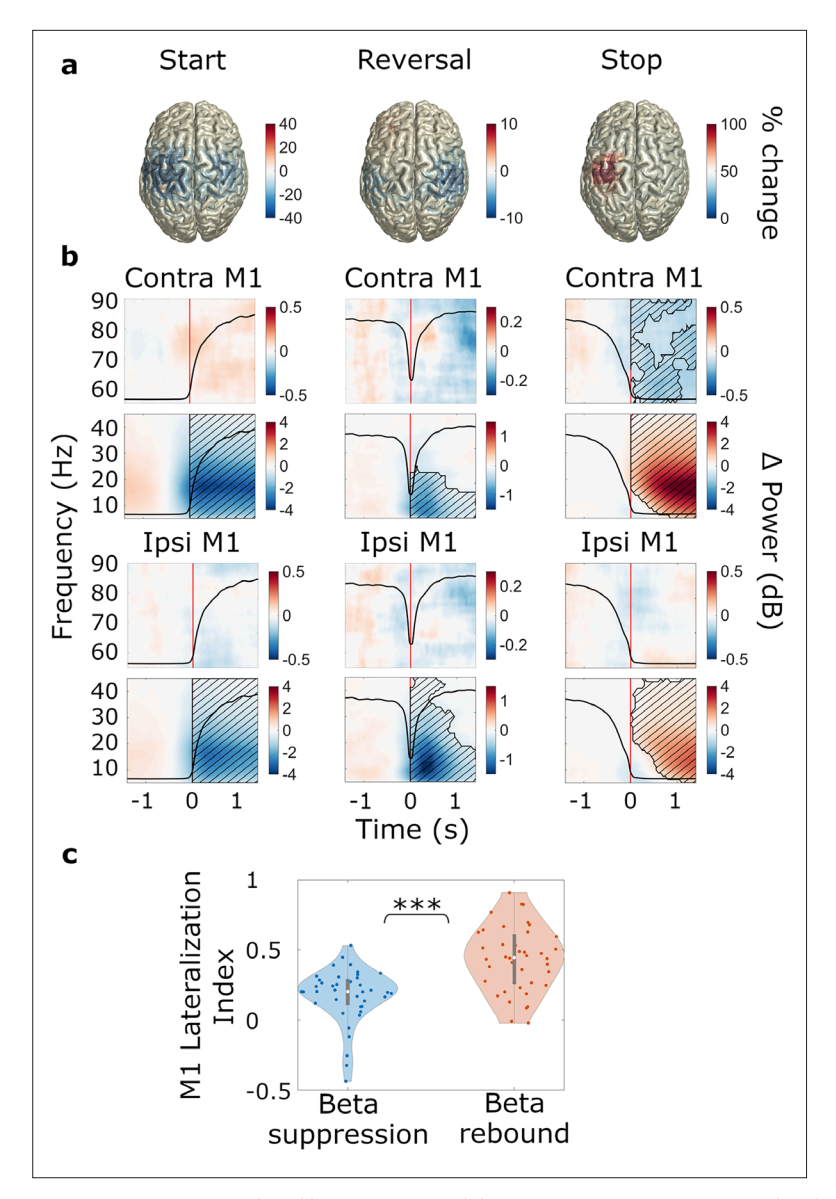


Figure 4. Movement-related beta power modulations in M1. N=20. (a) Source-localized movement-related modulation of beta power at movement start, reversal, and stop (Montreal Neurological Institute, MNI space, group average, trials averaged across predictability conditions). The hemisphere contralateral to movement is on the left. (b) Time-frequency spectra of start, reversal, and stop trials for M1. Time 0 marks the time point turning began, was reversed in direction, and halted (red lines). The black line in each plot represents the average wheel turning speed (scale: 0–600 deg/s). Power was baseline-corrected (baseline: –1.6–0 s). Hatched lines within black contours indicate significant changes relative to baseline. (c) Lateralization index for M1. LI = 0 corresponds to no lateralization; positive values refer to a contralateral lateralization and negative values to an ipsilateral lateralization. Blue: beta suppression; red: beta rebound.

The online version of this article includes the following figure supplement(s) for figure 4:

Figure supplement 1. Cue-aligned beta power modulations in M1.

from the beta rebound, as occurring after termination of the movement sequence, with respect to amplitude and spectral content, often lacking the low-beta component of the beta rebound (*Figure 3b*). These findings demonstrate distinct processing of brief pauses of action vs. a complete halt of action.

Modulation of cortical beta power associated with reversals

With respect to cortical beta power dynamics during reversals (research aim 1), we observed that reversals were associated with a brief suppression of alpha and beta power in motor cortex, particularly



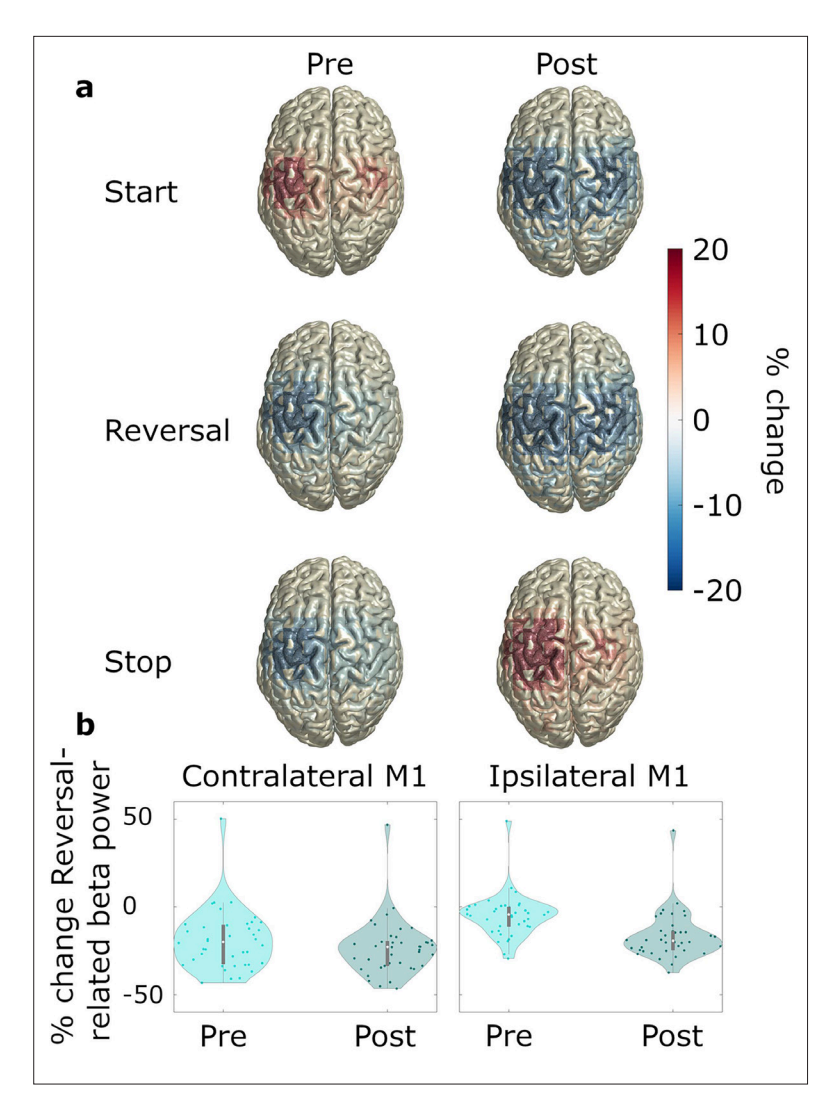


Figure 5. Pre- and post-event beta power. N=20. (a) Source-localized modulation of beta power before and after movement start, reversal, and stop (-1-0 and 0-1 s with respect to the movement of interest; baseline: power averaged over all time points and movement types). Plots are group-averages in Montreal Neurological Institute (MNI) space, trials were averaged across predictability conditions. (b) Relative change with respect to whole recording average baseline, of ipsilateral and contralateral beta power for pre-reversal and post-reversal time windows.

in M1 (contralateral M1: $t_{\text{clustersum}} = -1492.7$, p<0.001; ipsilateral M1: $t_{\text{clustersum}} = -3326.2$, p<0.001; **Figure 4a and b**). The suppression occurred after the turning point had been reached (**Figure 4b**) and was stronger in the hemisphere ipsilateral to movement, as demonstrated by a significant *ROI*movement* interaction effect on baseline-corrected beta power ($F_{\text{ROI*movement}}(10,6)=4.444$, $p_{\text{ROI*modulation}} = 0.041$, $\eta p^2=0.881$, refer to **Supplementary file 3** for the full results of the ANOVA). Post-hoc *t*-tests confirmed that beta power was at a lower level in ipsilateral M1 (M=-0.047, SD = 0.033) compared to contralateral M1 (M=-0.021, SD = 0.023) during reversal of movement direction (t=4.454, one-sided p<0.001, t=0.996).

To test whether the ipsilateral lateralization was related to pre-event baseline levels (i.e. pre-reversal, pre-start, and pre-stop), we re-computed the modulations using a whole recording average baseline (power averaged over all time points and movement types), thereby omitting the pre- vs. post-event contrast. *Figure 5a* illustrates that movement-related power modulations were generally stronger in the hemisphere contralateral to movement, with the exception of acceleration, which was associated with bilateral suppression of beta power (compare the bilateral beta power suppression at *post-start* and *post-reversal* to the contralateral beta power modulations in all other plots). The second

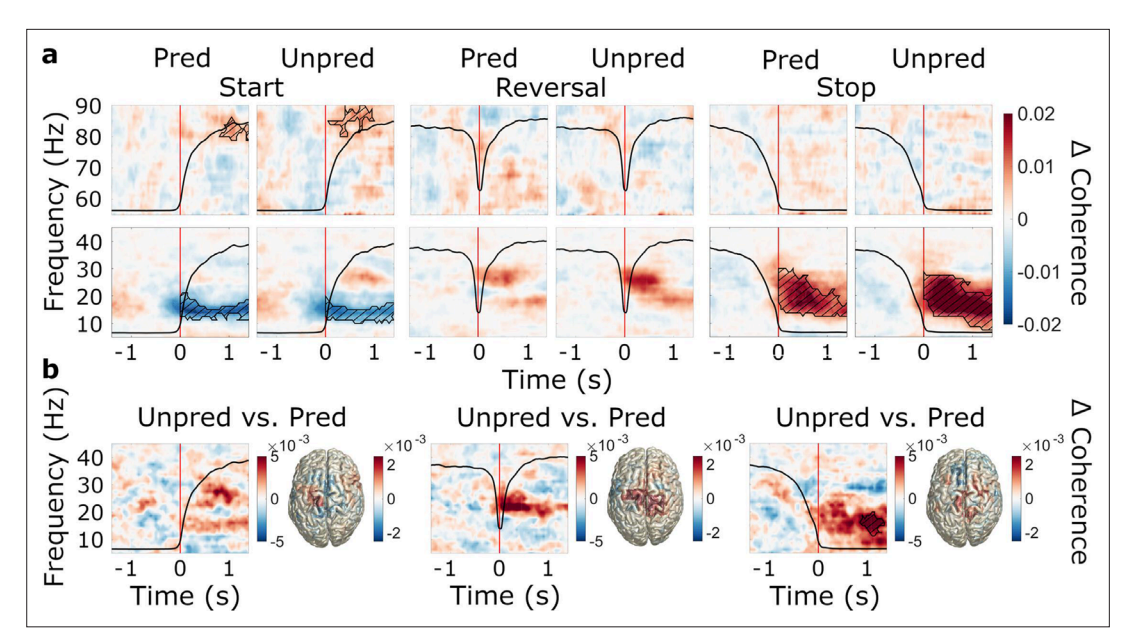


Figure 6. Event-related modulations of subthalamic nucleus (STN)-cortex coherence and the effect of predictability. N=20 (a) Baseline-corrected group average time-frequency representations of STN-cortex coherence (averaged over regions of interests, ROIs) during start, reversal, and stop for both the predictable and the unpredictable trials (baseline: –1.6–0 s). Time 0 marks the moment turning began, was reversed in direction, and was halted, respectively (red line). The black line in each plot represents the average wheel turning speed (scale: 0–600 deg/s). Hatched lines within black contours indicate significant changes relative to baseline. (b) Group average coherence difference between the unpredictable and predictable conditions. Left: Contrast of time-frequency representations. TFRs were averaged over ROIs. Right: Contrast of source-localized, event-related coherence modulations in the beta band.

The online version of this article includes the following figure supplement(s) for figure 6:

Figure supplement 1. Cue-aligned modulations of subthalamic nucleus (STN)-cortex coherence and the effect of predictability.

Figure supplement 2. Directionality of M1-subthalamic nucleus (STN) and MSMC-STN coupling.

before reversing, beta-power was at an intermediate level in the hemisphere ipsilateral to movement (Figure 5a). Thus, we observed a suppression relative to the pre-event baseline (Figure 4a-b). In the contralateral hemisphere, in contrast, beta power could not be suppressed much further because it was already close to floor level prior to reversing (Figure 5b). The lack of a pre-reversal increase of beta power is remarkable, because the second prior to reversing contained the deacceleration of the moving hand, which does not appear to involve an increase of beta power in primary motor cortex.

Effects of predictability on power

With respect to the effect of predictability of movement instructions on beta power dynamics (research aim 2), we observed an interaction between movement type and condition ($F_{\text{cond*mov}}$ (2,14)=4.206, $p_{\text{cond*mov}} = 0.037$, $\eta p^2 = 0.375$), such that the beta power suppression at movement start was generally stronger in the predictable (M=-0.170, SD = 0.065) than in the unpredictable (M=-0.154, SD = 0.070) condition across ROIs (t=-1.888, one-sided p=0.037, d=-0.422). We did not observe any modulation of gamma power by the predictability of movement instructions (F_{cond} (1,15)=0.792, P_{cond} = 0.388, ηp^2 =0.050, **Supplementary file 5**).

Connectivity

Movement-related modulations of STN-cortex connectivity

Beyond the local changes in beta power, we intended to investigate the dynamics of oscillatory coupling within the basal ganglia-cortex loop in the context of reversals of movement direction (research aim 1). The movement-related modulations of STN-cortex coherence were similar to modulations of



power, including beta suppression (predictable start: $t_{\text{clustersum}} = -489.4$, p=0.002; unpredictable start: $t_{\text{clustersum}} = -530.1$, p=0.003), beta rebound (predictable stop: $t_{\text{clustersum}} = 802.0$, p=0.002; unpredictable stop: $t_{\text{clustersum}} = 1252.2$, p<0.001), and increases in the gamma band at movement start (predictable start: $t_{\text{clustersum}} = 120.4$, p=0.005; unpredictable start: $t_{\text{clustersum}} = 197.8$, p<0.001). Unlike motor cortical beta power, however, STN-cortex beta coherence did not decrease in the re-acceleration phase of reversals. On a qualitative level, it even increased relative to baseline. *Figure 6* depicts the movement-related changes in coherence averaged across all ROIs.

Effects of predictability on STN-cortex coherence

With respect to the effect of predictability of movement instructions on beta coherence (research aim 2), we found that the pre-post event differences were generally more positive in the unpredictable condition (main effect of predictability: $F_{\rm cond}(1,15)=8.684$, $p_{\rm cond}=0.010$, $\eta p^2=0.367$; **Supplementary file 3**), meaning that the suppression following movement start was diminished and the increases following stop and reversal were enhanced in the unpredictable condition (**Figure 6a**). This effect was most pronounced in the MSMC (**Figure 6b**). When comparing region-average TFRs between the unpredictable and the predictable condition, we observed a significant difference only for stopping ($t_{\rm clustersum}=142.8$, p=0.023), suggesting that the predictability effect was mostly carried by increased beta coherence following stops. When repeating the rmANCOVA for pre-event coherence, we did not observe an effect of predictability ($F_{\rm cond}(1,15)=0.163$, $p_{\rm cond}=0.692$, $\eta p^2=0.011$), i.e., the effect was most likely not due to a shift of baseline levels. The increased tendency for upward modulations and decreased tendency for downward modulations rather suggests that the inability to predict the next cue prompted intensified event-related interaction between STN and cortex. STN-cortex gamma coherence was not modulated by predictability ($F_{\rm cond}(1,15)=0.005$, $p_{\rm cond}=0.944$, $\eta p^2=0.000$, **Supplementary file 5**).

Granger causality

In general, cortex appeared to drive the STN in the beta band, regardless of the movement type and predictability condition. This was reflected in a main effect of ROI on Granger causality estimates ($F_{ROI}(7,9) = 3.443$, $p_{ROI} = 0.044$, $\eta p^2 = 0.728$; refer to **Supplementary file 4** for the full results of the ANOVA). In the hemisphere contralateral to movement, follow-up t-tests revealed significantly greater Granger causality from M1 to the STN (t = 3.609, one-sided p<0.001, d = 0.807) and from MSMC to the STN (t = 2.051, one-sided p<0.027, d = 0.459) than the other way around. The same picture emerged in the hemisphere ipsilateral to movement (M1 to STN: t = 3.082, one-sided p=0.003, d = 0.689; MSMC to STN: t = 1.833, one-sided p<0.041, d = 0.410). In the gamma band, we did not detect a significant drive from one area to the other ($F_{ROI}(7,9) = 0.338$, $p_{ROI} = 0.917$, $\eta p^2 = 0.208$, **Supplementary file 6**). **Figure 6—figure supplement 2** demonstrates the differences in Granger causality between original and time-reversed data for the beta and gamma bands.

Discussion

Our study demonstrates that initiating, reversing, and stopping a continuous movement involves modulation of local and long-range beta synchronization in basal ganglia-cortex loops. Accelerating, stopping briefly, and coming to a complete halt have distinct and region-specific effects on beta oscillations in the motor system. These effects are context-dependent, with event-related increases of subcortico-cortical coupling intensifying when the upcoming movement instructions cannot be anticipated.

The dynamics of STN-cortex coherence

Simultaneous measurements of subthalamic and cortical oscillations in a comparably complex motor task allowed us to study the context-dependent dynamics of STN-cortex coupling. STN-M1 and STN-MSMC beta coherence decreased at movement initiation and increased after movement termination, while gamma coherence increased at movement start, corresponding to similar power changes in STN and motor cortex. A pre-movement suppression of beta coherence has been reported previously (Cassidy et al., 2002; Talakoub et al., 2016; van Wijk et al., 2017). Similarly, increases in gamma coherence have been found for the performance of ballistic movements (Alegre et al., 2013;



Litvak et al., 2012). Stopping a planned movement has been found to be linked with reduced suppression of beta coherence (Alegre et al., 2013), but a post-movement increase of coherence has thus far only been described for ballistic movements (Tan et al., 2014). Considering the timing of the increase observed here, the STN's role in movement inhibition (Benis et al., 2014; Ray et al., 2012) and the fact that frontal and prefrontal cortical areas are believed to drive subthalamic beta activity via the hyperdirect pathway (Chen et al., 2020; Oswal et al., 2021) it seems plausible that the increase of beta coherence reflects feedback of sensorimotor cortex to the STN in the course of post-movement processing. In line with this idea, we observed a cortical drive of subthalamic activity in the beta band.

Beta coherence and beta power are modulated by predictability

In the present paradigm, patients were presented with cues that were either temporally predictable or unpredictable. We found that unpredictable movement prompts were associated with stronger upward modulations and weaker downward modulations of STN-cortex beta coherence, likely reflecting the patients adopting a more cautious approach, paying greater attention to instructive cues. Enhanced STN-cortex interactions might indicate the recruitment of additional neural resources, which might have allowed patients to maintain the same movement speed in both conditions.

The notion of beta oscillations reflecting motor and cognitive processes such as action selection, clearing, and error-monitoring has gained growing support (Fonken et al., 2016; Schmidt et al., 2019; Turner and Desmurget, 2010). Purely cognitive inhibition processes, such as inhibition of thoughts, have been found to be associated with prefrontal beta power modulations (Castiglione et al., 2019; Schmidt et al., 2019). Furthermore, the STN has been suggested to implement its hold your horses function, reflected by beta-band synchronization, in situations of cognitive conflict (Brittain et al., 2012). Simultaneous measurements of MEG and STN LFPs revealed that STN-cortex beta coherence increases after conflict cues in an expanded judgment task (Patai et al., 2022). Though the present paradigm did not involve any conflict as such, the context of unpredictable movement instructions possibly engaged similar cognitive processes in response to surprise/uncertainty.

With respect to power, we observed reduced beta suppression in the unpredictable condition at movement start, consistent with the effect on coherence, likely demonstrating a lower level of motor preparation. This finding aligns with MEG research that found reduced beta suppression with enhanced uncertainty in a motor task (*Tzagarakis et al., 2010*), and findings from an EEG study that demonstrated reduced beta suppression in response to an unpredictable sequence of rhythmic stimuli (*Alegre et al., 2003*). Although previous research has reported modulations of the beta rebound by cognitive factors (*Fischer et al., 2016*; *Tan et al., 2016*; *Zavala et al., 2018*), we did not find an effect of predictability on the beta power rebound here.

Acceleration involves the recruitment of ipsilateral M1

As expected, we found sustained beta suppression at movement start and a strong beta power rebound at movement stop in STN, M1, and MSMC. During reversals, beta power was suppressed briefly in M1, particularly in the ipsilateral hemisphere where beta was not fully desynchronized prior to reversing. In contrast, the contralateral hemisphere revealed a floor effect: the ongoing movement resulted in persistent beta power suppression that was only slightly intensified when reversing. Bilateral modulation of beta power, as reported during reversals, was otherwise observed during the initiation of movement, but not during ongoing movement or after movement termination, suggesting that the recruitment of ipsilateral M1 may be selective to acceleration.

Our findings are consistent with prior studies that have demonstrated a bilateral (Alegre et al., 2004; Zaepffel et al., 2013) and spatially diffuse (Jurkiewicz et al., 2006) beta suppression, and more focal (Jurkiewicz et al., 2006) and predominantly contralateral (Espenhahn et al., 2017) topography of the beta rebound. Furthermore, past research has posited a role of ipsilateral motor cortex in motor control and preparation (Jurkiewicz et al., 2006; Olson et al., 2022). Beta suppression in the ipsilateral hemisphere has been found to be related to increased corticospinal excitability, to facilitate finger movements (Rau et al., 2003), and to have a role in higher order cortical processing of fine motor programs (Chen et al., 1997).



Brief pauses and complete stops have distinct effects on beta oscillations

We did not find evidence of a beta rebound following the short pause of movement during reversals in motor cortex. Instead, we observed a transient broadband beta power suppression in cortex, which was likely related to re-acceleration in the opposite direction. In contrast, the STN exhibited increases of high beta power in some patients, compatible with post-processing of the brief pause of movement occurring during reversals. On an observational level, the spectral patterns of these increases did not entirely match the individual stop-related beta pattern, lacking the low-beta component of the beta rebound. Thus, STN low-beta oscillations might not re-emerge when stopping briefly within a movement sequence, corroborating a dissociation of low- and high-beta oscillations, as proposed previously (*Chandrasekaran et al., 2019*; *Oswal et al., 2021*; *Patai et al., 2022*). Given that the beta rebound has been reported to slow reaction times (*Muralidharan and Aron, 2021*) and to reduce corticospinal excitability (*Wessel et al., 2016*), and that beta power must decrease for movement to start (*Heinrichs-Graham and Wilson, 2016*; *Khanna and Carmena, 2017*), it is likely that at least the low-beta portion of the beta rebound needs to be avoided during changes of ongoing action because it would slow down re-acceleration otherwise.

In agreement with the current findings, previous research assessing STN- and cortical beta activity reported no beta rebound around the time a movement changed (Alegre et al., 2004; London et al., 2021), except for one study, which did report a cortical beta rebound between two successive movements (Muralidharan and Aron, 2021). It should be noted, however, that the pauses were ~1–2 s long. In our study, the beta rebound occurred only at the end of the movement sequence, when patients were already in the process of stopping and movement had already slowed. This picture emerged irrespective of whether power dynamics were analyzed in a movement- or cue-aligned fashion (see Figure 3—figure supplement 1, Figure 4—figure supplement 1, Figure 6—figure supplement 1). A causal role of the beta rebound in stopping is, therefore, implausible. More likely, the rebound serves as a post-movement feedback signal reflecting task-dependent contextual information used to either confirm or update motor plans (Alegre et al., 2004; Cao and Hu, 2016). Alternatively, it might indicate the clear-out of the entire motor program (Schmidt et al., 2019).

With respect to gamma activity, we observed increases in power at movement start in the contralateral STN and decreases in power at movement termination in contralateral STN and M1. While movement-related increases in gamma power are an established finding in the literature (*Litvak et al.*, 2012; *Lofredi et al.*, 2018), there appears to be no consensus on its functional role during movement stopping. Previous studies using auditory stop signals reported STN gamma power increases in response to stop signals (*Fischer et al.*, 2017; *Ray et al.*, 2012). When assessed within a brief critical window between the stop signal and the average time of the upcoming finger tap, gamma power even correlated with stopping success, i.e., gamma was stronger when the downward movement was stopped earlier (*Fischer et al.*, 2017). Conversely, another study using visual stop signals reported decreased STN gamma power (*Alegre et al.*, 2013). We are unaware of studies that have assessed gamma power changes when stopping a continuous movement in response to visual cues and, therefore, provide first evidence for a decrease in this scenario, although we cannot rule out that focusing on different DBS contacts or using auditory stop signals and shorter event-locked analysis windows might produce different results.

Limitations and future directions

Invasive measurements of STN activity are only possible in patients who are undergoing or have undergone brain surgery. Studies drawing from this limited pool of candidate participants are typically limited in terms of sample size and cohort stratification, particularly when carried out in a perioperative setting. Here, we had a sample size of 20, which is rather high for a peri-operative MEG-LFP study, but still low in terms of absolute numbers.

We further acknowledge that most of our participants were older than 60 y. To diminish any confounding effects of age on movement-related modulations of neural oscillations, such as beta suppression and rebound (*Bardouille and Bailey, 2019*; *Espenhahn et al., 2019*), we included age as a covariate in the statistical analyses.

Furthermore, we cannot be sure to what extent the present study's findings relate to PD pathology rather than general motor processing. We suggest that our approach at least approximates healthy



brain functioning as patients were on their usual dopaminergic medication. Dopaminergic medication has been demonstrated to normalize power within the STN and globus pallidus internus, as well as STN-globus pallidus internus and STN-cortex coherence (Brown et al., 2001; Hirschmann et al., 2013). Additionally, several of our findings match observations made in other patient populations and in healthy participants, who exhibit the same beta power dynamics at movement start and stop (Alegre et al., 2004) that we observed here. Notably, our finding of enhanced cortical involvement in face of uncertainty aligns well with established theories of cognitive processing, given the cortex' prominent role in managing higher cognitive functions (Altamura et al., 2010). Yet, transferring our approach and task to patients with different disorders, e.g., obsessive compulsive disorder, or examining young and healthy participants solely at the cortical level, could contribute to elucidating whether the synchronization dynamics reported here are indeed independent of PD and age. Additionally, future research could capitalize on sensing-capable devices to circumvent the necessity to record brain activity peri-operatively, allowing for larger sample sizes and to circumvent the stun effect, an immediate improvement in motor symptoms arising as a consequence of electrode implantation (Mann et al., 2009). Lastly, given the present study's focus on understanding movement-related rhythms, particularly in the beta range, future research could further explore the role of gamma oscillations in continuous movement and their relation to action potentials in motor areas (Fischer et al., 2020; Igarashi et al., 2013), which form the basis of movement encoding in the brain.

Due to the diversity of modulations across patients, we cannot provide a general description of how the STN responds to reversals. The variability may result from the fact that the exact recording site varied across patients, although all recording contacts were located in the dorsolateral STN. Furthermore, stop processes, mediated by the hyperdirect and the indirect pathway as well as corticostriatal go processes, may emerge in the basal ganglia close in time (*Muralidharan et al., 2022*;

Table 1. Patient clinical characteristics.

Disease duration refers to the time since diagnosis. For patient 4, the time since first symptom manifestation is given. MoCa = Montreal Cognitive Assessment Test.

ID	Age	sex	Pre-surgical MDS-UPDRS III ON	Pre-surgical MoCa	Used hand	Disease duration (y)	Motor subtype	DBS Lead
1	70	m	20	27	R	3	tremor	Abbott Infinity
2	67	m	31	27	R	32	mixed	Abbott Infinity
3	64	М	23	25	R	6	akinetic-rigid	Abbott Infinity
4	57	М	53	27	L	2	tremor	Abbott Infinity
5	66	F	33	26	R	18	mixed	Abbott Infinity
6	75	М	11	24	R	13	akinetic-rigid	Abbott Infinity
7	66	М	10	27	R	13	mixed	Abbott Infinity
8	83	F	7	25	R	13	tremor	Abbott Infinity
9	68	F	15	20	L	11	akinetic-rigid	Abbott Infinity
10	58	F	21	14	R	5	mixed	Medtronic
11	69	М	17	27	L	12	mixed	Abbott Infinity
12	73	F	17	28	L	9	mixed	Abbott Infinity
13	65	М	28	21	L	13	mixed	Abbott Infinity
14	65	М	12	20	R	4	tremor	Abbott Infinity
15	64	М	25	23	R	17	mixed	Medtronic
16	68	М	15	28	R	5	mixed	Abbott Infinity
17	65	М	9	18	R	4	akinetic-rigid	Abbott Infinity
18	50	М	11	26	R	4	tremor	Abbott Infinity
19	68	F	42	23	L	12	mixed	Abbott Infinity
20	56	F	20	26	R	3	tremor	Medtronic



Schmidt and Berke, 2017), potentially overlapping. The sub-populations processing these signals in the STN (Isoda and Hikosaka, 2008; Schmidt and Berke, 2017; Schmidt et al., 2013) might not be resolvable with macro-electrode LFP recordings.

Conclusion

In conclusion, we have revealed distinct local and long-range synchronization dynamics of motor cortex and STN during changes of ongoing action in different movement contexts. We found that stopping briefly in the course of changing movement direction and terminating a movement sequence have distinct oscillatory profiles. Moreover, movement scenarios that do not permit movement preparation and require higher levels of caution appear to involve enhanced levels of subthalamo-cortical beta synchronization, highlighting that long-range beta coherence plays an important role in coordinating movements in response to unpredictable events.

Materials and methods

Patients

23 PD patients with a mean age of 66.13 y (±7.72 y) participated in the study (*Table 1*). DBS surgery was performed by the Department of Functional Neurosurgery and Stereotaxy of the University Hospital Düsseldorf under full anesthesia and according to standard procedures. 21 patients were implanted with Abbott Infinity segmented leads (Abbott Laboratories, Chicago, Illinois, USA) and three patients with Medtronic SenSight electrodes (Medtronic Inc, Minneapolis, MN, USA). DBS surgery was performed in two steps, and the measurements took place in between the implantation of the electrodes and the implantation of the pulse generator. Prior to participating, all patients provided their written informed consent in agreement with the Declaration of Helsinki. The study was approved by the Ethics Committee of the Medical Faculty of Heinrich Heine University Düsseldorf. The medication schedule was not changed for this experiment (Med ON state). Three participants were excluded from the analyses, two of whom were physically unable to perform the paradigm. The data of the third patient were contaminated by excessive artifacts.

Recordings

Measurements took place the day after the implantation of DBS electrodes. Externalization of leads allowed us to measure LFPs from the STN in combination with MEG. For LFP recordings, we used a mastoid reference and re-referenced the signals using a bipolar montage post-measurement. MEG signals were acquired simultaneously, using a 306-channel whole-head MEG system (VectorView, MEGIN). Muscle and ocular activity were monitored via electromyography (EMG) and vertical and horizontal electrooculography (EOG), respectively. EMG surface electrodes were placed on patients' right and left forearms, referenced to the muscle tendons at the wrist. We first recorded 5 min of resting-state data, followed by the motor task, which lasted for about 32 min in total. During the task, patients were required to turn a wheel clockwise or counterclockwise, according to visual instructions presented on a screen in front of them.

Experimental design

Patients were seated in the MEG scanner in a magnetically shielded room with a turning device ('wheel,' *Figure 2b*) placed on a table in front of them. The wheel (diameter = 14 cm, height = 6.5 cm) could be turned into both directions and had indentations, allowing comfortable placement of one index finger for turning. An MEG-compatible plastic fiber optic position sensor system (MR430 Series ZapFREE Fiber Optic Absolute Encoder System, MICRONER Inc, Camarillo, CA, USA) was used to measure wheel turning. The absolute angular position was continuously measured and updated at a frequency of 1.2 kHz. Given its design, the sensing system did not introduce any magnetic interference.

Movement prompts were presented on a screen. The visual stimuli consisted of two curved arrows pointing either clockwise or counterclockwise, respectively, and a stop sign with white font on a red background (*Figure 1a*). Patients were instructed to turn the wheel with their index finger following the direction of the arrows and to stop when a stop cue appeared. We did not impose requirements on turning speed or body side, so that patients could use their less affected hand and adjust the speed to their individual motor capabilities.



The experiment was conducted in two distinct blocks, where stimuli differed in their order and timing of presentation. In the predictable condition, trials consisted of a blue arrow cueing the patients to start turning clockwise, followed by a cue to change the turning direction after 4 s, and a stop cue after another 4 s. Each trial was followed by a pause lasting for 4 s. The condition was termed *predictable*, as the fixed timing and the fixed order of cues allowed patients to easily predict and prepare what they had to do next and when. In the unpredictable condition, the start cue was either clockwise or counterclockwise and was followed by 0, 1, or 2 reversals before the stop cue appeared. Each alternative occurred equally often (go, stop: 33%; go, reverse, stop: 33%; go, reverse, reverse, stop: 33%; clockwise and counterclockwise start directions were balanced). Additionally, the intervals between the visual stimuli were unpredictable (ranging between 4–7 s), with 50% of all inter-stimulus intervals kept at 4 s, as in the predictable condition. Hence, patients could not foresee the sequence and the timing of instructions, calling for a more cautious/attentive monitoring of cues.

We recorded two blocks per condition, with 36 trials each, in a pseudo-randomized fashion. To enhance compliance, we split each block in half, allowing for a short break, and also offered breaks between blocks.

Materials availability statement

The code used for analyses is available at https://github.com/luciewinkler/Subthalamo-Cortical-Synchronization (copy archived at *Hirschmann and Winkler*, 2025).

Data analysis

Data were analyzed using MATLAB R2019b (The Mathworks, Natick, Massachusetts, USA) and the toolbox FieldTrip (*Oostenveld et al., 2011*). For statistical testing, we used IBM SPSS Statistics 28 (IBM Corporation, Somers, USA).

Preprocessing

The data were visually inspected to identify and tag noisy channels and subsequently cleaned using temporal Signal Space Separation to remove artifacts originating from outside the MEG sensor array (*Taulu and Simola, 2006*). Then, the data were downsampled to 500 Hz. We applied a high-pass finite impulse response filter with a cut-off frequency of 1 Hz to remove low-frequency drifts and screened the data for remaining artifacts.

We used custom MATLAB scripts for semi-automated detection of movement start, reversal, and stop in the wheel data. This was achieved by applying an event-specific combination of amplitude and duration thresholds to the first temporal derivative of the rotation angle measurements. To ensure that events were correctly marked, all events were visually inspected and manually corrected if needed. Then, we epoched MEG and LFP data with respect to the behavioral events. Trials were centered around movement events of interest, i.e., start, stop, and reversal of movement, and encompassed 4 s. Movement-aligned angular speed was calculated within those time windows and averaged over trials. Reaction times to cues were defined as the time from cue presentation until movement.

LFP Channel Selection

The positions of DBS electrodes were localized with the MATLAB toolbox Lead-DBS (**Neudorfer et al., 2023**) using the patients' pre-operative T1- and T2-weighted MRIs (Magnetom Trio MRI scanner, Siemens, Erlangen, Germany) and postoperative CT scans (**Figure 1b**). In order to select one LFP channel for each patient and hemisphere, we identified the bipolar LFP channel with the strongest beta suppression and beta rebound, as previous research has demonstrated the presence of these modulations in the dorsolateral motor STN (**Benis et al., 2014**; **Wessel et al., 2016**). Moreover, the source of subthalamic beta oscillations has been localized to the dorsal STN (**Tamir et al., 2020**).

Regions of interest

Similarly, we selected cortical regions of interest (ROIs) by localizing the strongest event-related modulations of beta power/beta coherence. For source localization, we first co-registered the pre-operative T1-weighted MRI scans to the MEG coordinate system. Using the segmented MRIs, we prepared forward models based on single-shell realistic head models (**NoIte**, **2003**). Beamformer grids, specifying the position of sources, covered the entire brain and were aligned to the Montreal Neurological



Institute (MNI) space. Subsequently, we applied *Dynamic Imaging of Coherent Sources (DICS)* (**Gross et al., 2001**) to beta-band LFP-MEG cross-spectral densities pooled across predictability conditions. Next, we computed contrasts between post-event (0–2 s) and pre-event (–2–0 s) beta power/coherence and averaged the absolute changes across patients and events (movement start, reversal, and stop). This served to identify the regions with the strongest change in general, irrespective of sign, event, and predictability condition.

The strongest beta power modulations localized to the hand knob area of primary motor cortex (M1; *Figure 1a*) and the strongest changes in STN-cortex beta coherence to medial sensorimotor cortex (MSMC; *Figure 1b*). Thus, we focused our analysis on bilateral STN, M1, and MSMC. For time-frequency analysis, we represented each cortical ROI by the grid point of strongest modulation and its six nearest neighbors and extracted a time-series for each grid point, using a linearly constrained minimum variance spatial filter (*Van Veen and Buckley, 1988*).

Time-frequency analyses

While our main focus was the beta band, we also included other frequencies in our time-frequency analyses to get a more complete picture of power and coherence changes. Specifically, we considered the frequency ranges 5–45 Hz and 55–90 Hz, omitting the 50 Hz line noise artifact, and the time range from –1.6–1.6 s with respect to the movement event. Fourier spectra were computed using a multitaper approach (four Slepian tapers for the low frequency range and seven Slepian tapers for the high frequency range), a window size of 800 ms and a step size of 50 ms. Using the Fourier coefficients, we computed power and STN-cortex across-trial coherence for each time-frequency bin.

For illustration, we applied baseline correction, using the mean of the pre-event time window (-1.6-0 s) as baseline. In case of power, we expressed changes with respect to baseline in decibel. In case of coherence, we subtracted the baseline values. Time-frequency spectra of cortical sources were averaged over neighboring grid points belonging to the same ROI.

Granger causality analysis

We computed beta and gamma band non-parametric Granger causality (*Dhamala et al., 2008*) between cortical ROIs and the STN for the post-event time windows (0–2 s with respect to start, reversal, and stop). Because estimates of Granger causality are often biased, we compared the original data to time-reversed data to suppress non-causal interactions. True directional influence is reflected by a higher causality measure in the original data than in its time-reversed version, resulting in a positive difference between the two, the opposite being the case for a signal that is 'Granger-caused' by the other. Directionality is thus reflected by the sign of the estimate (*Haufe et al., 2013*). Because rmANCOVA results indicated no significant effects for predictability and movement type, and post-hoc tests did not show significant differences between hemispheres, we averaged Granger causality estimates over movement types, hemispheres, and predictability conditions in *Figure 6*—*figure supplement 2*.

Statistical analysis

Repeated measures analyses of (co)variance (rmANCOVA), implemented in SPSS, were our main tool for statistical analysis. This approach provides a comprehensive, multi-factorial analysis, but requires pre-selection of brain areas (see Regions of Interest), a frequency range, and a time range of interest (see Power and coherence). The dependent variable was either the event-related change in power or coherence, the hemispheric lateralization of the event-related power change (see Lateralization), or Granger causality. The main independent variable of interest was *predictability. Brain area* and *movement type* were also included as factors due to their clear effects on power and coherence, but their main effects are not reported in the main paper. They can be found in the Supplementary material. Because Mauchly's test indicated violations of the sphericity assumption, we report results from the multivariate test (*Rasch et al., 2021*). To account for their potential influence on brain activity, we added age, pre-operative UPDRS score, and disease duration as covariates to all ANOVAs. Covariates were standardized by means of z-scoring.

The rmANCOVAs were complemented by cluster-based permutation tests for detecting significant power/coherence modulations relative to baseline. These tests are mono-factorial but have the advantage of not requiring any preselection of time or frequency ranges while providing correction



for multiple comparisons. The cluster-defining and the cluster significance threshold was set to 0.05 (two-sided test). The cluster statistic was the sum of *t*-values within a cluster. We performed 1000 permutations per test.

Power and connectivity

To assess the effect of predictability on power, we conducted a repeated measures ANCOVA testing the influence of the factors movement (start, stop, reversal), predictability (predictable, unpredictable) and brain area (STN, M1, MSMC, ipsilateral, and contralateral to the moving hand), as well as interactions between these factors, on the event-related modulation of beta power. Here, modulation refers to the difference between post-event (0-1.6 s) and pre-event (-1.6-0 s) beta power in decibel (dB). A similar rmANCOVA was computed for event-related modulations of STN-cortex beta coherence. In this case, we considered the difference between pre- and post-event coherence. Here, the factor brain area contained of the following pairs: contralateral M1-contralateral STN, contralateral MSMCcontralateral STN, ipsilateral M1-ipsilateral STN, ipsilateral MSMC-ipsilateral STN, with the terms ipsilateral and contralateral referring to the moving hand. In an additional rmANCOVA, we considered post-event (0–2 s) Granger causality. The factor brain area included these pairs: contralateral M1->contralateral STN, contralateral STN->contralateral M1, contralateral MSMC->contralateral STN, contralateral STN->contralateral MSMC, ipsilateral M1->ipsilateral STN, ipsilateral STN->ipsilateral M1, ipsilateral MSMC-ipsilateral STN, ipsilateral STN->ipsilateral MSMC. This rmANCOVA was supplemented by t-tests assessing whether the difference in Granger causality between the reversed and the original data differed from zero, indicating significant directionality.

Because beta power is known to correlate with movement speed (*Lisi and Morimoto, 2015*; *Lofredi et al., 2023*; *Pogosyan et al., 2009*), we added standardized turning speed, averaged over trials and timepoints, as an additional covariate to the above-mentioned rmANCOVAS.

Lateralization

We compared the beta power suppression and the beta power rebound with respect to their hemispheric lateralization, using a rmANOVA with the factors *brain area* (STN, M1, MSMC), *predictability* (predictable, unpredictable), and *modulation type* (beta suppression, beta rebound). Lateralization was quantified by the lateralization index, defined as the difference between contralateral and ipsilateral power, normalized by power summed over both hemispheres.

Behavior

To assess whether the predictability of movement prompts had an effect on the patients' performance in the task, we performed a rmANOVA with the factors *predictability* (predictable, unpredictable), *movement* (start, stop, reversal) and their interaction on reaction times and movement-aligned wheel turning speed, averaged over trials and time points, respectively. Epochs without movement (pre-start and post-stop) were disregarded in this analysis.

Acknowledgements

This research was funded by the Brunhilde Moll Stiftung. The authors thank all participants for their time, cooperation, and willingness to participate. Furthermore, the authors thank Hannah Feldmann for her contributions to developing the paradigm, Dafina Sylaj for her help with patient recruitment, and Lilli Ahrenberg for her work localizing the patients' DBS electrodes.

Additional information

Funding

Funder	Grant reference number	Author
Brunhilde Moll Stiftung		Alfons Schnitzler Jan Hirschmann



Funder Grant reference number Author

The funders had no role in study design, data collection and interpretation, or the decision to submit the work for publication.

Author contributions

Lucie Winkler, Formal analysis, Validation, Investigation, Visualization, Writing - original draft; Markus Butz, Investigation, Writing – review and editing; Abhinav Sharma, Methodology, Writing – review and editing; Jan Vesper, Resources, Writing – review and editing; Alfons Schnitzler, Resources, Funding acquisition, Writing – review and editing; Petra Fischer, Conceptualization, Resources, Supervision, Methodology, Writing – review and editing; Jan Hirschmann, Conceptualization, Supervision, Funding acquisition, Investigation, Methodology, Project administration, Writing – review and editing

Author ORCIDs

Lucie Winkler https://orcid.org/0009-0005-8558-9428
Markus Butz https://orcid.org/0000-0003-1438-5792
Petra Fischer https://orcid.org/0000-0001-5585-8977
Jan Hirschmann https://orcid.org/0000-0001-6315-1912

Ethics

Prior to participating, all patients provided their written informed consent in agreement with the declaration of Helsinki. The study was approved by the Ethics Committee of the Medical Faculty of Heinrich Heine University Düsseldorf (approval identifier: 14-264).

Peer review material

Reviewer #1 (Public review): https://doi.org/10.7554/eLife.101769.3.sa1 Reviewer #2 (Public review): https://doi.org/10.7554/eLife.101769.3.sa2 Reviewer #3 (Public review): https://doi.org/10.7554/eLife.101769.3.sa3 Author response https://doi.org/10.7554/eLife.101769.3.sa4

Additional files

Supplementary files

Supplementary file 1. Behavioral effects. (A) Effects of condition (predictable, unpredictable) and movement (start, reverse, stop) on movement-aligned speed, controlling for age, pre-operative UPDRS score, and disease duration. (B) Effects of condition (predictable, unpredictable) and movement (start, reverse, stop) on reaction times to cues, controlling for age, pre-operative UPDRS score, and disease duration.

Supplementary file 2. Effects on lateralization. Effects of modulation type (beta suppression, beta rebound), condition (predictable, unpredictable), and ROI (STN, M1, MSMC) on lateralization index, controlling for age, pre-operative UPDRS score, and disease duration.

Supplementary file 3. Effects on beta power and coherence. (A) Effects of condition (predictable, unpredictable), movement (start, reverse, stop), and regions of interest ROI (contralateral and ipsilateral STN, M1, MSMC) on normalized power, controlling for movement speed, age, preoperative UPDRS score, and disease duration. (B) Effects of condition (predictable, unpredictable), movement (start, reverse, stop), and ROI (contralateral STN-M1, contralateral STN-MSMC, ipsilateral STN-M1, ipsilateral STN-MSMC) on coherence modulation, controlling for movement speed, age, pre-operative UPDRS score, and disease duration.

Supplementary file 4. Effects on beta Granger causality. (A) Effects of condition (predictable, unpredictable), movement (start, reverse, stop), and regions of interest (ROI) (contralateral and ipsilateral M1->STN, STN->M1, MSMC->STN, STN->MSMC) on Granger causality, controlling for movement speed, age, pre-operative UPDRS score, and disease duration.

Supplementary file 5. Effects on gamma power and coherence. (**A**) Effects of condition (predictable, unpredictable), movement (start, reverse, stop), and regions of interest (ROI) (contralateral and ipsilateral STN, M1, MSMC) on normalized power, controlling for movement speed, age, preoperative UPDRS score and disease duration. (**B**) Effects of condition (predictable, unpredictable), movement (start, reverse, stop), and ROI (contralateral STN-M1, contralateral STN-MSMC, ipsilateral STN-M1, ipsilateral STN-MSMC) on coherence modulation, controlling for movement speed, age,



pre-operative UPDRS score, and disease duration.

Supplementary file 6. Effects on gamma Granger causality. (A) Effects of condition (predictable, unpredictable), movement (start, reverse, stop), and regions of interest (ROI) (contralateral and ipsilateral M1->STN, STN->M1, MSMC->STN, STN->MSMC) on Granger causality, controlling for movement speed, age, pre-operative UPDRS score, and disease duration.

Supplementary file 7. Excel file containing reaction times and movement speed.

Supplementary file 8. Excel file containing beta and gamma power values.

Supplementary file 9. Excel file containing beta lateralization index values.

Supplementary file 10. Excel file containing the beta and gamma coherence values.

Supplementary file 11. Excel file containing the beta and gamma Granger causality values.

MDAR checklist

Data availability

The data tables that formed the input to the statistical analyses (band-average power and coherence) are provided as Supplementary Excel files. The raw data is not openly available because patients did not consent to data sharing. Researchers interested in accessing others parts of the data which can be completely de-identifed may contact Jan.Hirschmann@uni-duesseldorf.de for help with seeking approval from the Data Protection Office of the University Clinic Düsseldorf.

References

- Alegre M, Gurtubay IG, Labarga A, Iriarte J, Malanda A, Artieda J. 2003. Alpha and beta oscillatory changes during stimulus-induced movement paradigms: effect of stimulus predictability. *Neuroreport* **14**:381–385. DOI: https://doi.org/10.1097/00001756-200303030-00017, PMID: 12634488
- Alegre M, de Gurtubay IG, Labarga A, Iriarte J, Malanda A, Artieda J. 2004. Alpha and beta oscillatory activity during a sequence of two movements. *Clinical Neurophysiology* **115**:124–130. DOI: https://doi.org/10.1016/s1388-2457(03)00311-0, PMID: 14706479
- Alegre M, Lopez-Azcarate J, Obeso I, Wilkinson L, Rodriguez-Oroz MC, Valencia M, Garcia-Garcia D, Guridi J, Artieda J, Jahanshahi M, Obeso JA. 2013. The subthalamic nucleus is involved in successful inhibition in the stop-signal task: a local field potential study in Parkinson's disease. Experimental Neurology 239:1–12. DOI: https://doi.org/10.1016/j.expneurol.2012.08.027, PMID: 22975442
- Altamura M, Goldberg TE, Elvevåg B, Holroyd T, Carver FW, Weinberger DR, Coppola R. 2010. Prefrontal cortex modulation during anticipation of working memory demands as revealed by magnetoencephalography. International Journal of Biomedical Imaging 2010:Article . DOI: https://doi.org/10.1155/2010/840416, PMID: 20689717
- Aron AR, Poldrack RA. 2006. Cortical and subcortical contributions to Stop signal response inhibition: role of the subthalamic nucleus. The Journal of Neuroscience 26:2424–2433. DOI: https://doi.org/10.1523/JNEUROSCI. 4682-05.2006, PMID: 16510720
- Bardouille T, Bailey L. 2019. Evidence for age-related changes in sensorimotor neuromagnetic responses during cued button pressing in a large open-access dataset. *NeuroImage* **193**:25–34. DOI: https://doi.org/10.1016/j.neuroimage.2019.02.065, PMID: 30849530
- Bastin J, Polosan M, Benis D, Goetz L, Bhattacharjee M, Piallat B, Krainik A, Bougerol T, Chabardès S, David O. 2014. Inhibitory control and error monitoring by human subthalamic neurons. *Translational Psychiatry* **4**:e439. DOI: https://doi.org/10.1038/tp.2014.73, PMID: 25203170
- Benis D, David O, Lachaux J-P, Seigneuret E, Krack P, Fraix V, Chabardès S, Bastin J. 2014. Subthalamic nucleus activity dissociates proactive and reactive inhibition in patients with Parkinson's disease. *NeuroImage* 91:273–281. DOI: https://doi.org/10.1016/j.neuroimage.2013.10.070, PMID: 24368260
- Bonnevie T, Zaghloul KA. 2019. The subthalamic nucleus: unravelling new roles and mechanisms in the control of action. *The Neuroscientist* **25**:48–64. DOI: https://doi.org/10.1177/1073858418763594, PMID: 29557710
- Brittain J-S, Watkins KE, Joundi RA, Ray NJ, Holland P, Green AL, Aziz TZ, Jenkinson N. 2012. A role for the subthalamic nucleus in response inhibition during conflict. *The Journal of Neuroscience* **32**:13396–13401. DOI: https://doi.org/10.1523/JNEUROSCI.2259-12.2012, PMID: 23015430
- Brown P, Oliviero A, Mazzone P, Insola A, Tonali P, Di Lazzaro V. 2001. Dopamine dependency of oscillations between subthalamic nucleus and pallidum in Parkinson's disease. *The Journal of Neuroscience* **21**:1033–1038. DOI: https://doi.org/10.1523/JNEUROSCI.21-03-01033.2001, PMID: 11157088
- Cao L, Hu YM. 2016. Beta rebound in visuomotor adaptation: still the status quo? The Journal of Neuroscience 36:6365–6367. DOI: https://doi.org/10.1523/JNEUROSCI.1007-16.2016, PMID: 27307225
- Cassidy M, Mazzone P, Oliviero A, Insola A, Tonali P, Di Lazzaro V, Brown P. 2002. Movement-related changes in synchronization in the human basal ganglia. Brain 125:1235–1246. DOI: https://doi.org/10.1093/brain/awf135, PMID: 12023312



- Castiglione A, Wagner J, Anderson M, Aron AR. 2019. Preventing a thought from coming to mind elicits increased right frontal beta just as stopping action does. Cerebral Cortex 29:2160–2172. DOI: https://doi.org/ 10.1093/cercor/bhz017, PMID: 30806454
- Chandrasekaran C, Bray IE, Shenoy KV. 2019. Frequency Shifts and depth dependence of premotor beta band activity during perceptual decision-making. The Journal of Neuroscience 39:1420–1435. DOI: https://doi.org/10.1523/JNEUROSCI.1066-18.2018
- Chen R, Gerloff C, Hallett M, Cohen LG. 1997. Involvement of the ipsilateral motor cortex in finger movements of different complexities. Annals of Neurology 41:247–254. DOI: https://doi.org/10.1002/ana.410410216, PMID: 9029074
- Chen W, de Hemptinne C, Miller AM, Leibbrand M, Little SJ, Lim DA, Larson PS, Starr PA. 2020. Prefrontal-subthalamic hyperdirect pathway modulates movement inhibition in humans. *Neuron* **106**:579–588. DOI: https://doi.org/10.1016/j.neuron.2020.02.012, PMID: 32155442
- Dhamala M, Rangarajan G, Ding M. 2008. Analyzing information flow in brain networks with nonparametric Granger causality. *NeuroImage* **41**:354–362. DOI: https://doi.org/10.1016/j.neuroimage.2008.02.020, PMID: 18394927
- Engel AK, Fries P. 2010. Beta-band oscillations--signalling the status quo? Current Opinion in Neurobiology 20:156–165. DOI: https://doi.org/10.1016/j.conb.2010.02.015, PMID: 20359884
- Espenhahn S, de Berker AO, van Wijk BCM, Rossiter HE, Ward NS. 2017. Movement-related beta oscillations show high intra-individual reliability. *NeuroImage* 147:175–185. DOI: https://doi.org/10.1016/j.neuroimage. 2016.12.025, PMID: 27965146
- Espenhahn S, van Wijk BCM, Rossiter HE, de Berker AO, Redman ND, Rondina J, Diedrichsen J, Ward NS. 2019. Cortical beta oscillations are associated with motor performance following visuomotor learning. *NeuroImage* 195:340–353. DOI: https://doi.org/10.1016/j.neuroimage.2019.03.079, PMID: 30954709
- Fischer P, Tan H, Pogosyan A, Brown P. 2016. High post-movement parietal low-beta power during rhythmic tapping facilitates performance in a stop task. *The European Journal of Neuroscience* **44**:2202–2213. DOI: https://doi.org/10.1111/ejn.13328, PMID: 27364852
- Fischer P, Pogosyan A, Herz DM, Cheeran B, Green AL, Fitzgerald J, Aziz TZ, Hyam J, Little S, Foltynie T, Limousin P, Zrinzo L, Brown P, Tan H. 2017. Subthalamic nucleus gamma activity increases not only during movement but also during movement inhibition. *eLife* 6:e23947. DOI: https://doi.org/10.7554/eLife.23947, PMID: 28742498
- Fischer P, Pogosyan A, Green AL, Aziz TZ, Hyam J, Foltynie T, Limousin P, Zrinzo L, Samuel M, Ashkan K, Da Lio M, De Cecco M, Fornaser A, Brown P, Tan H. 2019. Beta synchrony in the cortico-basal ganglia network during regulation of force control on and off dopamine. *Neurobiology of Disease* 127:253–263. DOI: https://doi.org/10.1016/j.nbd.2019.03.004, PMID: 30849510
- Fischer P, Lipski WJ, Neumann W-J, Turner RS, Fries P, Brown P, Richardson RM. 2020. Movement-related coupling of human subthalamic nucleus spikes to cortical gamma. eLife 9:e51956. DOI: https://doi.org/10.7554/eLife.51956
- Fonken YM, Rieger JW, Tzvi E, Crone NE, Chang E, Parvizi J, Knight RT, Krämer UM. 2016. Frontal and motor cortex contributions to response inhibition: evidence from electrocorticography. *Journal of Neurophysiology* 115:2224–2236. DOI: https://doi.org/10.1152/jn.00708.2015, PMID: 26864760
- Gross J, Kujala J, Hamalainen M, Timmermann L, Schnitzler A, Salmelin R. 2001. Dynamic imaging of coherent sources: Studying neural interactions in the human brain. *PNAS* **98**:694–699. DOI: https://doi.org/10.1073/pnas.98.2.694, PMID: 11209067
- Haufe S, Nikulin W, Müller K-R, Nolte G. 2013. A critical assessment of connectivity measures for EEG data: a simulation study. *NeuroImage* 64:120–133. DOI: https://doi.org/10.1016/j.neuroimage.2012.09.036, PMID: 23006806
- Heinrichs-Graham E, Wilson TW. 2016. Is an absolute level of cortical beta suppression required for proper movement? Magnetoencephalographic evidence from healthy aging. NeuroImage 134:514–521. DOI: https://doi.org/10.1016/j.neuroImage.2016.04.032, PMID: 27090351
- Hirschmann J, Özkurt TE, Butz M, Homburger M, Elben S, Hartmann CJ, Vesper J, Wojtecki L, Schnitzler A. 2013. Differential modulation of STN-cortical and cortico-muscular coherence by movement and levodopa in Parkinson's disease. NeuroImage 68:203–213. DOI: https://doi.org/10.1016/j.neuroimage.2012.11.036, PMID: 23247184
- HirschmannJ, WinklerL. 2025. Subthalamo-cortical-synchronization.
- swh:1:rev:a63b3ce5947c1aca5bfabbc6a992a510ab3f2aa0. Software Heritage. https://archive.softwareheritage.org/swh:1:dir:7c0ae01b3e8443813c9e4177c4c556f661f8e1dc;origin=https://github.com/luciewinkler/Subthalamo-Cortical-Synchronization;visit=swh:1:snp:84886525a95aeb37ea9e1c6950fe85a86408cde2;anchor=swh:1:rev:a63b3ce5947c1aca5bfabbc6a992a510ab3f2aa0
- **Igarashi** J, Isomura Y, Arai K, Harukuni R, Fukai T. 2013. A θ-γ oscillation code for neuronal coordination during motor behavior. *The Journal of Neuroscience* **33**:18515–18530. DOI: https://doi.org/10.1523/JNEUROSCI. 2126-13.2013, PMID: 24259574
- Isoda M, Hikosaka O. 2008. Role for subthalamic nucleus neurons in switching from automatic to controlled eye movement. The Journal of Neuroscience 28:7209–7218. DOI: https://doi.org/10.1523/JNEUROSCI.0487-08. 2008, PMID: 18614691
- Jurkiewicz MT, Gaetz WC, Bostan AC, Cheyne D. 2006. Post-movement beta rebound is generated in motor cortex: evidence from neuromagnetic recordings. NeuroImage 32:1281–1289. DOI: https://doi.org/10.1016/j. neuroimage.2006.06.005, PMID: 16863693



- Khanna P, Carmena JM. 2017. Beta band oscillations in motor cortex reflect neural population signals that delay movement onset. eLife 6:e24573. DOI: https://doi.org/10.7554/eLife.24573, PMID: 28467303
- Lisi G, Morimoto J. 2015. EEG single-trial detection of gait speed changes during treadmill walk. PLOS ONE 10:e0125479. DOI: https://doi.org/10.1371/journal.pone.0125479, PMID: 25932947
- Litvak V, Eusebio A, Jha A, Oostenveld R, Barnes G, Foltynie T, Limousin P, Zrinzo L, Hariz MI, Friston K, Brown P. 2012. Movement-related changes in local and long-range synchronization in Parkinson's disease revealed by simultaneous magnetoencephalography and intracranial recordings. *Journal of Neuroscience* 32:10541–10553. DOI: https://doi.org/10.1523/JNEUROSCI.0767-12.2012
- Lofredi R, Neumann W-J, Bock A, Horn A, Huebl J, Siegert S, Schneider G-H, Krauss JK, Kühn AA. 2018. Dopamine-dependent scaling of subthalamic gamma bursts with movement velocity in patients with Parkinson's disease. *eLife* 7:e31895. DOI: https://doi.org/10.7554/eLife.31895, PMID: 29388913
- Lofredi R, Auernig GC, Irmen F, Nieweler J, Neumann W-J, Horn A, Schneider G-H, Kühn AA. 2021. Subthalamic stimulation impairs stopping of ongoing movements. *Brain* 144:44–52. DOI: https://doi.org/10.1093/brain/awaa341, PMID: 33253351
- Lofredi R, Scheller U, Mindermann A, Feldmann LK, Krauss JK, Saryyeva A, Schneider G-H, Kühn AA. 2023. Pallidal beta activity is linked to stimulation-induced slowness in Dystonia. *Movement Disorders* **38**:894–899. DOI: https://doi.org/10.1002/mds.29347, PMID: 36807626
- London D, Fazl A, Katlowitz K, Soula M, Pourfar MH, Mogilner AY, Kiani R. 2021. Distinct population code for movement kinematics and changes of ongoing movements in human subthalamic nucleus. eLife 10:e64893. DOI: https://doi.org/10.7554/eLife.64893, PMID: 34519273
- Mann JM, Foote KD, Garvan CW, Fernandez HH, Jacobson CE, Rodriguez RL, Haq IU, Siddiqui MS, Malaty IA, Morishita T, Hass CJ, Okun MS. 2009. Brain penetration effects of microelectrodes and DBS leads in STN or GPi. Journal of Neurology, Neurosurgery, and Psychiatry 80:794–797. DOI: https://doi.org/10.1136/jnnp.2008. 159558, PMID: 19237386
- Mosher CP, Mamelak AN, Malekmohammadi M, Pouratian N, Rutishauser U. 2021. Distinct roles of dorsal and ventral subthalamic neurons in action selection and cancellation. *Neuron* 109:869–881.. DOI: https://doi.org/10.1016/j.neuron.2020.12.025, PMID: 33482087
- Muralidharan V, Aron AR. 2021. Behavioral induction of a high beta state in sensorimotor cortex leads to movement Slowing. *Journal of Cognitive Neuroscience* 33:1311–1328. DOI: https://doi.org/10.1162/jocn_a_01717, PMID: 34496400
- Muralidharan V, Aron AR, Schmidt R. 2022. Transient beta modulates decision thresholds during human action-stopping. *NeuroImage* **254**:119145. DOI: https://doi.org/10.1016/j.neuroimage.2022.119145
- Neudorfer C, Butenko K, Oxenford S, Rajamani N, Achtzehn J, Goede L, Hollunder B, Ríos AS, Hart L, Tasserie J, Fernando KB, Nguyen TAK, Al-Fatly B, Vissani M, Fox M, Richardson RM, van Rienen U, Kühn AA, Husch AD, Opri E, et al. 2023. Lead-DBS v3.0: Mapping deep brain stimulation effects to local anatomy and global networks. NeuroImage 268:119862. DOI: https://doi.org/10.1016/j.neuroimage.2023.119862, PMID: 36610682
- Nolte G. 2003. The magnetic lead field theorem in the quasi-static approximation and its use for magnetoencephalography forward calculation in realistic volume conductors. *Physics in Medicine and Biology* 48:3637–3652. DOI: https://doi.org/10.1088/0031-9155/48/22/002, PMID: 14680264
- Olson JW, Nakhmani A, Irwin ZT, Edwards LJ, Gonzalez CL, Wade MH, Black SD, Awad MZ, Kuhman DJ, Hurt CP, Guthrie BL, Walker HC. 2022. Cortical and subthalamic nucleus spectral changes during limb movements in parkinson's disease patients with and without Dystonia. *Movement Disorders* 37:1683–1692. DOI: https://doi.org/10.1002/mds.29057, PMID: 35702056
- Oostenveld R, Fries P, Maris E, Schoffelen JM. 2011. FieldTrip: open source software for advanced analysis of MEG, EEG, and invasive electrophysiological data. *Computational Intelligence and Neuroscience* 2011:1–9. DOI: https://doi.org/10.1155/2011/156869
- Oswal A, Litvak V, Sauleau P, Brown P. 2012. Beta reactivity, prospective facilitation of executive processing, and its dependence on dopaminergic therapy in Parkinson's disease. *The Journal of Neuroscience* 32:9909–9916. DOI: https://doi.org/10.1523/JNEUROSCI.0275-12.2012, PMID: 22815506
- Oswal A, Litvak V, Brücke C, Huebl J, Schneider GH, Kühn AA, Brown P. 2013. Cognitive factors modulate activity within the human subthalamic nucleus during voluntary movement in Parkinson's disease. *The Journal of Neuroscience* 33:15815–15826. DOI: https://doi.org/10.1523/JNEUROSCI.1790-13.2013, PMID: 24089489
- Oswal A, Cao C, Yeh C-H, Neumann W-J, Gratwicke J, Akram H, Horn A, Li D, Zhan S, Zhang C, Wang Q, Zrinzo L, Foltynie T, Limousin P, Bogacz R, Sun B, Husain M, Brown P, Litvak V. 2021. Neural signatures of hyperdirect pathway activity in Parkinson's disease. *Nature Communications* 12:5185. DOI: https://doi.org/10.1038/s41467-021-25366-0, PMID: 34465771
- Patai EZ, Foltynie T, Limousin P, Akram H, Zrinzo L, Bogacz R, Litvak V. 2022. Conflict detection in a sequential decision task is associated with increased cortico-subthalamic coherence and prolonged subthalamic oscillatory response in the β Band. *The Journal of Neuroscience* 42:4681–4692. DOI: https://doi.org/10.1523/JNEUROSCI.0572-21.2022, PMID: 35501153
- Pfurtscheller G, Neuper C, Brunner C, da Silva FL. 2005. Beta rebound after different types of motor imagery in man. Neuroscience Letters 378:156–159. DOI: https://doi.org/10.1016/j.neulet.2004.12.034, PMID: 15781150
- Pogosyan A, Gaynor LD, Eusebio A, Brown P. 2009. Boosting cortical activity at Beta-band frequencies slows movement in humans. Current Biology 19:1637–1641. DOI: https://doi.org/10.1016/j.cub.2009.07.074, PMID: 19800236
- Rasch B, Friese M, Hofmann W, Neumann E. 2021. Quantitative Methoden. Springer. DOI: https://doi.org/10.1007/978-3-662-63284-0



- Rau C, Plewnia C, Hummel F, Gerloff C. 2003. Event-related desynchronization and excitability of the ipsilateral motor cortex during simple self-paced finger movements. *Clinical Neurophysiology* **114**:1819–1826. DOI: https://doi.org/10.1016/s1388-2457(03)00174-3, PMID: 14499743
- Ray NJ, Brittain JS, Holland P, Joundi RA, Stein JF, Aziz TZ, Jenkinson N. 2012. The role of the subthalamic nucleus in response inhibition: evidence from local field potential recordings in the human subthalamic nucleus. *NeuroImage* 60:271–278. DOI: https://doi.org/10.1016/j.neuroimage.2011.12.035, PMID: 22209815
- Salmelin R, Hämäläinen M, Kajola M, Hari R. 1995. Functional segregation of movement-related rhythmic activity in the human brain. NeuroImage 2:237–243. DOI: https://doi.org/10.1006/nimg.1995.1031, PMID: 9343608
- Schmidt R, Leventhal DK, Mallet N, Chen F, Berke JD. 2013. Canceling actions involves a race between basal ganglia pathways. *Nature Neuroscience* **16**:1118–1124. DOI: https://doi.org/10.1038/nn.3456, PMID: 23852117
- Schmidt R, Berke JD. 2017. A Pause-then-Cancel model of stopping: evidence from basal ganglia neurophysiology. Philosophical Transactions of the Royal Society of London. Series B, Biological Sciences 372:20160202. DOI: https://doi.org/10.1098/rstb.2016.0202, PMID: 28242736
- Schmidt R, Herrojo Ruiz M, Kilavik BE, Lundqvist M, Starr PA, Aron AR. 2019. Beta oscillations in working memory, executive control of movement and thought, and sensorimotor function. The Journal of Neuroscience 39:8231–8238. DOI: https://doi.org/10.1523/JNEUROSCI.1163-19.2019, PMID: 31619492
- Struber L, Baumont M, Barraud PA, Nougier V, Cignetti F. 2021. Brain oscillatory correlates of visuomotor adaptive learning. NeuroImage 245:118645. DOI: https://doi.org/10.1016/j.neuroimage.2021.118645, PMID: 34687861
- Swann N, Tandon N, Canolty R, Ellmore TM, McEvoy LK, Dreyer S, DiSano M, Aron AR. 2009. Intracranial EEG reveals a time- and frequency-specific role for the right inferior frontal gyrus and primary motor cortex in stopping initiated responses. *The Journal of Neuroscience* 29:12675–12685. DOI: https://doi.org/10.1523/JNEUROSCI.3359-09.2009, PMID: 19812342
- Talakoub O, Neagu B, Udupa K, Tsang E, Chen R, Popovic MR, Wong W. 2016. Time-course of coherence in the human basal ganglia during voluntary movements. *Scientific Reports* **6**:34930. DOI: https://doi.org/10.1038/srep34930, PMID: 27725721
- Tamir I, Wang D, Chen W, Ostrem JL, Starr PA, de Hemptinne C. 2020. Eight cylindrical contact lead recordings in the subthalamic region localize beta oscillations source to the dorsal STN. *Neurobiology of Disease* 146:105090. DOI: https://doi.org/10.1016/j.nbd.2020.105090, PMID: 32977021
- Tan H, Zavala B, Pogosyan A, Ashkan K, Zrinzo L, Foltynie T, Limousin P, Brown P. 2014. Human subthalamic nucleus in movement error detection and its evaluation during visuomotor adaptation. *The Journal of Neuroscience* 34:16744–16754. DOI: https://doi.org/10.1523/JNEUROSCI.3414-14.2014, PMID: 25505327
- Tan H, Wade C, Brown P. 2016. Post-movement beta activity in sensorimotor cortex indexes confidence in the estimations from internal models. *The Journal of Neuroscience* **36**:1516–1528. DOI: https://doi.org/10.1523/JNEUROSCI.3204-15.2016, PMID: 26843635
- Taulu S, Simola J. 2006. Spatiotemporal signal space separation method for rejecting nearby interference in MEG measurements. Physics in Medicine and Biology 51:1759–1768. DOI: https://doi.org/10.1088/0031-9155/51/7/008, PMID: 16552102
- Tinkhauser G, Pogosyan A, Tan H, Herz DM, Kühn AA, Brown P. 2017. Beta burst dynamics in Parkinson's disease OFF and ON dopaminergic medication. *Brain* 140:2968–2981. DOI: https://doi.org/10.1093/brain/awx252
- **Toledo DR**, Manzano GM, Barela JA, Kohn AF. 2016. Cortical correlates of response time slowing in older adults: ERP and ERD/ERS analyses during passive ankle movement. *Clinical Neurophysiology* **127**:655–663. DOI: https://doi.org/10.1016/j.clinph.2015.05.003, PMID: 26024982
- Turner RS, Desmurget M. 2010. Basal ganglia contributions to motor control: a vigorous tutor. Current Opinion in Neurobiology 20:704–716. DOI: https://doi.org/10.1016/j.conb.2010.08.022, PMID: 20850966
- Tzagarakis C, Ince NF, Leuthold AC, Pellizzer G. 2010. Beta-band activity during motor planning reflects response uncertainty. *The Journal of Neuroscience* **30**:11270–11277. DOI: https://doi.org/10.1523/JNEUROSCI.6026-09.2010, PMID: 20739547
- Van Veen BD, Buckley KM. 1988. Beamforming: a versatile approach to spatial filtering. *IEEE ASSP Magazine* 5:4–24. DOI: https://doi.org/10.1109/53.665
- van Wijk BCM, Neumann W-J, Schneider G-H, Sander TH, Litvak V, Kühn AA. 2017. Low-beta cortico-pallidal coherence decreases during movement and correlates with overall reaction time. *NeuroImage* **159**:1–8. DOI: https://doi.org/10.1016/j.neuroimage.2017.07.024, PMID: 28712991
- Wagner J, Wessel JR, Ghahremani A, Aron AR. 2018. Establishing a right frontal beta signature for stopping action in scalp eeg: implications for testing inhibitory control in other task contexts. *Journal of Cognitive Neuroscience* 30:107–118. DOI: https://doi.org/10.1162/jocn_a_01183, PMID: 28880766
- Wessel JR, Ghahremani A, Udupa K, Saha U, Kalia SK, Hodaie M, Lozano AM, Aron AR, Chen R. 2016. Stop-related subthalamic beta activity indexes global motor suppression in Parkinson's disease. *Movement Disorders* 31:1846–1853. DOI: https://doi.org/10.1002/mds.26732, PMID: 27474845
- Wessel JR, Waller DA, Greenlee JDW. 2019. Non-selective inhibition of inappropriate motor-tendencies during response-conflict by a fronto-subthalamic mechanism. *eLife* **8**:e42959. DOI: https://doi.org/10.7554/eLife. 42959, PMID: 31063130
- Wessel JR. 2020. β-bursts reveal the trial-to-trial dynamics of movement initiation and cancellation. *The Journal of Neuroscience* **40**:411–423. DOI: https://doi.org/10.1523/JNEUROSCI.1887-19.2019, PMID: 31748375

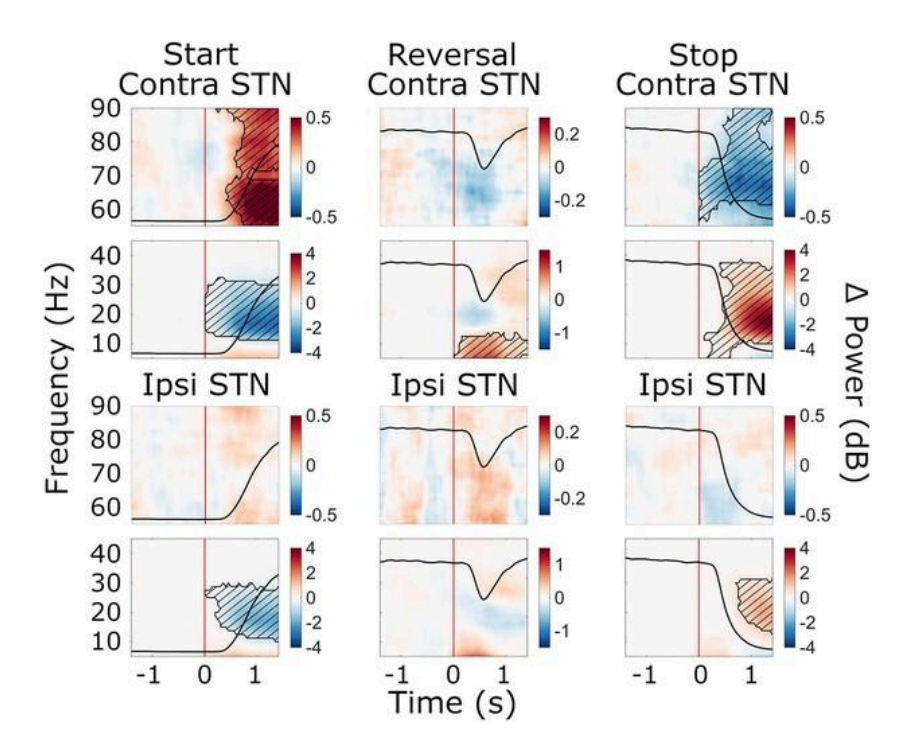


Zaepffel M, Trachel R, Kilavik BE, Brochier T. 2013. Modulations of EEG beta power during planning and execution of grasping movements. PLOS ONE 8:e60060. DOI: https://doi.org/10.1371/journal.pone.0060060, PMID: 23555884

Zavala BA, Jang AI, Zaghloul KA. 2017. Human subthalamic nucleus activity during non-motor decision making. eLife 6:e31007. DOI: https://doi.org/10.7554/eLife.31007, PMID: 29243587

Zavala B, Jang A, Trotta M, Lungu CI, Brown P, Zaghloul KA. 2018. Cognitive control involves theta power within trials and beta power across trials in the prefrontal-subthalamic network. *Brain* 141:3361–3376. DOI: https://doi.org/10.1093/brain/awy266, PMID: 30358821

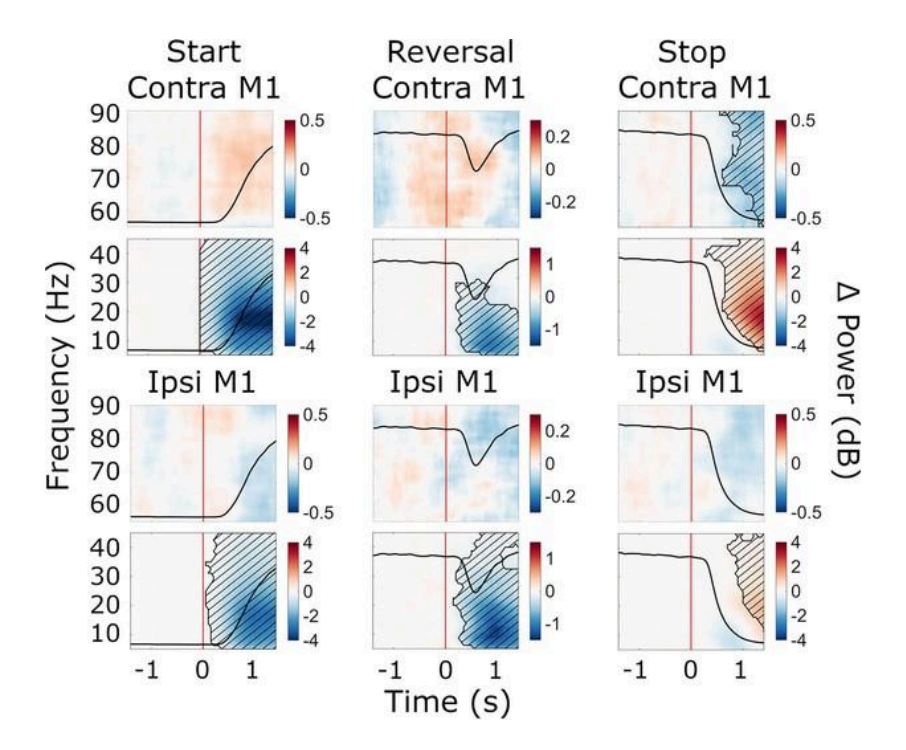
Figure 3—figure supplement 1



Cue-aligned beta power modulations in the subthalamic nucleus (STN).

Time-frequency spectra of cue-aligned start, reversal, and stop trials for the STN (group average, trials averaged across predictability conditions). Time 0 marks the appearance of the cue to start, reverse, or stop turning (red lines). The black line in each plot represents the average wheel turning speed (scale: 0–600 deg/s). Power was baseline-corrected (baseline: –1.6–0 s). Hatched lines within black contours indicate significant changes relative to baseline. N=20.

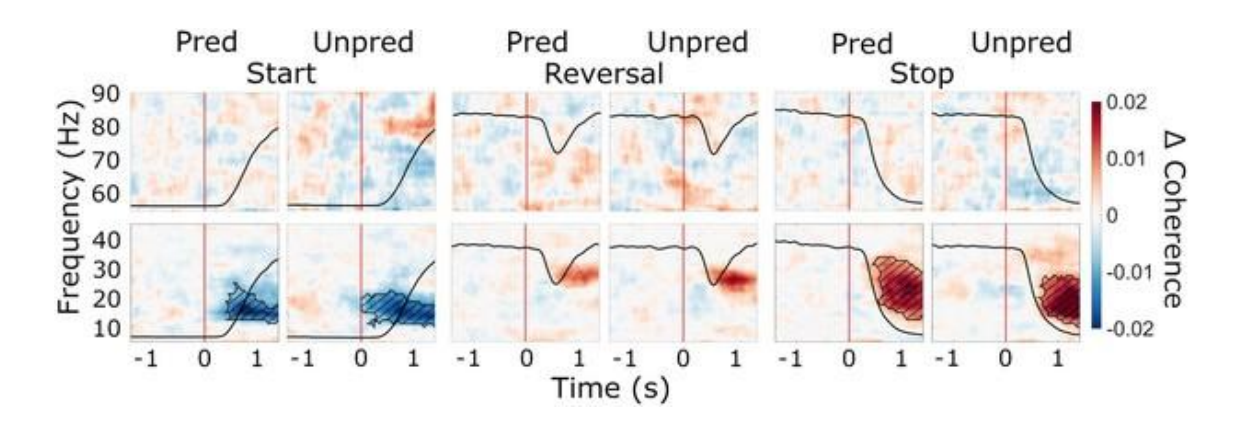
Figure 4—figure supplement 1



Cue-aligned beta power modulations in M1.

Time-frequency spectra of cue-aligned start, reversal, and stop trials for M1. Time 0 marks the appearance of the cue to start, reverse, or stop turning (red lines). The black line in each plot represents the average wheel turning speed (scale: 0-600 deg/s). Power was baseline-corrected (baseline: -1.6-0 s). Hatched lines within black contours indicate significant changes relative to baseline. N=20.

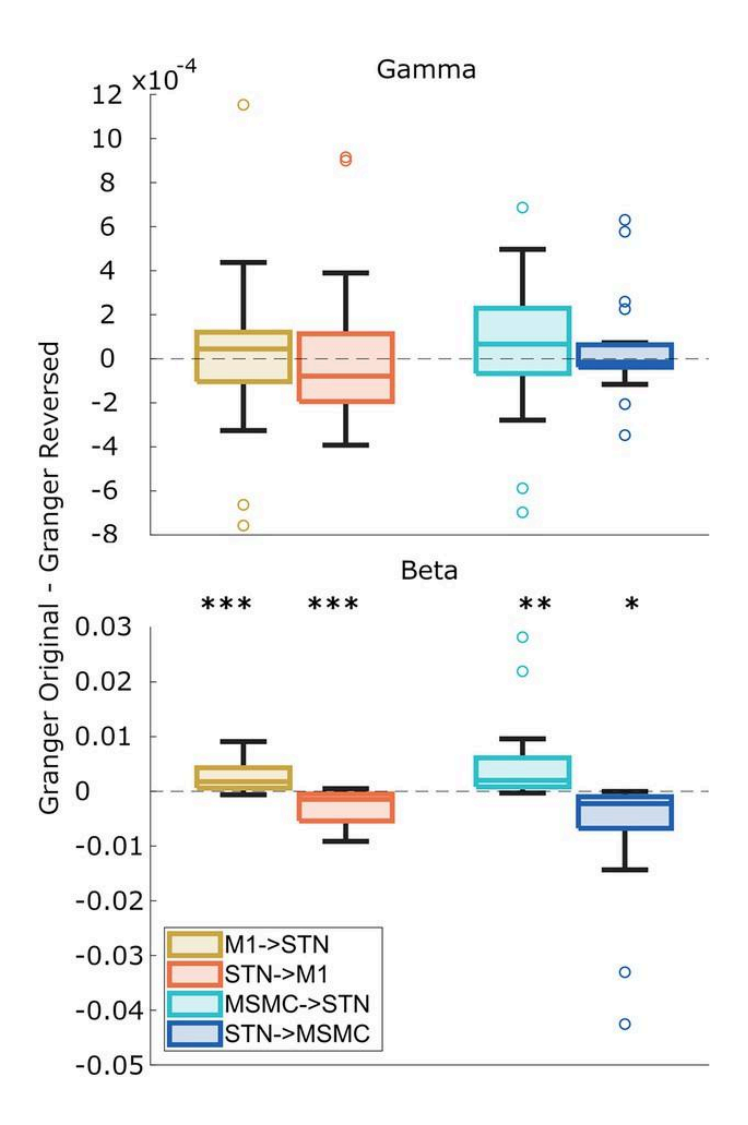
Figure 6—figure supplement 1



Cue-aligned modulations of subthalamic nucleus (STN)-cortex coherence and the effect of predictability.

Baseline-corrected group average of time-frequency representations of STN-cortex coherence (averaged over regions of interest, ROIs) during start, reversal, and stop (cue-aligned) for both the predictable and the unpredictable trials (baseline: –1.6–0 s). Time 0 marks the appearance of the cue to start, reverse, or stop turning (red lines). The black line in each plot represents the average wheel turning speed (scale: 0–600 deg/s). Hatched lines within black contours indicate significant changes relative to baseline. N=20.

Figure 6—figure supplement 2



Directionality of M1-subthalamic nucleus (STN) and MSMC-STN coupling.

Beta and gamma Granger causality estimates were averaged over predictability conditions, movements, and hemispheres. Boxplots illustrate the differences in Granger causality between the original data and the time-reversed data. Differences significantly deviating from zero indicate significant directionality, as indicated by asterisks. Positive values suggest a given area drives the other. N=20.

Supplementary File 1: Behavioral effects. (**A**) Effects of condition (predictable, unpredictable) and movement (start, reverse, stop) on movement-aligned speed, controlling for age, pre-operative UPDRS score and disease duration. (**B**) Effects of condition (predictable, unpredictable) and movement (start, reverse, stop) on reaction times to cues, controlling for age, pre-operative UPDRS score and disease duration.

Α

Factor	Wilk's	F	Hypothesis	Error	Sig.	${\eta_p}^2$
	Lambda		df	df		
Condition	0.998	0.037	1	16	0.850	0.002
Condition*age	0.974	0.425	1	16	0.524	0.026
Condition*UPDRS	1,000	0.002	1	16	0.966	0,000
Condition*disease duration	0.894	1.897	1	16	0.187	0.106
Movement	0.412	10.695	2	15	0.001	0.588
Movement*age	0.987	0.098	2	15	0.908	0.013
Movement*UPDRS	0.971	0.223	2	15	0.803	0.029
Movement*disease duration	0.992	0.059	2	15	0.943	0.008
Condition*movement	0.762	2.345	2	15	0.130	0.238
Condition*movement*age	0.983	0.129	2	15	0.880	0.017
Condition*movement*UPDRS	0.848	1.344	2	15	0.291	0.152
Condition*movement*disease duration	0.939	0.483	2	15	0.626	0.061

Condition	0.705	6.698	1	16	0.020	0.295
Condition*age	0.987	0.205	1	16	0.657	0.013
Condition*UPDRS	0.967	0.544	1	16	0.472	0.033
Condition*disease duration	0.998	0.031	1	16	0.862	0.002
Movement	0.278	19.482	2	15	<0.001	0.722
Movement*age	0.968	0.251	2	15	0.781	0.032
Movement*UPDRS	0.906	0.780	2	15	0.476	0.094
Movement*disease duration	0.815	1.708	2	15	0.215	0.185
Condition*movement	0.604	4.916	2	15	0.023	0.396
Condition*movement*age	0.828	1.556	2	15	0.243	0.172
Condition*movement* UPDRS	0.881	1.015	2	15	0.386	0.119
Condition*movement* disease duration	0.900	0.832	2	15	0.454	0.100

Supplementary File 2: Effects on lateralization. Effects of modulation type (beta suppression, beta rebound), condition (predictable, unpredictable) and ROI (STN, M1, MSMC) on lateralization index, controlling for age, pre-operative UPDRS score and disease duration.

Factor	Wilk's Lambda	F	Hypothesis <i>df</i>	Error <i>df</i>	Sig.	${\eta_p}^2$
		40.000	,	40	.0.004	0.700
Modulation type	0.467	18.233	1	16	<0.001	0.533
Modulation type*age	0.989	0.185	1	16	0.673	0.011
Modulation	0.987	0.213	1	16	0.651	0.013
type*UPDRS						
Modulation	0.892	1.931	1	16	0.184	0.108
type*disease duration						
ROI	0.597	5.071	2	15	0.021	0.403
RO*age	0.960	0.313	2	15	0.736	0.040
ROI*UPDRS	0.861	1.210	2	15	0.326	0.139
ROI*disease duration	0.921	0.639	2	15	0.542	0.079
Condition	0.950	0.836	1	16	0.374	0.050
Condition*age	0.998	0.035	1	16	0.854	0.002
Condition*UPDRS	0.919	1.411	1	16	0.252	0.081
Condition*disease	0.975	0.407	1	16	0.532	0.025
ROI*condition	0.849	1.332	2	15	0.294	0.151

ROI*condition*age	0.816	1.689	2	15	0.218	0.184
ROI*condition*UPDRS	0.895	0.876	2	15	0.437	0.105
ROI*condition*disease	0.994	0.043	2	15	0.958	0.006
ROI*modulation type	0.372	12.648	2	15	<0.001	0.628
ROI*modulation	0.963	0.292	2	15	0.751	0.037
ROI*modulation type*UPDRS	0.821	1.636	2	15	0.228	0.179
ROI*modulation type*disease duration	0.888	0.949	2	15	0.409	0.112
Modulation type type*condition	0.990	0.161	1	16	0.693	0.010
Modulation type type*condition*age	0.998	0.028	1	16	0.870	0.002
Modulation type type*condition*UPDRS	0.968	0.524	1	16	0.480	0.032
Modulation type type*condition*disease duration	0.919	1.411	1	16	0.252	0.081
ROI*condition* modulation type	0.770	2.237	2	15	0.141	0.230

ROI*condition*	0.712	3.035	2	15	0.078	0.288
modulation type*age						
ROI*condition*	0.970	0.231	2	15	0.796	0.030
modulation						
type*UPDRS						
ROI*condition*	0.770	2.239	2	15	0.141	0.230

modulation

type*disease

duration

Supplementary File 3: Effects on beta power and coherence. (A) Effects of condition (predictable, unpredictable), movement (start, reverse, stop) and ROI (contralateral and ipsilateral STN, M1, MSMC) on normalized power, controlling for movement speed, age, pre-operative UPDRS score and disease duration. (B) Effects of condition (predictable, unpredictable), movement (start, reverse, stop) and ROI (contralateral STN-M1, contralateral STN-MSMC, ipsilateral STN-M1, ipsilateral STN-MSMC) on coherence modulation, controlling for movement speed, age, pre-operative UPDRS score and disease duration.

Α

Factor	Wilk's	F	Hypothesis	Error	Sig.	${\eta_p}^2$
	Lambda		df	df		
Condition	0.938	0.992	1	15	0.335	0.062
Condition*speed	0.936	1.034	1	15	0.325	0.064
Condition*age	0.938	0.991	1	15	0.335	0.062
Condition*UPDRS	0.960	0.632	1	15	0.439	0.040
Condition*disease duration	0.951	0.777	1	15	0.392	0.049
ROI	0.239	6.988	5	11	0.004	0.761
ROI*speed	0.595	1.500	5	11	0.267	0.405
ROI*age	0.900	0.245	5	11	0.934	0.100
ROI*UPDRS	0.740	0.773	5	11	0.589	0.260
ROI*disease duration	0.898	0.250	5	11	0.931	0.102
Movement	0.111	56.281	2	14	<0.001	0.889
Movement*speed	0.832	1.414	2	14	0.276	0.168

Movement*age	0.952	0.355	2	14	0.707	0.048
Movement*UPDRS	0.968	0.228	2	14	0.799	0.032
Movement*disease duration	0.919	0.618	2	14	0.553	0.081
ROI*condition	0.832	0.446	5	11	0.808	0.168
ROI*condition*speed	0.830	0.450	5	11	0.805	0.170
ROI*condition*age	0.800	0.550	5	11	0.736	0.200
ROI*condition*UPDRS	0.715	0.876	5	11	0.528	0.285
ROI*condition*disease	0.567	1.683	5	11	0.219	0.433
ROI*movement	0.119	4.444	10	6	0.041	0.881
ROI*movement*speed	0.368	1.031	10	6	0.508	0.632
ROI*movement*age	0.128	4.078	10	6	0.049	0.872
ROI*movement*UPDRS	0.331	1.212	10	6	0.424	0.669
ROI*movement*disease	0.494	0.616	10	6	0.763	0.506
Condition*movement	0.625	4.206	2	14	0.037	0.375
Condition*movement*speed	0.710	2.866	2	14	0.091	0.290
Condition*movement*age	0.938	0.463	2	14	0.639	0.062
Condition*movement*UPDRS	0.752	2.308	2	14	0.136	0.248
Condition*movement*disease duration	0.936	0.481	2	14	0.628	0.064

ROI*condition*movement	0.083	6.666	10	6	0.015	0.917
ROI*condition*movement*	0.429	0.800	10	6	0.641	0.571
speed						
ROI*condition*movement*	0.177	2.769	10	6	0.110	0.823
age						
ROI*condition*movement*	0.520	0.554	10	6	0.805	0.480
UPDRS						
ROI*condition*movement*	0.387	0.952	10	6	0.551	0.613
disease duration						
В						
Condition	0.633	8.684	1	15	0.010	0.367
Condition Condition*speed	0.633 0.962	8.684 0.595	1	15 15	0.010	0.367
Condition*speed	0.962	0.595	1	15	0.453	0.038
Condition*speed Condition*age	0.962	0.595 0.113	1	15 15	0.453	0.038
Condition*speed Condition*age Condition*UPDRS	0.962 0.992 0.942	0.595 0.113 0.929	1 1 1	15 15 15	0.453 0.741 0.350	0.038 0.008 0.058
Condition*speed Condition*age Condition*UPDRS Condition*disease duration	0.962 0.992 0.942 0.772	0.595 0.113 0.929 4.427	1 1 1	15 15 15	0.453 0.741 0.350 0.053	0.038 0.008 0.058 0.228
Condition*speed Condition*age Condition*UPDRS Condition*disease duration ROI	0.962 0.992 0.942 0.772 0.453	0.595 0.113 0.929 4.427 5.239	1 1 1 3	15 15 15 15	0.453 0.741 0.350 0.053 0.014	0.038 0.008 0.058 0.228 0.547
Condition*speed Condition*age Condition*UPDRS Condition*disease duration ROI ROI*speed	0.962 0.992 0.942 0.772 0.453	0.595 0.113 0.929 4.427 5.239 1.714	1 1 1 3	15 15 15 13	0.453 0.741 0.350 0.053 0.014 0.213	0.038 0.008 0.058 0.228 0.547 0.283
Condition*speed Condition*age Condition*UPDRS Condition*disease duration ROI ROI*speed ROI*age	0.962 0.992 0.942 0.772 0.453 0.717 0.682	0.595 0.113 0.929 4.427 5.239 1.714 2.017	1 1 1 3 3 3	15 15 15 15 13 13	0.453 0.741 0.350 0.053 0.014 0.213 0.161	0.038 0.008 0.058 0.228 0.547 0.283 0.318

Movement	0.370	11.907	2	14	<0.001	0.630
Movement*speed	0.959	0.296	2	14	0.749	0.041
Movement*age	0.825	1.486	2	14	0.260	0.175
Movement*UPDRS	0.979	0.150	2	14	0.862	0.021
Movement*disease duration	0.991	0.061	2	14	0.941	0.009
ROI*condition	0.698	1.871	3	13	0.184	0.302
ROI*condition*speed	0.988	0.050	3	13	0.984	0.012
ROI*condition*age	0.892	0.526	3	13	0.672	0.108
ROI*condition*UPDRS	0.819	0.960	3	13	0.441	0.181
ROI*condition*disease	0.737	1.546	3	13	0.250	0.263
ROI*movement	0.518	1.548	6	10	0.258	0.482
ROI*movement*speed	0.457	1.982	6	10	0.162	0.543
ROI*movement*age	0.810	0.390	6	10	0.870	0.190
ROI*movement*UPDRS	0.619	1.026	6	10	0.462	0.381
ROI*movement*disease	0.528	1.487	6	10	0.276	0.472
Condition*movement	0.956	0.319	2	14	0.732	0.044
Condition*movement	0.939	0.453	2	14	0.644	0.061

^{*}speed

Condition*movement*age	0.888	0.880	2	14	0.436	0.112
Condition*movement*UPDRS	0.925	0.565	2	14	0.581	0.075
Condition*movement*disease duration	0.817	1.572	2	14	0.242	0.183
ROI*condition*movement	0.642	0.930	6	10	0.513	0.358
ROI*condition*movement *speed	0.614	1.048	6	10	0.451	0.386
ROI*condition*movement*	0.777	0.479	6	10	0.810	0.223
ROI*condition*movement* UPDRS	0.819	0.367	6	10	0.884	0.181
ROI*condition*movement*	0.484	1.780	6	10	0.201	0.516

disease duration

Supplementary File 4: Effects on beta granger causality. (A) Effects of condition (predictable, unpredictable), movement (start, reverse, stop) and ROI (contralateral and ipsilateral M1->STN, STN->M1, MSMC->STN, STN->MSMC) on Granger causality, controlling for movement speed, age, preoperative UPDRS score and disease duration.

Α

Factor	Wilk's	F	Hypothesis	Error	Sig.	${\eta_p}^2$
	Lambda		df	df		
Condition	0.911	1.459	1	15	0.246	0.089
Condition*speed	0.824	3.199	1	15	0.094	0.176
Condition*age	0.999	0.008	1	15	0.931	0.001
Condition*UPDRS	1.000	0.000	1	15	0.999	0.000
Condition*disease duration	0.998	0.023	1	15	0.881	0.002
ROI	0.272	3.443	7	9	0.044	0.728
ROI*speed	0.663	0.653	7	9	0.707	0.337
ROI*age	0.414	1.820	7	9	0.198	0.586
ROI*UPDRS	0.878	0.178	7	9	0.983	0.122
ROI*disease duration	0.590	0.893	7	9	0.549	0.410
Movement	0.774	2.045	2	14	0.166	0.226
Movement*speed	0.662	3.567	2	14	0.056	0.338
Movement*age	0.795	1.805	2	14	0.201	0.205
Movement*UPDRS	0.745	2.398	2	14	0.127	0.255

Movement*disease duration	0.990	0.072	2	14	0.931	0.010
ROI*condition	0.753	0.421	7	9	0.866	0.247
ROI*condition*speed	0.633	0.745	7	9	0.643	0.367
ROI*condition*age	0.741	0.450	7	9	0.848	0.259
ROI*condition*UPDRS	0.805	0.312	7	9	0.931	0.195
ROI*condition*disease	0.663	0.652	7	9	0.707	0.337
duration						
ROI*movement	0.062	2.178	14	2	0.359	0.938
ROI*movement*speed	0.150	0.808	14	2	0.680	0.850
ROI*movement*age	0.131	0.946	14	2	0.627	0.869
ROI*movement*UPDRS	0.232	0.474	14	2	0.842	0.768
ROI*movement*disease	0.139	0.887	14	2	0.648	0.861
duration						
Condition*movement	0.727	2.632	2	14	0.107	0.273
Condition*movement	0.798	1.767	2	14	0.207	0.202
*speed						
Condition*movement*age	0.658	3.638	2	14	0.053	0.342
Condition*movement*UPDRS	0.955	0.333	2	14	0.722	0.045
Condition*movement*disease	0.898	0.794	2	14	0.471	0.102
duration						
ROI*condition*movement	0.078	1.698	14	2	0.432	0.922

ROI*condition*movement	0.149	0.816	14	2	0.677	0.851
*speed						
ROI*condition*movement*	0.133	0.931	14	2	0.632	0.867
ROI*condition*movement*	0.157	0.766	14	2	0.698	0.843
UPDRS						
ROI*condition*movement*	0.106	1.200	14	2	0.545	0.894
disease duration						

Supplementary File 5: Effects on gamma power and coherence. (A) Effects of condition (predictable, unpredictable), movement (start, reverse, stop) and ROI (contralateral and ipsilateral STN, M1, MSMC) on normalized power, controlling for movement speed, age, pre-operative UPDRS score and disease duration. (B) Effects of condition (predictable, unpredictable), movement (start, reverse, stop) and ROI (contralateral STN-M1, contralateral STN-MSMC, ipsilateral STN-M1, ipsilateral STN-MSMC) on coherence modulation, controlling for movement speed, age, pre-operative UPDRS score and disease duration.

Α

Factor	Wilk's Lambda	F	Hypothesis df	Error df	Sig.	${\eta_p}^2$
Condition	0.950	0.792	1	15	0.388	0.050
Condition*speed	0.849	2.667	1	15	0.123	0.151
Condition*age	0.998	0.032	1	15	0.861	0.002
Condition*UPDRS	0.904	1.592	1	15	0.226	0.096
Condition*disease duration	0.929	1.145	1	15	0.302	0.071
ROI	0.440	2.789	5	11	0.072	0.560
ROI*speed	0.593	1.510	5	11	0.264	0.407
ROI*age	0.788	0.592	5	11	0.707	0.212
ROI*UPDRS	0.807	0.526	5	11	0.753	0.193
ROI*disease duration	0.290	5.276	5	11	0.010	0.710
Movement	0.607	4.537	2	14	0.030	0.393
Movement*speed	0.966	0.247	2	14	0.784	0.034

Movement*age	0.925	0.567	2	14	0.580	0.075
Movement*UPDRS	0.940	0.450	2	14	0.647	0.060
Movement*disease duration	0.852	1.215	2	14	0.326	0.148
ROI*condition	0.745	0.752	5	11	0.602	0.255
ROI*condition*speed	0.598	1.447	5	11	0.273	0.402
ROI*condition*age	0.864	0.347	5	11	0.874	0.136
ROI*condition*UPDRS	0.645	1.212	5	11	0.366	0.355
ROI*condition*disease	0.766	0.671	5	11	0.654	0.234
ROI*movement	0.163	3.073	10	6	0.091	0.837
ROI*movement*speed	0.389	0.944	10	6	0.555	0.611
ROI*movement*age	0.227	2.045	10	6	0.197	0.773
ROI*movement*UPDRS	0.537	0.518	10	6	0.829	0.463
ROI*movement*disease	0.234	1.962	10	6	0.212	0.766
Condition*movement	0.962	0.276	2	14	0.763	0.038
Condition*movement*speed	0.916	0.639	2	14	0.542	0.084
Condition*movement*age	0.992	0.054	2	14	0.947	0.008
Condition*movement*UPDRS	0.991	0.063	2	14	0.939	0.009
Condition*movement*disease duration	0.978	0.160	2	14	0.853	0.022

ROI*condition*movement	0.316	1.301	10	6	0.389	0.684
ROI*condition*movement*	0.386	0.953	10	6	0.550	0.614
speed						
ROI*condition*movement*	0.041	14.067	10	6	0.002	0.959
age						
ROI*condition*movement*	0.083	6.643	10	6	0.015	0.917
UPDRS						
ROI*condition*movement*	0.475	0.662	10	6	0.731	0.525
disease duration						
В						
Condition	1.000	0.005	1	15	0.944	0.000
Condition Condition*speed	1.000 0.949	0.005 0.804	1	15 15	0.384	0.000
Condition*speed	0.949	0.804	1	15	0.384	0.051
Condition*speed Condition*age	0.949	0.804	1	15 15	0.384	0.051
Condition*speed Condition*age Condition*UPDRS	0.949 1.000 0.997	0.804 0.002 0.040	1 1 1	15 15 15	0.384 0.969 0.844	0.051 0.000 0.003
Condition*speed Condition*age Condition*UPDRS Condition*disease duration	0.949 1.000 0.997 0.983	0.804 0.002 0.040 0.257	1 1 1	15 15 15	0.384 0.969 0.844 0.619	0.051 0.000 0.003 0.017
Condition*speed Condition*age Condition*UPDRS Condition*disease duration ROI	0.949 1.000 0.997 0.983 0.921	0.804 0.002 0.040 0.257 0.371	1 1 1 3	15 15 15 15	0.384 0.969 0.844 0.619	0.051 0.000 0.003 0.017 0.079
Condition*speed Condition*age Condition*UPDRS Condition*disease duration ROI ROI*speed	0.949 1.000 0.997 0.983 0.921 0.812	0.804 0.002 0.040 0.257 0.371 1.006	1 1 1 3	15 15 15 13	0.384 0.969 0.844 0.619 0.775	0.051 0.000 0.003 0.017 0.079 0.188
Condition*speed Condition*age Condition*UPDRS Condition*disease duration ROI ROI*speed ROI*age	0.949 1.000 0.997 0.983 0.921 0.812 0.956	0.804 0.002 0.040 0.257 0.371 1.006 0.200	1 1 1 3 3	15 15 15 13 13	0.384 0.969 0.844 0.619 0.775 0.422 0.894	0.051 0.000 0.003 0.017 0.079 0.188 0.044

Movement	0.687	3.195	2	14	0.072	0.313
Movement*speed	0.918	0.626	2	14	0.549	0.082
Movement*age	0.819	1.547	2	14	0.247	0.181
Movement*UPDRS	0.645	3.851	2	14	0.047	0.355
Movement*disease duration	0.920	0.605	2	14	0.560	0.080
ROI*condition	0.809	1.025	3	13	0.414	0.191
ROI*condition*speed	0.944	0.256	3	13	0.856	0.056
ROI*condition*age	0.764	1.339	3	13	0.305	0.236
ROI*condition*UPDRS	0.929	0.330	3	13	0.804	0.071
ROI*condition*disease	0.562	3.373	3	13	0.051	0.438
ROI*movement	0.569	1.263	6	10	0.354	0.431
ROI*movement*speed	0.870	0.248	6	10	0.949	0.130
ROI*movement*age	0.976	0.042	6	10	1.000	0.024
ROI*movement*UPDRS	0.788	0.448	6	10	0.831	0.212
ROI*movement*disease	0.502	1.655	6	10	0.230	0.498
Condition*movement	0.681	3.274	2	14	0.068	0.319
Condition*movement	0.852	1.214	2	14	0.326	0.148

^{*}speed

Condition*movement*age	0.808	1.665	2	14	0.225	0.192
Condition*movement*UPDRS	0.908	0.709	2	14	0.509	0.092
Condition*movement*disease duration	0.937	0.467	2	14	0.636	0.063
ROI*condition*movement	0.641	0.935	6	10	0.511	0.359
ROI*condition*movement *speed	0.659	0.862	6	10	0.553	0.341
ROI*condition*movement*	0.554	1.344	6	10	0.323	0.446
ROI*condition*movement* UPDRS	0.650	0.897	6	10	0.532	0.350
ROI*condition*movement*	0.632	1.972	6	10	0.490	0.368

disease duration

Supplementary File 6: Effects on gamma granger causality. (A) Effects of condition (predictable, unpredictable), movement (start, reverse, stop) and ROI (contralateral and ipsilateral M1->STN, STN->M1, MSMC->STN, STN->MSMC) on Granger causality, controlling for movement speed, age, preoperative UPDRS score and disease duration.

Α

Factor	Wilk's	F	Hypothesis	Error	Sig.	${\eta_p}^2$
	Lambda		df	df		
Condition	0.814	3.435	1	15	0.084	0.186
Condition*speed	0.995	0.077	1	15	0.786	0.005
Condition*age	0.999	0.015	1	15	0.904	0.001
Condition*UPDRS	0.989	0.164	1	15	0.691	0.011
Condition*disease duration	0.984	0.238	1	15	0.633	0.016
ROI	0.792	0.338	7	9	0.917	0.208
ROI*speed	0.372	2.170	7	9	0.138	0.628
ROI*age	0.590	0.893	7	9	0.549	0.410
ROI*UPDRS	0.539	1.098	7	9	0.437	0.461
ROI*disease duration	0.773	0.378	7	9	0.894	0.227
Movement	0.774	2.043	2	14	0.167	0.226
Movement*speed	0.812	1.620	2	14	0.233	0.188
Movement*age	0.950	0.371	2	14	0.697	0.050
Movement*UPDRS	0.824	1.497	2	14	0.258	0.176

Movement*disease duration	0.966	0.245	2	14	0.786	0.034
ROI*condition	0.712	0.520	7	9	0.800	0.288
ROI*condition*speed	0.641	0.720	7	9	0.660	0.359
ROI*condition*age	0.541	1.090	7	9	0.441	0.459
ROI*condition*UPDRS	0.541	1.089	7	9	0.442	0.459
ROI*condition*disease	0.758	0.411	7	9	0.873	0.242
duration						
ROI*movement	0.039	3.478	14	2	0.246	0.961
ROI*movement*speed	0.133	0.932	14	2	0.631	0.867
ROI*movement*age	0.204	0.556	14	2	0.798	0.796
ROI*movement*UPDRS	0.250	0.428	14	2	0.867	0.750
ROI*movement*disease	0.149	0.813	14	2	0.678	0.851
duration						
Condition*movement	0.665	3.519	2	14	0.058	0.335
Condition*movement	0.955	0.333	2	14	0.722	0.045
*speed						
Condition*movement*age	0.791	1.846	2	14	0.194	0.209
Condition*movement*UPDRS	0.894	0.831	2	14	0.456	0.106
Condition*movement*disease	0.983	0.119	2	14	0.889	0.017
duration						
ROI*condition*movement	0.191	0.604	14	2	0.774	0.809

ROI*condition*movement	0.157	0.768	14	2	0.697	0.843
*speed						
ROI*condition*movement*	0.314	0.313	14	2	0.928	0.686
ROI*condition*movement*	0.402	0.212	14	2	0.973	0.598
UPDRS						
ROI*condition*movement*	0.084	1.565	14	2	0.458	0.916
disease duration						

Deep brain stimulation-responsive subthalamo-cortical coupling

in obsessive-compulsive disorder

Lucie Winkler MSc1, Lucy M. Werner MSc1, Markus Butz PhD1, Christian J. Hartmann MD12,

Alfons Schnitzler MD¹², Jan Hirschmann PhD^{1*}

¹ Institute of Clinical Neuroscience and Medical Psychology, Medical Faculty and University Hospital Düsseldorf,

Heinrich Heine University, 40225, Düsseldorf, Germany

² Center for Movement Disorders and Neuromodulation, Department of Neurology, Medical Faculty and

University Hospital Düsseldorf, 40225, Düsseldorf, Germany

*Jan Hirschmann

Email: Jan.Hirschmann@med.uni-duesseldorf.de

Abstract

Deep brain stimulation (DBS)-responsive oscillations have been implicated in motor

symptoms of Parkinson's disease (PD). Their role in non-movement disorders, such as

obsessive-compulsive disorder (OCD), is less clear. Here, we aimed to characterize the effect

of DBS on subthalamic and cortical oscillations in OCD.

Local field potential recordings from the subthalamic nucleus (STN) were combined with

magnetoencephalography in one OCD patient at rest (DBS OFF and ON) and in a Go/NoGo

task (DBS OFF). A PD patient completed the same task for comparison.

In the OCD patient, we observed right-lateralized beta peaks in STN power and STN-cortex

coherence. These were diminished by DBS. Task-related modulations of STN power occurred

in the theta band for the OCD patient, and in the beta band for the PD patient.

We conclude that resting-state, DBS-responsive beta oscillations are not necessarily a sign of

Parkinsonism. Task-related spectral modulations might be more disease-specific than resting-

state oscillations.

NOTE: This preprint reports new research that has not been certified by peer review and should not be used to guide clinical practice.

1

Introduction

Beta oscillations within the subthalamic nucleus (STN) are central to understanding the pathophysiology of Parkinson's disease (PD) and the therapeutic mechanisms of deep brain stimulation (DBS). In PD patients, beta activity is pathologically enhanced in the STN and other structures of the cortico-basal ganglia loop ¹⁻³, and is widely recognized to contribute to PD motor symptoms such as bradykinesia and rigidity ^{4,5}. DBS of the STN alleviates motor symptoms, presumably by reducing excessive beta activity in the STN ⁶⁻⁸ and sensorimotor cortex ^{6,9}. These findings suggest a causal role of subthalamic beta oscillations in motor slowing. This notion, however, is mostly based on observations in PD patients.

Here, we examined a patient with obsessive-compulsive disorder (OCD), a psychiatric condition marked by persistent thoughts and urges (obsessions), and repetitive actions or mental operations (compulsions) ¹⁰. OCD is characterized by pathologically enhanced overconnectivity in a network spanning limbic cortical regions, the striatum, and the STN ¹¹⁻¹⁵. Altered theta activity in the STN ^{16,17} and cortex ¹⁸⁻²⁰ has been identified as a potential biomarker of OCD pathology.

Importantly, OCD is a condition for which, despite the absence of motor slowing, DBS of the STN is being applied as a therapeutic intervention. The therapeutic benefit possibly acts through a reduction of theta oscillations in the fronto-basal ganglia pathway ^{21,22}. The role of beta oscillations in OCD has not been studied extensively, but some studies suggest that beta activity is altered in cortex ²³ and the STN ¹⁶ and that DBS is associated with both increases ²² and decreases ²⁴ of beta activity in the stria terminalis/anterior limb of the internal capsule and frontal cortex. However, while it has been demonstrated that beta oscillations are present in the dorsal ¹⁷ and anteromedial STN ¹¹ in OCD, it remains unknown whether and how DBS influences these oscillations. Therefore, we aimed to examine the effect of DBS in OCD.

2

Materials and methods

Patients

A female patient in her fifties suffering from severe OCD (first manifestation in the third decade), marked by excessive washing of the hands, participated in the present study. She was implanted with DBS electrodes (3389) 12 years before measurement, and received a new stimulator one day before participating in the present study. DBS reduced her Yale-Brown Compulsive Obsessive Scale score substantially, from 39/40 pre-operatively to 7 at the time of measurement. The patient's scores on the MDS-UPDRS III were 3 and 4 in the DBS OFF and ON setting, respectively. No medications were taken at the time of measurement.

For comparison, we present data from a female tremor-dominant idiopathic PD patient in her sixties in the Med ON state (first disease manifestation approximately 8 years ago at the time of participation; DBS system implanted 3 years ago; UPDRS Part III: Med OFF/DBS OFF: 51, Med ON/DBS ON: 18, Med OFF/DBS ON: 42). Both patients were implanted with a Medtronic Percept PC (Medtronic Inc., Minneapolis, MN, USA), capable of measuring local field potentials (LFPs) from the implanted DBS leads. DBS surgery was performed at the department of Functional Neurosurgery and Stereotaxy of the University Hospital Düsseldorf in adherence to standard procedures.

Both patients gave their written informed consent to participate in the study, according to the declaration of Helsinki. The study was approved by the Ethics Committee of the Medical Faculty of Heinrich Heine University Düsseldorf. Both patients consented to publication.

Recordings and stimulation

MEG was measured using a 306-channel MEG system (VectorView, MEGIN, Espoo, Finland) with a sampling rate of 2 kHz. We additionally monitored horizontal and vertical ocular using electrooculography (EOG). Muscular activity was recorded activity electromyography (EMG), with EMG surface electrodes placed on the patients' right and left forearms, referenced to EMG electrodes on the wrist. Additional surface electrodes were placed on the left chest to track the electrocardiogram (ECG), above the implanted stimulator, as well as on the neck above the subcutaneous extension to record the DBS artifact, with

reference electrodes positioned over the cervical vertebrae. We performed a 5 min resting-state recording in DBS OFF and subsequently applied monopolar, unilateral DBS using the second ring from the bottom (ring 1) at 130 Hz for 5 min in each hemisphere (amplitude: $1.2 \, \text{mA}$; pulse width: $60 \, \mu \text{s}$). We recorded bipolar LFPs with the Percept system in the BrainSense streaming mode from the rings above and below (0 and 2). Both patients additionally participated in a Go/NoGo task (see below). No stimulation was applied during the task.

Electrode localization

DBS electrode localizations (Fig. 1) were performed with the advanced processing pipeline in Lead-DBS v3.1 (lead-dbs.org) ²⁵. Briefly, postoperative CT images were linearly coregistered with pre-operative MRIs (T1 and T2) using advanced normalization tools ANTs; stnava.github.io/ANTs/; ²⁶. If necessary, co-registrations were reviewed and refined. Brain shift corrections were performed using Lead-DBS standard tools. We used all preoperative volumes to estimate a precise multispectral normalization to ICBM 2009b NLIN asymmetric ("MNI") space ²⁷ using the ANTs SyN Diffeomorphic Mapping ²⁸ with the preset "effective: low variance default+subcortical refinement." The reconstruction of DBS contacts was performed manually or using the PaCER method ²⁹. Atlas segmentations are based on the DISTAL atlas ³⁰. Finally, using the Lead group toolbox, visualizations of the electrode reconstructions were generated for both patients ³¹.

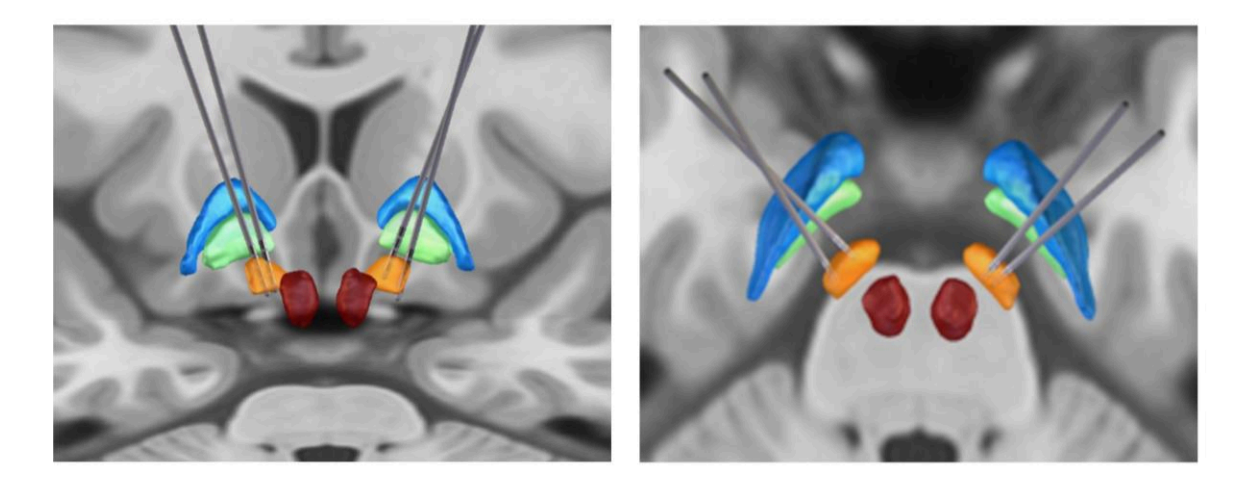


Figure 1. Electrode localization. Left: front view. Right: top view. Subthalamic nucleus: orange, external pallidum: blue, internal pallidum: green, red nucleus: red. The electrodes of the OCD patient are the ones that are positioned more medial on the level of the STN.

Paradigm

Both patients completed a visually cued Go/NoGo task (OCD patient: 4 blocks; PD patient: 3 blocks; 120 trials per block) while seated in the MEG scanner (Fig. 2). Visual stimuli were presented using the software PsychoPy (version 2023.2.3) in Python (3.12.0). Individual reaction time was estimated at the beginning of the experiment through a sequence of Go trials. In the main experiment, each trial began with a black fixation cross, lasting 500 ms, and ended with feedback (on screen for 1 s). Following the fixation cross, we presented the outlines of a bar in either horizontal or vertical orientation (cue). After 500 ms, the bar acquired either an orange or a blue color fill, corresponding to the Go stimulus or the NoGo stimulus, respectively. In case of Go, the patient had to press a button with the right index finger as fast as possible (time limit: individual reaction time + 2 SD). In case of NoGo, the patient was instructed to withhold any response. The NoGo stimulus was on screen for the individual reaction time + 4 SD. The orientation of the bar predicted the upcoming stimulus (Go or NoGo), i.e. each orientation was preferentially paired with a particular color, and this preference needed to be learned on task. We refer to the more common pairing as congruent trials, and to the less common pairing as incongruent trials. The distribution of trials was: 55% congruent Go, 12.5% incongruent Go, 20% congruent NoGo and 12.5% incongruent NoGo.

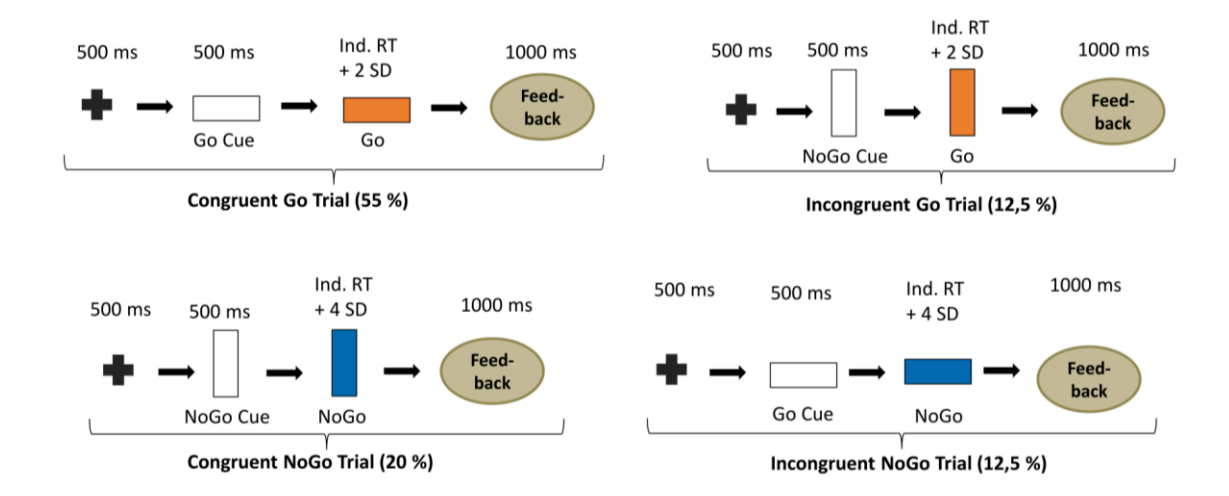


Figure 2. Cued Go/NoGo task. The association between bar orientation and expected instruction (here: horizontal – likely Go, vertical – likely NoGo) and between colour fill and instruction (here: orange – Go, blue - NoGo) was counterbalanced across subjects. Trial frequencies are noted below each trial type.

Data analysis

Data were analyzed using MATLAB R2019b (The Mathworks, Natick, Massachusetts, USA) and the toolbox FieldTrip ³², as well as Python (Version 3.12) and the fitting oscillations and one over F (FOOOF) toolbox 33.

Preprocessing

We first visually identified noisy channels and subsequently applied temporal Signal Space Separation to the MEG data ³⁴. The MEG data was downsampled to 250 Hz to match the sampling rate of the LFP data. We then applied a high-pass finite impulse response filter with a cut-off frequency of 1 Hz to remove low-frequency drifts and a low pass filter with a cut-off frequency of 100 Hz to both the MEG and LFP data to ease the detection of cardiac artifacts (see below).

We switched DBS on briefly at the beginning and at the end of each measurement, resulting in DBS artifacts, which we used for temporal alignment of MEG and LFP signals ³⁵. Given the presence of strong cardiac artifacts in the resting-state STN LFP data when DBS was ON, this initial alignment could be improved further in a second step based on the ECG. First, the ECG

signal was z-scored over the entire recording. Then, the R-peaks, features of the prominent

QRS waveform in ECG signals, were identified using the Matlab function findpeaks() with two

criteria: the peak height exceeded the mean signal level by 2.5 standard deviations, and the

interval between successive peaks was at least 500 ms. Next, we defined epochs centered on

the R-peak and averaged the epochs to obtain a mean QRS waveform for both LFP and ECG.

Finally, we computed the cross-covariance between the two versions of the heartbeat and

finetuned the initial alignment by correcting any delay visible in the cross-correlogram.

Spectral analysis and time-frequency analysis

LFP power and LFP-MEG coherence were computed using Welch's method in combination

with a Hanning taper ³². For LFP power, we isolated the oscillatory components from the

aperiodic background using the FOOOF toolbox ³³.

For the Go/NoGo task data, we source-reconstructed the activity of left and right

primary motor cortices (M1, hand-knob) using Linearly Constrained Minimum Variance

beamforming ³⁶. Time-frequency spectra (2-45 Hz) were computed for STN and M1 bilaterally

using a Hanning taper. As baseline, we used power averaged over all trial types

(i.e. congruent/incongruent Go/NoGo trials) and all time points within those trials. In Fig. 4,

we pooled congruent and incongruent trials, as we did not observe any effect of congruency.

Source reconstruction

To localize the sources of STN-cortex beta coherence, we first co-registered the pre-operative

T1-weighted MRI scan with the MEG coordinate system. Using the segmented MRI, a forward

model was generated based on a single-shell realistic head model ³⁷. Beamformer grid points

covered the whole brain, with their coordinates standardized to Montreal Neurological

Institute (MNI) space. Dynamic Imaging of Coherent Sources (DICS) 38 was applied to beta-

band LFP-MEG cross-spectral densities (13-30 Hz). To contrast the DBS ON and OFF conditions

(Fig. 3), we averaged the source images for left and right stimulation and subtracted the DBS

7

off image from the average.

it is made available under a CC-BT 4.0 international license

Statistical analysis

Differences in power and coherence between DBS ON and OFF in resting-state, and power

differences between Go and NoGo trials were identified through cluster-based permutation

tests ³⁹. We performed 1000 permutations, and used a cluster defining threshold of 0.05 (two-

sided test) and an alpha level of 0.025. The cluster statistic was defined as the sum of t-values

within a cluster.

Data availability

Data can be made available in anonymized form upon reasonable request.

Results

DBS reduced STN beta power and STN-cortex beta coherence in OCD

When analyzing the resting-state data of the OCD patient, we observed a prominent peak

in the beta-band for right STN power and for coherence between right STN and right

sensorimotor cortex (Fig. 3A). The beta power peak was reduced by stimulation of the left

 $(t_{\text{clustersum}} \le -10.775, p < 0.001)$ and particularly of the right $(t_{\text{clustersum}} \le -95.168, p < 0.001)$ STN

(Fig. 3C). Similarly, the beta peak in STN-sensorimotor cortex coherence was suppressed by

DBS of the right ($t_{clustersum} \le -14.258$, $p \le 0.02$) or left STN ($t_{clustersum} \le -14.704$, $p \le 0.002$;

8

Fig. 3C, D). Detailed statistical results can be found in Supplemental Tables 1-2.

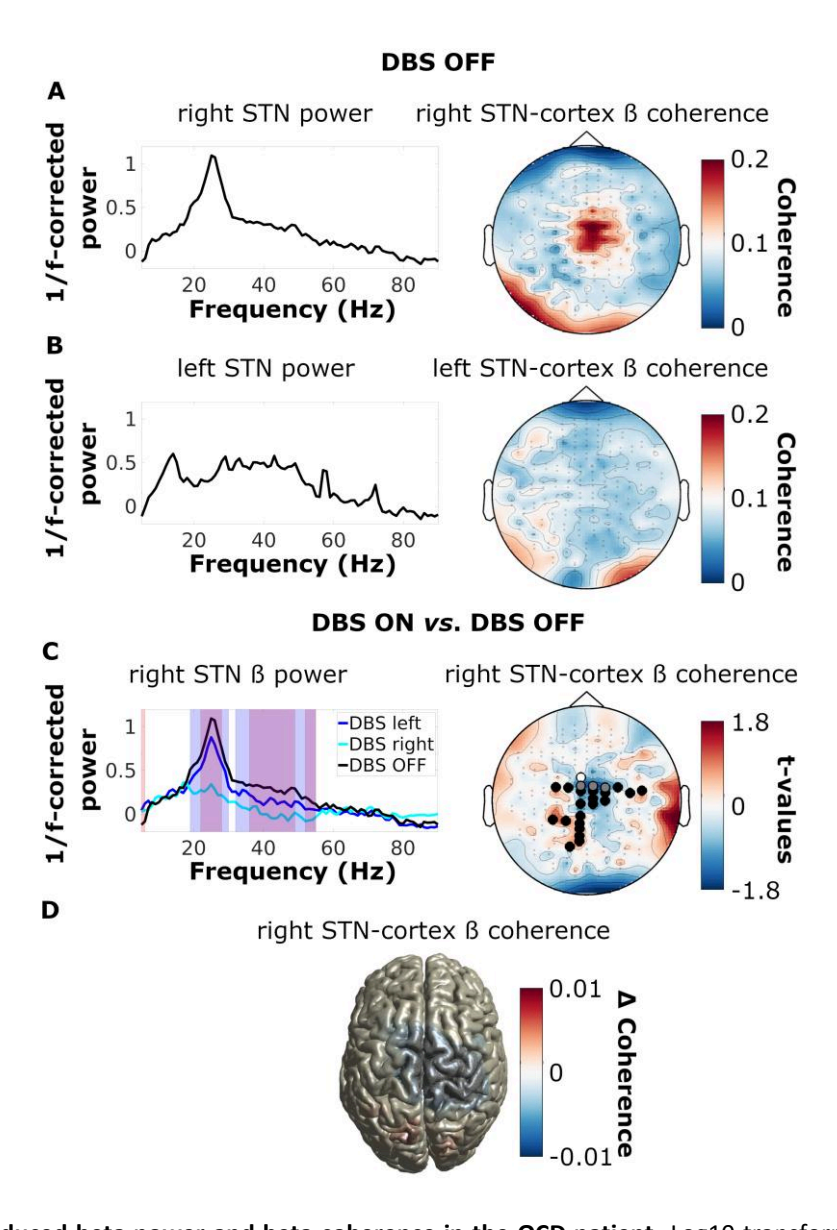


Figure 3. DBS reduced beta power and beta coherence in the OCD patient. Log10-transformed resting-state power spectra (aperiodic fit subtracted) and topographies of beta (13-30 Hz) STN-MEG sensor coherence for the right (A) and left (B) STN. (C; left) Log10-transformed resting-state power spectra (aperiodic fit subtracted) of the right STN during DBS OFF and during right and left DBS ON. Significant differences for right DBS ON vs. OFF: blue shade; left DBS ON vs. OFF: red shade; overlapping clusters: purple shade. (C; right) Topography of coherence between the right STN and the MEG sensors during right DBS ON vs. OFF and left DBS ON vs. OFF. Channels significantly modulated by right DBS are marked in black (left DBS: white, overlap: grey). (D) Sourcelocalized contrast between DBS ON and DBS OFF (left and right DBS averaged).

Task-related modulations of subthalamic oscillations differed between the OCD and the PD patient

Surprised by how closely the resting-state patterns of the OCD patient resembled those reported for PD, we wondered whether we would find a more distinct oscillatory signature in a task. Thus, we had the OCD patient perform a Go/NoGo task and compared the recordings to a PD patient measured with the same setup.

On the cortical level, the responses were rather similar (Fig. 4). In Go trials, we observed movement-related beta suppression after the Go stimulus, followed by a beta rebound. In NoGo trials, the suppression was interrupted by an early increase in beta power, differentiating response inhibition from execution (OCD M1: $t_{\rm clustersum}$ = -561.202, p < 0.001; PD M1: $t_{\rm clustersum}$ = -711.0559, p < 0.001). On the level of the STN, the beta-dominated pattern seen in cortex repeated in the PD patient ($t_{\rm clustersum}$ = -312.723, p < 0.001), but appeared to be shifted in frequency in the OCD patient, with differences arising in the theta band in left (Fig. 4) and right STN (Supplemental Fig. 1). Specifically, NoGo trials were associated with higher theta power than Go trials ($t_{\rm clustersum}$ = -333.027, p < 0.001; Fig. 4A). Details are reported in Supplemental Tables 3-4.

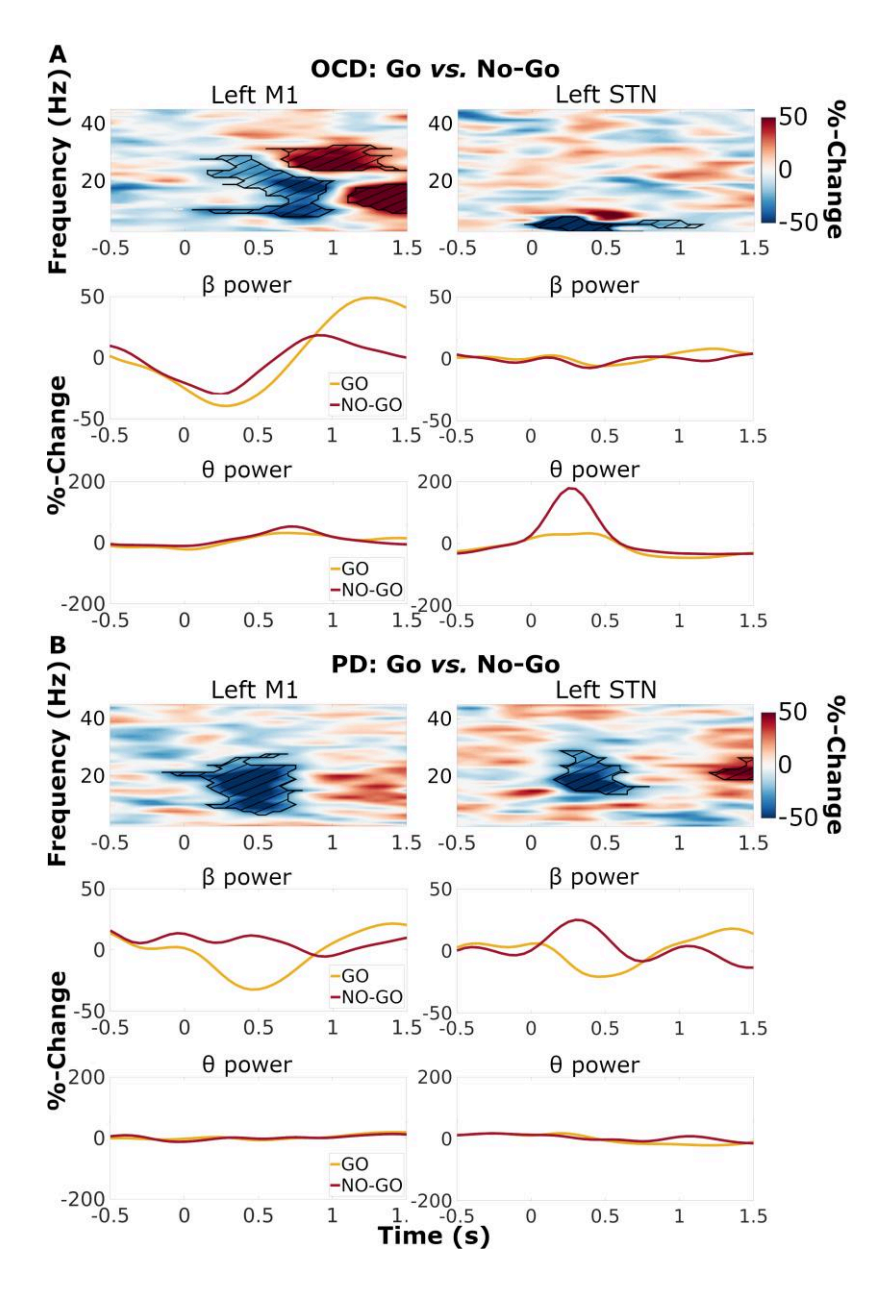


Figure 4. Modulations of left subthalamic power associated with response inhibition differed between the OCD and the PD patient. Top: time-frequency power spectra, contrast between Go and NoGo trials (pooled over cue types), for the OCD patient (A) and the PD patient (B). The difference between baseline-corrected Go trials and baseline-corrected NoGo trials is color-coded. Significant differences are marked by hatched lines within contours. Bottom: band-average power time course, for beta (13-30 Hz), and theta (3-8 Hz) frequencies.

Discussion

DBS in OCD is rare and its effects on neural oscillations and their synchronization across basal ganglia cortex loops are underexplored. Here, we demonstrate the existence of prominent

beta oscillations, synchronized across STN and motor cortex in the resting-state, in a single OCD patient. Interestingly, DBS suppressed these oscillations, as reported previously for PD patients ^{7,9,40}. Notably, we did not observe any DBS-entrained gamma activity in the OCD patient at half the stimulation frequency, in line with the idea that it is related to dopaminergic medication intake 41.

By providing a non-movement disorder control, this paper makes an important contribution to the discussion on the link between two major effects of DBS: the dampening of beta oscillations and the concurrent improvement of motor symptoms. Our results clearly indicate that these two effects can (but need not) dissociate, with beta-suppression occurring in the absence of any changes in motor performance. We thus conclude that DBS-responsive beta oscillations are not necessarily a sign of PD. The fact that they do occur in several diseases suggests that they might relate to physiological functions 42, such as somatosensory processing, the integration of sensory feedback with existing knowledge 43, and the maintenance of current motor/cognitive output 44. Alternatively, they might represent a common feature of PD and OCD, such as a high level of inhibition, arising either as a consequence of neurodegeneration (PD) or from volitional processes such as withstanding compulsions (OCD). The STN is likely involved in either process, as it integrates cognitive, limbic and motor processes 42, with beta oscillations occurring in both motor- 17 and nonmotor ^{11,45} regions.

In contrast to the resting-state recordings, the Go/NoGo task revealed an oscillatory pattern not familiar from the PD literature, which emphasizes the involvement of beta oscillations ⁴⁶. In the OCD patient, however, we found the strongest responses in the theta band. This finding aligns with previous research linking altered theta activity to OCD symptoms ^{16,17}, such as the inability to inhibit compulsive behaviors or deal with conflict, an established correlate of theta activity ⁴⁷. To ensure that the deviation was not due to the methodology applied here, we repeated the experiment in a single PD patient. As expected, we observed marked modulations of STN beta power, possibly reflecting the disease's characteristic overactivity of STN-cortical pathways. Notably, motor cortex exhibited task-related beta modulations in both patients. This might have led to corresponding beta-band modulations of subthalamic activity in PD only, due to insufficient shielding of the STN from motor cortical drive 3.

Of course, these ideas need to be tested in group studies. Case studies are limited by design,

particularly when comparing DBS patients with different electrode placements (Fig. 1). We

cannot rule out that a more anteromedial vs. dorsolateral electrode placement explains the

spectral shift observed here (beta modulation in PD, theta modulation in OCD). Yet, both of

the subthalamic compartments sampled here feature both theta and beta oscillations ^{45,48},

suggesting that the spectral shift is due to the disease rather than the subthalamic

compartment.

In summary, this case study illustrates how a task may uncover disease-specific STN

oscillations that are not apparent in resting-state. This aligns with functional MRI research,

demonstrating that task-based connectivity patterns contain more behaviorally relevant

information than resting-state connectivity ^{49,50}. Importantly, our study proves that DBS-

responsive beta oscillations exist in non-movement disorders, demonstrating that these

13

oscillations are not necessarily a sign of motor impairment.

Funding

This project was funded by Brunhilde Moll Stiftung.

Competing interests

The authors report no competing interests.

References

- 1. Brown P, Oliviero A, Mazzone P, Insola A, Tonali P, Di Lazzaro V. Dopamine dependency of oscillations between subthalamic nucleus and pallidum in Parkinson's disease. J Neurosci. 2001;21(3):1033-1038.
- 2. Hirschmann J, Özkurt TE, Butz M, et al. Distinct oscillatory STN-cortical loops revealed by simultaneous MEG and local field potential recordings in patients with Parkinson's disease. *NeuroImage*. 2011;55(3):1159-1168.
- 3. Oswal A, Cao C, Yeh C-H, et al. Neural signatures of hyperdirect pathway activity in Parkinson's disease. Nature Communications. 2021;12(1):5185.
- 4. Kühn AA, Tsui A, Aziz T, et al. Pathological synchronisation in the subthalamic nucleus of patients with Parkinson's disease relates to both bradykinesia and rigidity. Experimental Neurology. 2009;215(2):380-387.
- 5. Lofredi R, Tan H, Neumann W-J, et al. Beta bursts during continuous movements accompany the velocity decrement in Parkinson's disease patients. Neurobiol Dis. 2019;127:462-471.
- 6. Muthuraman M, Bange M, Koirala N, et al. Cross-frequency coupling between gamma oscillations and deep brain stimulation frequency in Parkinson's disease. Brain. 2020;143(11):3393-3407.
- 7. Mathiopoulou V, Lofredi R, Feldmann LK, et al. Modulation of subthalamic beta oscillations by movement, dopamine, and deep brain stimulation in Parkinson's disease. npj Parkinson's Disease. 2024;10(1):77.
- 8. Wilkins KB, Petrucci MN, Lambert EF, et al. Beta burst-driven adaptive deep brain stimulation improves gait impairment and freezing of gait in Parkinson's disease. medRxiv: the preprint server for health sciences. 2024.
- 9. Abbasi O, Hirschmann J, Storzer L, et al. Unilateral deep brain stimulation suppresses alpha and beta oscillations in sensorimotor cortices. NeuroImage. 2018;174:201-207.
- 10. American Psychiatric Association. Diagnostic and statistical manual of mental disorders 5ed: American Psychiatric Publishing; 2013.
- Wojtecki L, Hirschmann J, Elben S, et al. Oscillatory coupling of the subthalamic 11. nucleus in obsessive compulsive disorder. Brain. 2017;140(9):e56.
- 12. Qing X, Gu L, Li D. Abnormalities of localized connectivity in obsessive-compulsive disorder: A voxel-wise meta-analysis. Frontiers in Human Neuroscience. 2021;15:739175.
- 13. Beucke JC, Sepulcre J, Talukdar T, et al. Abnormally high degree connectivity of the orbitofrontal cortex in obsessive-compulsive disorder. JAMA2013;70(6):619-629.
- Smith EE, Schüller T, Huys D, et al. A brief demonstration of frontostriatal connectivity 14. in OCD patients with intracranial electrodes. *NeuroImage*. 2020;220:117138.
- Horn A, Li N, Meyer GM, Gadot R, Provenza NR, Sheth SA. Deep Brain Stimulation 15. response circuits in Obsessive Compulsive Disorder. *Biological Psychiatry*.
- 16. Bastin J, Polosan M, Piallat B, et al. Changes of oscillatory activity in the subthalamic nucleus during obsessive-compulsive disorder symptoms: Two case reports. Cortex. 2014;60:145-150.
- 17. Rappel P, Marmor O, Bick AS, et al. Subthalamic theta activity: a novel human subcortical biomarker for obsessive compulsive disorder. Transl Psychiatry. 2018;8(1):118.

- 18. Desarkar P, Sinha VK, Jagadheesan K, Nizamie SH. Subcortical functioning in obsessive-compulsive disorder: an exploratory EEG coherence study. The World Journal of Biological Psychiatry. 2007;8(3):196-200.
- 19. Lee I, Kim KM, Lim MH. Theta and gamma activity differences in obsessivecompulsive disorder and panic disorder: Insights from resting-state eeg with eLORETA. Brain sciences. 2023;13(10).
- 20. Perera MPN, Mallawaarachchi S, Bailey NW, Murphy OW, Fitzgerald PB. Obsessivecompulsive disorder (OCD) is associated with increased electroencephalographic (EEG) delta and theta oscillatory power but reduced delta connectivity. Journal of Psychiatric Research. 2023;163:310-317.
- 21. Figee M, Luigies J, Smolders R, et al. Deep brain stimulation restores frontostriatal activity in obsessive-compulsive disorder. network Nature Neuroscience. 2013;16(4):386-387.
- Schwabe K, Alam M, Saryyeva A, et al. Oscillatory activity in the BNST/ALIC and the 22. frontal cortex in OCD: Acute effects of DBS. Journal of Neural Transmission. 2021;128(2):215-224.
- 23. Koh MJ, Seol J, Kang JI, et al. Altered resting-state functional connectivity in patients with obsessive-compulsive disorder: A magnetoencephalography study. *International* Journal of Psychophysiology. 2018;123:80-87.
- 24. Xiong B, Wen R, Gao Y, Wang W. Longitudinal changes of local field potential oscillations in nucleus accumbens and anterior limb of the internal capsule in obsessivecompulsive disorder. Biological Psychiatry. 2023;93(11):e39-e41.
- 25. Horn A, Kühn AA. Lead-DBS: A toolbox for deep brain stimulation electrode localizations and visualizations. NeuroImage. 2015;107:127-135.
- 26. Avants BB, Tustison NJ, Song G, Cook PA, Klein A, Gee JC. A reproducible evaluation of ANTs similarity metric performance in brain image registration. NeuroImage. 2011;54(3):2033-2044.
- 27. Fonov V, Evans AC, Botteron K, Almli CR, McKinstry RC, Collins DL. Unbiased average age-appropriate atlases for pediatric studies. *NeuroImage*. 2011;54(1):313-327.
- Avants BB, Epstein CL, Grossman M, Gee JC. Symmetric diffeomorphic image 28. registration with cross-correlation: Evaluating automated labeling of elderly and neurodegenerative brain. Medical Image Analysis. 2008;12(1):26-41.
- 29. Husch A, V. Petersen M, Gemmar P, Goncalves J, Hertel F. PaCER - A fully automated method for electrode trajectory and contact reconstruction in deep brain stimulation. NeuroImage: Clinical. 2018;17:80-89.
- 30. Ewert S, Plettig P, Li N, et al. Toward defining deep brain stimulation targets in MNI space: A subcortical atlas based on multimodal MRI, histology and structural connectivity. NeuroImage. 2018;170:271-282.
- 31. Treu S, Strange B, Oxenford S, et al. Deep brain stimulation: Imaging on a group level. NeuroImage. 2020;219:117018.
- 32. Oostenveld R, Fries P, Maris E, Schoffelen JM. FieldTrip: Open source software for advanced analysis of MEG, EEG, and invasive electrophysiological data. Computational Intelligence and Neuroscience. 2011;2011(1):156869.
- Donoghue T, Haller M, Peterson EJ, et al. Parameterizing neural power spectra into 33. periodic and aperiodic components. Nature Neuroscience. 2020;23(12):1655-1665.
- 34. Taulu S, Simola J. Spatiotemporal signal space separation method for rejecting nearby interference in MEG measurements. Phys Med Biol. 2006;51(7):1759-1768.
- 35. Hnazaee MF, Sure M, O'Neill GC, et al. Combining magnetoencephalography with telemetric streaming of intracranial recordings and deep brain stimulation—A feasibility study. *Imaging Neuroscience*. 2023;1:1-22.

- 36. Van Veen BD, Buckley KM. Beamforming: A versatile approach to spatial filtering. *IEEE ASSP Magazine*. 1988;5(2):4-24.
- 37. Nolte G. The magnetic lead field theorem in the quasi-static approximation and its use for magnetoencephalography forward calculation in realistic volume conductors. *Phys Med Biol.* 2003;48(22):3637-3652.
- 38. Gross J, Kujala J, Hämäläinen M, Timmermann L, Schnitzler A, Salmelin R. Dynamic imaging of coherent sources: Studying neural interactions in the human brain. *Proceedings of the National Academy of Sciences*. 2001;98(2):694-699.
- 39. Maris E, Oostenveld R. Nonparametric statistical testing of EEG- and MEG-data. *Journal of neuroscience methods*. 2007;164(1):177-190.
- 40. Oswal A, Beudel M, Zrinzo L, et al. Deep brain stimulation modulates synchrony within spatially and spectrally distinct resting state networks in Parkinson's disease. *Brain*. 2016;139(5):1482-1496.
- 41. Colombo A, Bernasconi E, Alva L, et al. Finely tuned γ tracks medication cycles in Parkinson's disease: An ambulatory brain-sense study. *Movement Disorders*. 2025.
- 42. Accolla EA, Horn A, Herrojo-Ruiz M, Neumann W-J, Kühn AA. Reply: Oscillatory coupling of the subthalamic nucleus in obsessive compulsive disorder. *Brain*. 2017;140(9):e57-e57.
- 43. Barone J, Rossiter HE. Understanding the role of sensorimotor beta oscillations. *Front Syst Neurosci.* 2021;15(51).
- 44. Engel A, Fries P. Beta-band oscillation signalling the status quo? *Current Opinion in Neurobiology*. 2010;20(2):156-165.
- 45. Accolla EA, Herrojo Ruiz M, Horn A, et al. Brain networks modulated by subthalamic nucleus deep brain stimulation. *Brain*. 2016;139(Pt 9):2503-2515.
- 46. Kühn AA, Williams D, Kupsch A, et al. Event-related beta desynchronization in human subthalamic nucleus correlates with motor performance. *Brain*. 2004;127(4):735-746.
- 47. Zavala B, Brittain J-S, Jenkinson N, et al. Subthalamic nucleus local field potential activity during the Eriksen Flanker Task reveals a novel role for theta phase during conflict monitoring. *J Neurosci.* 2013;33(37):14758.
- 48. Olson JW, Nakhmani A, Irwin ZT, et al. Cortical and subthalamic nucleus spectral changes during limb movements in Parkinson's disease patients with and without dystonia. *Movement Disorders*. 2022;37(8):1683-1692.
- 49. Zhao W, Makowski C, Hagler DJ, et al. Task fMRI paradigms may capture more behaviorally relevant information than resting-state functional connectivity. *NeuroImage*. 2023;270:119946.
- 50. Elliott ML, Knodt AR, Cooke M, et al. General functional connectivity: Shared features of resting-state and task fMRI drive reliable and heritable individual differences in functional brain networks. *NeuroImage*. 2019;189:516-532.

Supplemental Results

Supplemental Table 1: Effects of left hemispheric DBS on STN power.

Freq. start [Hz]	Freq. end [Hz]	cluster statistic	<i>p</i> -value
36	49	-39.547	<0.001
22	28	-22.863	<0.001
52	55	-10.775	<0.001
5	6	7.3950	0.010

The results from the cluster-based permutation test describe the effects of left hemispheric DBS on right STN power (spectral test). The cluster statistic refers to the sum of t-values within a cluster. The sign of the statistic indicates whether STN power was increased or reduced by DBS. Only clusters significant in a two-sided test are listed.

Supplemental Table 2: Effects of right hemispheric DBS on STN power.

Freq. start [Hz]	Freq. end [Hz]	cluster statistic	<i>p</i> -value
32	55	-130.335	<0.001
19	30	-95.168	<0.001

The results from the cluster-based permutation test describe the effects of right hemispheric DBS on right STN power (spectral test). The cluster statistic refers to the sum of t-values within a cluster. The sign of the statistic indicates whether STN power was increased or reduced by DBS. Only clusters significant in a two-sided test are listed.

Supplemental Table 3: Effects of left hemispheric DBS on STN-cortex coherence.

location	cluster statistic	<i>p</i> -value
Bilateral sensorimotor cortices	-14.704	0.002

The results from the cluster-based permutation test describe the effects of left hemispheric DBS on beta coherence between right STN and cortex (spatial test, sensor level). The cluster statistic refers to the sum of t-values within a cluster. The sign of the statistic indicates whether coherence was increased or reduced by DBS. Only clusters significant in a two-sided test are listed.

Supplemental Table 4: Effects of right-hemispheric DBS on STN-cortex coherence.

location	cluster statistic	<i>p</i> -value
Left Sensorimotor cortex	-104.829	<0.001
Left parietal cortex	60.482	<0.001
Right Sensorimotor cortex	-24.462	0.004

The results from the cluster-based permutation test describe the effects of right hemispheric DBS on beta coherence between right STN and cortex (spatial test, sensor level). The cluster statistic refers to the sum of t-values within a cluster. The sign of the statistic indicates whether coherence was increased or reduced by DBS. Only clusters significant in a two-sided test are listed.

Supplemental Table 5: Left M1 power during Go vs. NoGo trials in OCD.

frequencies [Hz]	time points [s]	cluster statistic	<i>p</i> -value
7.568 - 28.809	0.052 – 1.000	-561.202	<0.001
23.682 - 32.471	0.548 - 1.500	316.069	<0.001
8.789 - 18.799	1.100 - 1.500	221.342	<0.001

The results from cluster-based permutation test describe the effects of trial type (Go or NoGo) on time-resolved power in the left M1 of the OCD patient (time-frequency test). The cluster statistic refers to the sum of t-values within a cluster. The sign of the statistic indicates whether baseline-corrected power increased or decreased in Go compared to NoGo trials. Only clusters significant in a two-sided test are listed.

Supplemental Table 6: Left STN power during Go vs. NoGo trials in OCD.

frequencies [Hz]	time points [s]	cluster statistic	<i>p</i> -value
2.441 - 7.568	-0.048 - 1.152	-333.027	<0.001

The results from cluster-based permutation test describe the effects of trial type (Go or NoGo) on time-resolved power in the left STN of the OCD patient (time-frequency test). The cluster statistic refers to the sum of t-values within a cluster. The sign of the statistic indicates whether baseline-corrected power increased or decreased in Go compared to NoGo trials. Only clusters significant in a two-sided test are listed.

Supplemental Table 7: Left M1 power during Go vs. NoGo trials in PD.

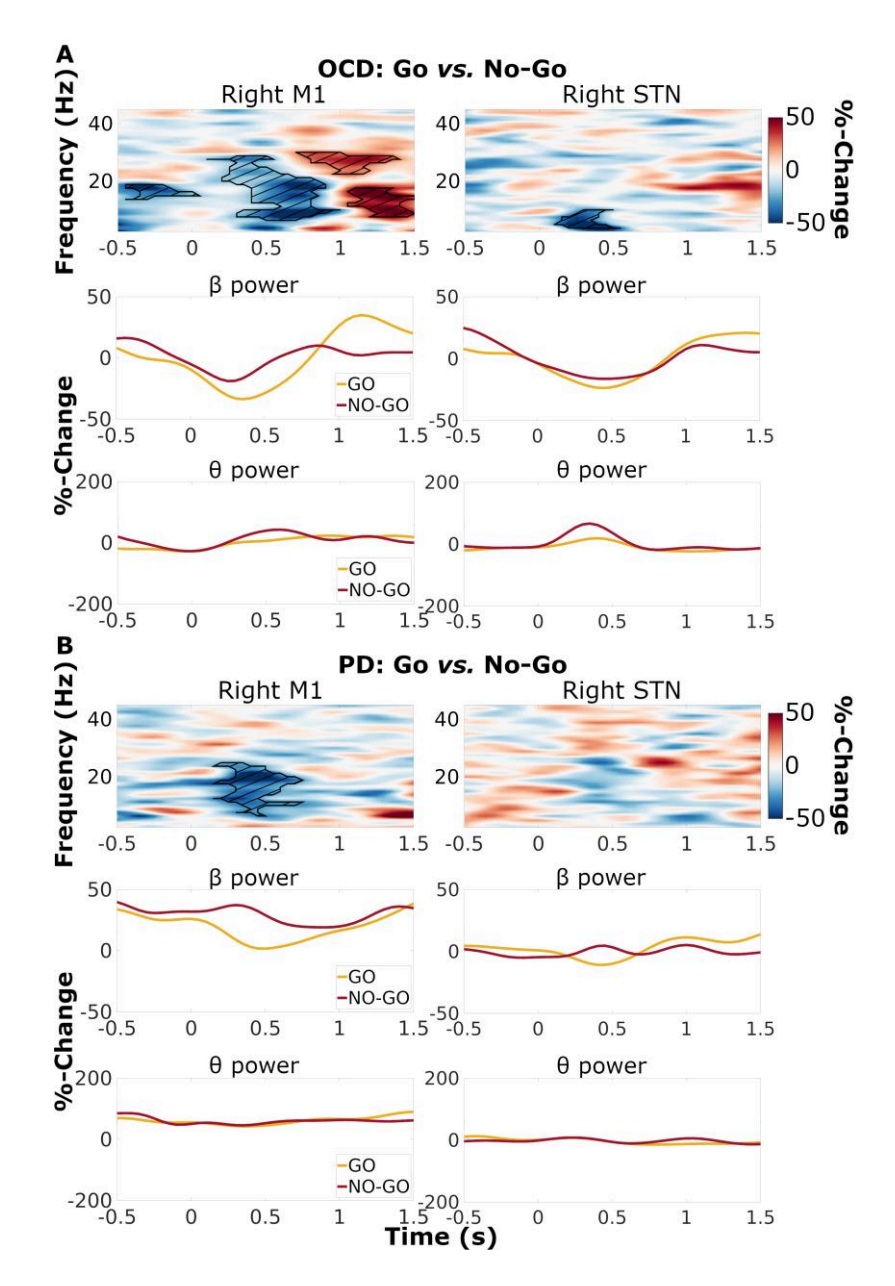
frequencies [Hz]	time points [s]	cluster statistic	<i>p</i> -value
6.348 - 27.588	-0.148 - 0.800	-711.056	<0.001

The results from cluster-based permutation test describe the effects of trial type (Go or NoGo) on time-resolved power in the left M1 of the PD patient (time-frequency test). The cluster statistic refers to the sum of t-values within a cluster. The sign of the statistic indicates whether baseline-corrected power increased or decreased in Go compared to NoGo trials. Only clusters significant in a two-sided test are listed.

Supplemental Table 8: Left STN power during Go vs. NoGo trials in PD.

13.672 - 28.809	0.152 - 0.800	-312.723	<0.001
18.799 - 26.367	1.200 - 1.500	81.775	0.004

The results from cluster-based permutation test describe the effects of trial type (Go or NoGo) on time-resolved power in the left STN of the PD patient (time-frequency test). The cluster statistic refers to the sum of t-values within a cluster. The sign of the statistic indicates whether baseline-corrected power increased or decreased in Go compared to NoGo trials. Only clusters significant in a two-sided test are listed.



Supplemental Figure 1: Modulations of right subthalamic power associated with response inhibition differed between the OCD and the PD patient. Top: time-frequency power spectra, contrast between Go and NoGo trials (pooled over cue types), for the OCD patient (A) and the PD patient (B). The difference between baseline-corrected Go trials (% change) and baseline-corrected NoGo trials (% change) is color-coded. Significant differences are marked by hatched lines within contours. Bottom: band-average power time course, for beta (13-30 Hz), and theta (3-8 Hz) frequencies.